Renewable Biomaterials from Bovine Serum Albumin

by

Kai Wang

A dissertation submitted to the Graduate Faculty of
Auburn University
in partial fulfillment of the
requirements for the Degree of
Doctor of Philosophy

Auburn, Alabama
December 13, 2014

Keywords: Bovine serum albumin, Biomaterials, Fibers, Injectable hydrogels, Artificial extracellular matrix

Approved by

Gisela Buschle-Diller, Chair, Professor of Polymer and Fiber Engineering
Yasser Gowayed, Professor of Polymer and Fiber Engineering
Maria Auad, Associate Professor and Interim Chair of Polymer and Fiber Engineering
Xinyu Zhang, Associate Professor of Polymer and Fiber Engineering
Yonnie Wu, Director, Mass Spec Center, Dept. of Chemistry and Biochemistry

Abstract

Bovine Serum Albumin (BSA) is one of the most abundant proteins from the livestock industry, and it has been widely used in biomedical research as a reagent. However, only limited areas of application and a very small amount of BSA is utilized. Comprehensive research to discover novel renewable protein based biomaterials as well as innovative cost-effective solution for its biomedical application is attempted in the following projects. These projects may have profound impacts on protein based biomaterials development and utility of by-product from agriculture.

In the first project, BSA was made to aggregate into long, linear fibers. Production of fibers occurs on a glass surface where dehydration conditions can be manipulated so that directional drying results in a linear protein aggregation. Interactions between BSA and salts suggest that removing the inner water shell surrounding the globular protein leads to protein unfolding and aggregation at the water/air interface. Fibril elongation is controlled by drying rate, chemical makeup, as well as solution geometry on the glass surface. Tensile testing of the product suggested crosslinked fibers are comparable with silk in mechanical properties. BSA fibers can be formed into larger assemblies such as yarns, and dyed with desired colorants, thus, possessing foreseeable potential for future industrial-scale development.

In the second project, BSA and low molecular weight polyethylene glycol (PEG) were reacted in a single-step reaction to synthesize translucent hydrogels with a Sol-Gel transition at temperatures between 37°C and 40°C. Gelation occurred by aggregation of smaller assemblies of BSA-PEG precursors at minutes time scale. The Sol-Gel transition concentration is depending on

the molecular weight of PEG and lies at temperatures below 35°C. Above 45°C, phase separation occurred that resulted in the precipitation of BSA-PEG from the solution. Microscopic examination of the gel revealed a porous structure with BSA-PEG forming the network with water filling in the spaces. At a low grafting ratio, BSA preserved its native secondary and tertiary structures and maintained its capacity for binding and enclosing small molecules. Drug delivery using the BSA-gel was assessed by a discontinuous method *in vitro* with 5-fluorouracil. Degradation tests with trypsin confirmed that the hydrogels were biodegradable. This novel material holds promise for biomedical applications as a potentially drug delivery vehicle for hydrophobic drugs which is difficult to be incorporated with other hydrogels.

In the third project, BSA was employed as a model protein to create a cost-effective artificial Model ECM (extracellular matrix) for potential tissue engineering applications. For this purpose, reduced BSA was PEGlyated and glycosylated to synthesize a linear glycoprotein as the major component of ECM. The glycosylated protein was crosslinked with EDC to mimic the mesh structures of native ECM. Coating and 3D porous structures were created by varying solution concentration and different fabrication steps. NIH 3T3 cells were cultured on 2D and 3D scaffold. Good cell adhesion, confluence and viability were achieved compared to those by collagen and tissue culture polystyrene. It is hypothesized that glycoprotein composition and specific morphology of the assembly will provide favorable circumstances for cell growth. Such ECM could eventually serve as an alternative culturing method for the more expensive collagen and fibronectin based materials currently in use and render tissue engineering more affordable.

Acknowledgments

The author owes a tremendous appreciation to his advisor, Dr. Gisela Buschle-Diller, for her guidance and encouragement during his study and research for completing the doctoral degree. The scientific method, insight of perspective and attitude learned from Dr. Buschle-Diller will benefit him lifelong. The author also expresses his gratitude to the other members of his academic committee, Dr. Yasser Gowayed, Dr. Maria Auad, Dr. Xinyu Zhang and Dr. Yonnie Wu for their interest and invaluable advice. The author would especially thank Dr. Yonnie Wu's cooperative work and contribution to those research projects. Many thanks to Dr. Allan E. David for evaluating dissertation and give suggestion as university reader, and thanks Dr. Ramsis Farag, Dr. Michael Miller and for their support in described experiments.

The author would also like to express gratitude to his group members Dr. Zhiwei Xie, Dr. Ahmet Karaaslan, Dr. Bo Yuan, Diana K. Lushington and Mei Li for their companionship and great work environment. The author would also like to thank anyone that assisted with the one or other aspect of his work, including but not limit to: Dr. Cihan Uzupinar, Xiaolong Wang, Bernal Sibaja, Chen Zheng, Yueru Li, Dr. Yu Wang, Dr. Ying Zhang, Dr. Young-Suk Choi, Xin Fan and Dr. Sharon K. Hamilton.

Last but not least, many thanks to his parents, Ziqiang Wang and Guanghui Cao for their continued love and support in his growth both physically and spiritually.

Table of Contents

List of Tables

List of Illustrations

List of Abbreviations

BSA	Bovine serum albumin
PEG	Polyethylene glycol
PVA	Polyvinyl alcohol
PLA	Polylactic acid (polylactide)
PLGA	Poly(lactic-co-glycolic acid)
PEO	Polyethylene oxide
PCL	Polycaprolactone
PNIPAM	Poly(N-isopropylacrylamide)
DOX	Doxorubicin
CTS	Chitosan
ALG	Alginate
HEP	Heparin
CS	Chondroitin sulfate
HA	Hyaluronic acid
TGF	Transformation growth factor
BMP	Bone morphogenetic protein
DEX	Dexamethasone
LCST	Lower critical solution temperature
ECM	Extracellular matrix

SEM	Scanning electron microscopy
TEM	Transmission electron microscopy
FT-IR	Fourier transform infrared spectroscopy
NMR	Nuclear magnetic resonance
UV-Vis	Ultraviolet-visible light spectroscopy
DTT	Dithiothreitol
EDC	1-Ethyl-3-(3-dimethylaminopropyl)carbodiimide
NHS	N-Hydroxysuccinimide
G’	Storage modulus
G”	Loss modulus
5-FU	5-Fluorouracil
DMSO	Dimethyl sulfoxide
D_2O	Deuterium oxide
CD	Circular dichroism
DMEM	Dulbecco's Modified Eagle's Medium
FBS	Fetal bovine serum
MTT	3-(4,5-dimethylthiazol-2-yl)-2,5-diphenyltetrazolium bromide
PEGDA	Polyethylene glycol diamine
GA	Gluconic acid
LA	Lactobionic acid
SA	Saccharide acid

TPS Tissue culture treated polystyrene

CHAPTER 1 INTRODUCTION

Bovine Serum Albumin

Bovine serum albumin (BSA) is the albumin purified from cattle plasma. BSA is ellipsoid in shape with the dimensions of 140 x 40 x 40 Å, and consists of 48.7% α-helix, 10.9% β-sheet and 30.7% random coils, or contains three domains which include two subdomains, with a total 583 amino acid residues with a molecular weight of 66,462 Da (Figure 1.1). In the two subdomains of BSA there are 17 disulfide bonds, which are not solvent accessible under its native conformation. BSA has non-uniformly distributed electric charges. With decreasing pH in the solution, the conformation of BSA could change significantly from globular to expanded linear structure with the loss of helical arrangements. Heating could also impact BSA secondary and tertiary structure, at 65-70°C, BSA lost its structure and denatured irreversibly In physiological system (in bovine), BSA serves the function of maintaining the osmotic pressure and stabilizing the pH of the blood. It is a carrier protein that binds to ligands such as metal ions, fatty acids and hormones, with different affinity, an indicator for the cleavage of a compound in the biological system.

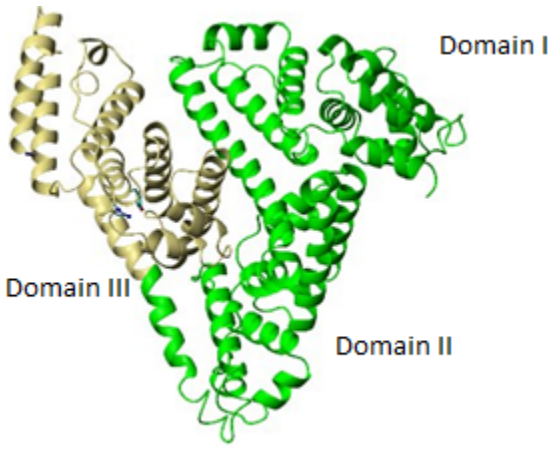

FIGURE1.1 3-D molecular structure of BSA

Motivation

Protein based biomaterials are currently used in the area of tissue engineering and drug delivery. Tissue engineering basically means the use of artificial tissue to restore, improve, or maintain tissue functions. Cells can be incorporated into scaffolds of biomaterials. These scaffolds may support cell growth as well as serve as a delivery vehicle of active compounds in the human body. In drug delivery, biomaterials are employed to improve drug administration and delivery effectiveness to target areas.

Protein based biomaterials, among other benefits, show biodegradability, non-inflammatory, and diversity in chemical composition, compared to synthetic polymers in biomedical applications. Synthetic polymers which have an aliphatic or aromatic backbone, are less likely to be degraded by metabolic enzymes, thus cannot match the degradability of nature-made proteins. In addition, proteins contain a variety of amino acids which enhances the likelihood for reacting with different substances and creates a favorable environment for interaction with cells and tissue. Proteins can be made precisely by controlling DNA transcription and translation, or by the use of a solid-phase synthesizer for smaller proteins, which guarantees a specific molecular weight, chemical, and biological properties. The potential high performance of protein based biomaterials may lead to an expanded field of applications in biomedical research. However, the cost of proteins (Table 1.1), especially proteins sourced from an extracellular matrix and in commercially available biological science grade, is extremely high limiting commercial applications to a certain degree. Cost effective materials with the known benefits of proteins need to be developed to replace those expensive materials currently in use.

Table 1.1 Price of commonly used protein and polysaccharide materials in biomedical science

Natural materials	**Price ($)[a)]**
Collagen (Type I)	656/100mg
Fibronectin	487/5mg
Hyaluronic acid	132/1g
Heparin (sodium salt)	417/1M Units (680mg)
Decellularized natural extracellular matrix (ECM)	231/1mg
BSA	1970/Kg

a) All materials' prices are from Sigma-Aldrich, 2014

For this research, BSA, with its relatively low cost and unique properties, has been selected for further exploration. BSA is the most abundant protein in bovine plasma with a typical concentration of 20 g/100 mL. A typical BSA product known as "Fraction V" is easily produced from bovine plasma by centrifuging and purifying via Edwin Cohn protein purification method by changing the pH, solvent (ethanol), salt content and concentration, etc. Albumin from animal blood is still considered a type of by-product that is not commonly utilized and often treated as waste. According to the statistics from USDA, there were over 70 million livestock slaughtered (54 million cattle) in the United States in 2011. Only a tiny fraction of animal blood protein is extracted and purified for research purposes. Currently, BSA is used for, including but not limited to microbial culture media, as blocking agent in western blot, as stabilizer in enzymatic reactions and as model protein in drug delivery systems. There is still a large amount of BSA available that could be utilized in prospective added-value products. The total amount of BSA currently adds up to 54.000 tons, calculated from 50% albumin obtained from an average 3.2 kg of cattle in the United States.

BSA has potential as inexpensive renewable material in a variety of biomedical areas. For instance, the domain 2 in BSA allows binding with hydrophobic drugs, which renders BSA a potential drug delivery vehicle. In addition, the conformation changes of BSA at the isoelectric point and under basic conditions enable property modifications of BSA and lead to materials distinctly different from native BSA. Furthermore, success in BSA utilization may guide the development of other proteins with similar structure and properties, which will significantly contribute to the amount of available renewable resources. These materials may replace expensive proteins or polysaccharide based materials listed in Table 1.1 in some areas of biomedical research and might have a profound impact on a variety of applications.

Objective

Research on BSA will broaden the utilization of serum proteins in the area of biomaterials, including the formation of fine fibers, injectable hydrogels or scaffolds for tissue engineering, which have not previously been developed. Long fine fibers can be obtained from BSA aggregation and, with enhanced mechanical properties, they might be excellent candidates for fibers in textiles, and for suture and wound dressing matrices. Injectable BSA-based hydrogels, with thermoresponsiveness introduced from grafted polymers, show rapid gelation rates and combine BSA's intrinsic property to bind small molecules. These hydrogels could become future drug delivery vehicles. Chemical modification and alteration of its structure may change the fact that BSA is incapable of cell adherence. The approach to mimic the extracellular matrix (EMC) based on BSA that has been chemically modified, could potentially overcome this problem.

Further, as part of this research, their properties and efficiency in application of BSA based biomaterials have to be established and approaches need to be developed that lead to

improvements. Therefore, the mechanical properties of BSA based fibers, the drug delivery effectiveness of the hydrogels, and the cell adhesion to scaffolds and, generally, the biocompatibility of all developed BSA based biomaterials has to be a focal point of this research and the key for improvements.

Finally, BSA could serve as a model protein that points to novel preparation methods for protein based biomaterials. The route to synthesize and modify BSA may be directly applied to other proteins or inspire preparation of new protein/polypeptide based biomaterials.

Chapter Arrangement

This dissertation is organized in six chapters with Chapter 1 being the introduction of the research area. Chapter 2 reviews the existing literature of biomaterials research related to three key projects. Chapters 3 to 5 represent the major body of each project in the sequence of BSA fiber formation from dehydration introduced aggregation, the preparation and properties of BSA-PEG thermoresponsive injectable hydrogels, and the potential use of glycosylated BSA as model ECM. Each chapter consists of an introduction, experimental section, results and discussion, and a conclusion. Chapter 6 closes with a summary of the most important findings and a perspective for future applications of these materials.

.

CHAPTER 2 LITERATURE REVIEW

In this chapter, current research progress on BSA as biomaterial and potential applications of BSA as fibers, injectable hydrogels and artificial ECM are summarized and reviewed. The advantages of protein based materials are described in the last chapter.

2.1 BSA BASED BIOMATERIALS

Bovine serum albumin (BSA) has been utilized in various areas of biomedical research. Traditionally, BSA has mostly been employed as nutrition medium in microbial culturing, as western blot blocking agent or enhancer [1]. However, the use of BSA as biomaterial has been relatively uncommon, and only a few types of BSA based materials were developed, mostly with the focus on serving as model compounds for further studies.

Chemical modification of BSA has been explored to potentially create a broader field of applications. One such modification constitutes the grafting of poly(ethylene glycol) (PEG) to the BSA backbone. BSA was first PEGylated in 1977 with methoxypolyethylene glycol of 2kDa and 5kDa by a two-step reaction. It could be illustrated that with PEG chains present in BSA, immunology reactions were significantly reduced in rabbits with a lower number of antibodies generated [2]. Following these findings, a variety of research studies on PEGylated BSA was conducted in order to explore the relationships of synthesis routes (via amino, thiol, carboxylate, carbonate groups, etc.), resulting properties (structure, stability and degradability) and applications of PEGylated protein products. Most studies targeted the development of a model for a protein or polypeptide delivery vehicle [3-6]. PEGylation provides desirable properties to BSA,

as well as to other types of proteins and polypeptides, such as nontoxicity, non-immunogenicity and non-antigenicity. Its residency in the living body can be prolonged by decreased degradation rate and a reduction in excretion rate.

In the course of these studies, PEGylated hydrogels were being developed for sustained drug delivery [7]. This research focused mostly on important hydrophilic drugs, but also on a number of hydrophobic drugs and a few polypeptides or low molecular weight proteins. For the first PEGylated BSA hydrogels nitrophenyl carbonate was used as crosslinking agent and PEG of various molecular weights. The hydrogels achieved high water content, and showed the capability of controlled drug release following a Fickian diffusion mechanism [8]. Subsequent research mainly focused on tailoring of the molecular structure towards an improvement of the properties of the hydrogels [9, 10]. Applications for enzyme or protein immobilization and the delivery of pharmaceuticals were conducted in later research [11, 12]. However, these hydrogels were formed *ex vivo,* which restrained the administration of drugs via an oral route, and which lowered the effective delivery rate. A more efficient approach of drug administration needs to be developed. One approach would be to use the thermoresponsiveness of low molecular weight PEG to easily transfer drug carrying PEGylated BSA and form gels *in vivo*. The details of injectable hydrogels will be discussed in section 2.3 of this chapter in more detail.

For the discovery of novel protein or polypeptide drug delivery systems, BSA served as a model for most of the proteins and polypeptides. Innumerous copolymers which are designed to improve protein drug carrier properties, such as PLGA, PNIPAM, PLA, alginate and chitosan, are based on BSA as a model to test the impact of drug entrapment or embedment [13, 14] for the reason that BSA is capable of forming reversible non-covalent bonds with polymers and/or drugs. Further, nanoscale BSA particles served as drug carriers for hydrophobic drugs [12]. BSA was

surface modified or copolymerized to enhance a specific type of bond to the drugs or to change the pharmacokinetic parameters (e.g. prolonged circulation life time for slow release) [7]. Additionally, BSA can take a variety of physical forms which is very useful. BSA can be electrospun into nanoscale fibrous webs and prepared as cell adherent coatings. In Dror's research [15], BSA was directly electrospun from solution without the use of a crosslinker and mechanical properties could be obtained that were comparable to natural fibrous materials. Unlike other proteins (see section 2.2), large scale production of BSA fibers, however, is still not available. Also, in the research of Kawamura [16] BSA was modified to introduce the capability to immobilize cells. However, cell migration and proliferation could not yet be achieved with this material. Subsequent research to enable more biological functions is still necessary. The related content will be presented in the section 2.4 of this chapter. Although exhibiting unique properties, BSA materials still has problems, such as variations from batch to batch, which restricted the industrial development of these nanomaterials.

2.2 PROTEIN FIBER ASSEMBLY

There are an abundance of fibrous materials constituted by naturally occurring proteins, mainly in cells, organelles and tissues. The biosynthesis of the specific protein precisely controls the composition and conformation by sequencing 20 types of amino acids to provide extraordinary diversity in protein functions [17]. The major types of natural protein fibers from animals consist of actin, collagen, elastin, fibrinogen, keratin, tubulin and silk. From plants sources, soy protein, zein and gluten are most significant [17, 18]. Those protein fibers play an important role in motility, scaffolding, stabilization and protection in the living body.

Research in the past fifty years has taken proteins from their natural function to develop textiles, biomedical and technical applications [18, 19]. Distinct assembly approaches, such as self-assembly, wet spinning, electrospinning and thermal aggregation were developed. The most common method is self-assembly which is also the predominant method *in vivo*. The method is a relative complex process to form organized structures but can be effective in manufacturing high performance materials for biomedical applications [17].

Among all of the protein fibers, silk is most significant for biomedical and textile applications, due to its unique chemical composition, structure, and biological properties which allow infinite possibilities for functionalization, processing and integration. Processing of silk materials is water based, at room temperature and neutral pH, and the fibers are biocompatible and mechanically stable. The self-assembly method was commonly employed in fibroin (silk protein) processing [20-22]. Products could be made from regenerated silk fibroin without sericin which may cause allergic reactions; these materials may cause minimal inflammation [20, 23-25]. A variety of applications in tissue engineering, implantable devices and drug delivery system have been devised from fibroin based materials [16, 18, 20, 25]. Additionally, the blend of silk fibroin with biocompatible PEO created fibrous composites with adequate mechanical properties for tissue engineering [26]. Introducing glycosaminoglycan, such as hyaluronic acid, rendered a more tissue mimicking environment [27]. Tripeptide RGD (Arginine-Glycine-Aspartic acid, obtained from AY genes) sequence (some silk from non-silkworm source may naturally contain RGD sequence) was immobilized onto silk for promoting cell adhesion [28]. Spider silk protein could also be regenerated from natural spider silk, however, with lower mechanical properties and a change in dimension [29].

Collagen is one of the most abundant proteins from the living body; there are over 20 types of collagens which are different in crosslink-sites of amino acid residues and degree of crosslinking [17]. For non-crosslinked collagen, hydrogen bond introduced self-assembly was employed for fiber fabrication [30].

In order to overcome the drawbacks of non-crosslinked collagen fibers, a variety of fibers from collagen blends with other materials were studied and produced for distinct applications. For instance, collagen-PAN fibers showed increased hydrophobicity and enhanced stability [31]. Blending collagen with chitosan in composites resolved the problem of too rapid degradation, and also introduced some antimicrobial properties [32].

Protein engineering as a relatively new method has also been used to create fibrous assemblies [19]. Engineered polypeptide and protein may form fibers at the scale of tens of nanometers, in the shape of branched fibrous matrices. However, it is challenging to scale up the fabrication as mass produced industrial products from self-assembly, for the reason that self-assembly may not meet the requirement of production rate in industry.

Wet spinning could be considered biomimicking of the formation process of spider fibers. Protein solution is extruded from tiny pores to stretch and draw fibers. Properties of spun fibers may be determined by a variety of factors, such as temperature, humidity, composition and concentration of solution, drawing speed, etc. [33]. A higher draw ratio may result in superior toughness, tenacity, and Young's modulus. Currently, with wet spinning protein, fibers are obtained in the range of 10-60 um diameter, thus is significantly higher than natural spider silk (1-4 um). In addition, the properties of fibers from wet spinning may be inferior than those of their natural counterpart (e.g. spider silk); nevertheless, some modifications in spinning condition

and solution may improve fiber properties to come close to those of natural fibers (e. g. fibroin) [20, 33].

Soy protein fibers can be produced from alkaline solution by wet spinning [34]. Fibers are crosslinked by aldehyde in order to enhance mechanical properties. Although suitable for the textile market, these fibers showed to be cytotoxic and could not be applied in the biomedical area [35]. Later research utilized extrusion from urea aged soy protein without use of a crosslinking agent. These fibers have better mechanical properties than non-crosslinked collagen and the capability for cell adhesion [36]. However, the stability at neutral conditions was limited. Soy protein was also mixed with other synthetic polymers or proteins in wet spinning, in order to solve the problem of low mechanical properties of the fibers. Zhang et al. [37] blended soy protein with PVA and formed fibers from extrusion. Controlling of extrusion conditions (salt/urea concentration, die L/D ratio and temperature) resulted in variant fibers. Later research of Deng et al. [38] on extrusion of soy protein/PAN fiber in ionic liquid created either hollow or solid fibers, depending on the processing temperature.

Zein is a protein of 44 kDa molecular weight that is isolated from corn and processed via wet spinning. Early attempts to use zein fibers started in the 1950s; chemical modification of zein rendered it suitable for textile and industrial applications [39]. However, the early product such as Vicara was withdrawn from the market because of its high cost. Later research documented the biocompatibility of zein fibers and its degradation products, its capability for cell adhesion, growth and proliferation [40]. Some research has been reported on zein blended with other materials to form fibers. These fibers may serve as drug carriers as well as may be made into packaging materials [41]. Among all the admixed components, nanocrystalline cellulose was found to most significantly increase the mechanical properties. The dispersion of nanocrystalline

cellulose in zein solution resulted in an oriented network within the fibers. Therefore, enhanced mechanical properties could be achieved without losing biocompatibility [42].

Casein is the phosphoprotein derived from mammal milk, making up 80% of the proteins in cow milk and 20-45% of the proteins in human milk. Fibers can be wet spun from the alkaline solution of casein with formaldehyde or aluminum sulfate as crosslinking agent [43]. To name a few commercialized products, Caslen (US), Lactofil (Holland), Cargan (Belgium), Tiolan (Germany), Silkool (Japan) and Fibrolane (UK) had been on the market. Instability at a higher pH and suspected carcinogenicity restrict the usage of these fibers to a narrow area, although they exhibited fair mechanical properties in tensile strength and elongation [35, 44]. Jiang and Yang [45] studied fibers from regenerated casein by using their alkaline solution and citric acid as crosslinking agent. These fibers achieved desirable mechanical properties and stability under acid conditions. However, these fibers were not biocompatible according to the cytotoxicity test. Casein-soy protein as well as casein-acrylonitrile blend was also studied and materials were obtained that exhibited resistance to weak alkaline conditions; however, these fibers still have a similar problem as other casein fibers in regard to biocompatibility [46].

Thermal aggregation was used as an advanced technology in commercial protein fiber production. Recent innovations such as QMilch© are offering a more refined use of the fiber for modern fabrics. The fibers underwent thermo-processing and were produced without the use of any additional chemicals as crosslinking agents [53]. These fibers have been promoted in the textile industry for high-end clothing, but the biocompatibility of these fibers still needs further investigation.

Electrospinning is another approach to form a thin fiber assembly. The difference between electrospinning and wet spinning is that in electrospinning a static electric field is used as driving

force. Fibers are deposited on a target rather than stretched and drawn. Most of the proteins capable of forming fibers in nature can be electrospun, and fibers are acquired in nano- or microscale [16-18]. It is still difficult though to obtain a single filament from electrospinning and current products are mostly obtained in form of a fibrous matrix or membrane.

In Section 2.1 electrospun fibers from BSA have been mentioned, however, this method of fiber formation is still less investigated for proteins compared to other natural polymers. Collagen was electrospun alone or with the other chemicals to fabricate ultrafine fibers. The early electrospinning efforts of collagen always involved using of fluoroethanol as the solvent for collagen, which caused the reduction in collagen triple helix structure and the high solubility of collagen at physiological conditions [47]. Fluoride containing chemicals are not biocompatible, which limits their application in biomedical engineering. Later attempts to electrospin collagen were performed with acetic acid to increase the biocompatibility, but it was found that the applied conditions decreased the amount of triple helix in the structure [48]. Studies were performed using weak organic acids as solvents, such as carboxylic acid, showed to preserve triple helix structure and to form fibers with higher strength. A combination of collagen, citric acid and hypophosphite seemed to improve biocompatibility and mechanical properties [49].

Proteins from plants sources, such as soy protein and zein were electrospun from water soluble polymer admixtures (PEO, PVA) [38, 50] for antimicrobial and scaffold purpose, along with higher mechanical properties. Chitosan-zein composites provided a material with some antimicrobial function [51]. Silk was also electrospun with zein to mimic the extracellular matrix (ECM) [52].

Although efforts to upscale manufacturing from laboratory experiments have been made, the commercial mass production of electrospun fibers is still under development.

2.3 INJECTABLE HYDROGELS

Besides as fibers, proteins can function in form of hydrogels which have important applications, especially in the biomedical field. Generally, hydrogels are materials with three-dimensional network structures that consist of hydrophilic polymer building blocks. They are capable of retaining large amounts of water. Hydrogels have been used as scaffolding materials for tissue engineering, for cell encapsulation and drug/gene delivery, and as barriers between tissue and materials' surfaces. Their suitability is based on their biocompatibility and biodegradability, excellent physical and chemical properties and ease of fabrication [54, 55].

Injectable hydrogels are three-dimensional network structures that can be formed *in vivo*, as opposed to a pre-formed hydrogel. The aqueous precursor of the hydrogel must have low viscosity before gelation, and be crosslinkable *in vivo* after injection. If targeted for biomedical applications, the gelation has to be possible in a physiologically benign environment without the use of toxic chemicals or heat beyond body temperature. Further, any release of gaseous by-products could cause tissue damage. This type of material, of course, also requires biocompatibility and biodegradability and, if used as drug or cell carrier, the homogeneous dispensation of the loaded active component. Due to the mobility of the injectable precursor, the hydrogel is able to adapt to defects but must achieve the necessary mechanical properties after injection. Injectable hydrogels should also exhibit pronounced porosity to allow the transportation, growth and rearrangement of cells [55-64].

By controlling the chemical composition of natural and/or synthetic polymers, a number of injectable hydrogels have been created for biomedical applications. They need to provide the appropriate chemical and morphological environment, correctly respond to cell cues, show

controllable gelation kinetics, and have good mechanical properties. They should biodegrade and be able to deliver drugs. Balancing the gelation and biodegradation plays an important role in any practical application.

Polymer systems suitable for injectable hydrogels

Materials for injectable hydrogels can generally be divided into natural and synthetic polymers. Natural polymers include polysaccharides (e.g., chitosan, hyaluronic acid, alginate), and proteins (e.g., gelatin, heparin, chondroitin sulfate). The major focus of synthetic polymers has been on synthetic peptides and block-copolymers, such as polyethylene glycol-poly(lactide) (PEG–PLA), poly(ethylene glycol)-b-poly(lactic acid co-glycolic acid) (PEG–PLGA) and poly(ethylene glycol)-b-poly (ε-caprolactone) (PEG–PCL), etc. [61, 71-75]. Synthetic polymers showed to reduce the immunologic reaction. Some examples for injectable hydrogels are listed in Table 2.1 [55].

Table 2.1 Typical gelation factors, properties, administrative routes and potential applications of injectable and biodegradable hydrogels (Data adopted from [55])

Polymers	Modification and Gelation	Properties	Potential applications
Chitosan (CS)	CS- PNIPAM	Tg = 32.1°C	Drug/cell delivery Wound healing
	N-Palmitoyl-CS	pH-triggered gelation	
Hyaluronic acid (HA)	CS in PEO–PPO–PEO	Heparin mediated b-TGF release	Cartilage Regeneration Bone regeneration Cell delivery/tissue constructs
	HA-PNIPAM	*In vivo* biocompatible	
	HA–TA(Tartaric acid) /apatite with H_2O_2	Reinforced (G' 46.5 kPa)	
	HA-Dextran	Hydrolytic mediated release	
Alginate	$CaSO_4$ (RGD grafted)	Optimized RGD spacer length	Tissue engineering
Heparin (HEP)	Alginate and $CaCl_2$	Increase growth factor release	Cartilage Regeneration of neurons
	HEP–TA with H_2O_2	Increase chondrogenesis	

	HEP/PEG EDC/NHS crosslinked	Synergistic biosignaling	Regeneration
	HEP-PEG-DAc	Increase chondrogenesis	
	PEG-HEP/VEGF	Receptor-mediated growth factor	
	GEL– Hydroxyapatite	Hydrogel fibers	
Gelatin (GEL)	GEL/Dextran–MA	Dually crosslinked	Neurogenesis Cell delivery
	GEL-HA-PEG	Accelerate gelation rate	
Fibronectin	Thrombin (With PLGA and heprain)	Increase growth factor release, angiogenesis	Hind limb ischemia Localized gene
	Thrombin	Fibrin-mediated gene delivery	Delivery
	Chitosan crosslinked	Increase cartilage adhesive strength	
	Elastin like peptide-PEG	Hyperthermia targeting, acid-labile release	
	PEG—peptide	Thermo-activated crosslinking	
	MMP-peptide-SH/PEG-VS	MMP-mediated DNA delivery	
	MB-PEG—PLLA	Gelation concentration l5wt%	
Polyethylene Glycol (PEG)	PEG —$(PLA)_8$	Increase G”, 7-l7 kPa, Gelation concentration 7 w/v%	Tissue engineering Drug delivery Adhesion prevention
	PEG —$(PLA)_8$—Ch	Increase G’, 10 kPa, Gelation concentration 3w/v%	
	PEG —PLLA / PEG —PDLA	Increased G” ,	
	PEG—PLGA—PEG	Gelation concentration 17wt%	
	PLGA— PLGA—PEG	*In vivo* biocompatible	
	PEG—PCL	*In vivo* BSA-FITC release	
	PCL — PEG — PCL	Increase gel domain, *in vivo* duration	
	PCLA — PEG — PCLA	Reduced peritoneal adhesion	
Purine nucleoside phosphorylase	PNP and IleOEt (RGD grafted)	Osteogenic differentiation	Bone regeneration
	PNP and IleOEt (DOX incorporated)	Increased antitumor activities	

Among polysaccharides, glycosaminoglycans are important candidates for biomedical hydrogels. Hyaluronic acid is the only non-sulfated glycosaminoglycan that is widely represented in connective, epithelial and neural tissues. Hyaluronic acid based hydrogels have served an important role in wound healing and angiogenesis, as well as in the construction of the extracellular matrix (ECM) [57]. Heparin is a highly sulfated negatively charged

glycosaminoglycan that is employed *in vitro* and *in vivo* in systems for the delivery of growth factors for bone generation, as well as for hydrogels [59]. This peptide with moieties in specific sequences may form hydrogels with various potential interactions. Furthermore, self-assembled peptide hydrogels are drawing more and more attention as drug delivery vehicles and scaffolds for tissue engineering [60, 61].

Chitosan is chemically similar to glycosaminoglycan and has excellent biocompatibility and low toxicity. The physical or chemical gelation of chitosan based injectable hydrogels is less invasive and can be initiated by either thermal or pH change. Chitosan based hydrogels have been employed for drug delivery and tissue engineering as well as in cancer treatment [55].

Alginate is an unbranched polysaccharide with debatable biocompatibility that depends on molecular weight. Alginate hydrogels could act as delivery systems for bioactive peptides and proteins, genes, and drugs [58].

Amphiphilic polymers have received considerable attention as potential biomaterials. For instance, PLA, PCL, and PLGA form copolymers with PEG in form of micelles at low concentrations and gels at higher concentrations. They are mainly used for delivery of active compounds and tissue regeneration [62].

In vivo gelation can take place by either a chemical or physical route ([54, 55], Figure 2.1). Temperature-responsive hydrogels and some types of physically crosslinked hydrogels are attractive materials primarily due to the ease of tailoring their physical properties for specific applications. These systems exhibit relatively high biological compatibility; cells, bioactive molecules or even complex 3D network structures can simply be mixed in solution at low temperatures and injected in the defect area to induce gelation [54, 55].

Injectable hydrogels can also be created by ionic crosslinking. They respond to controlled ionic interaction to form hydrogels *in situ*. Alginates are a relatively low cost choice for injectable hydrogels; they form under fairly mild conditions that are suitable for various medical applications [54].

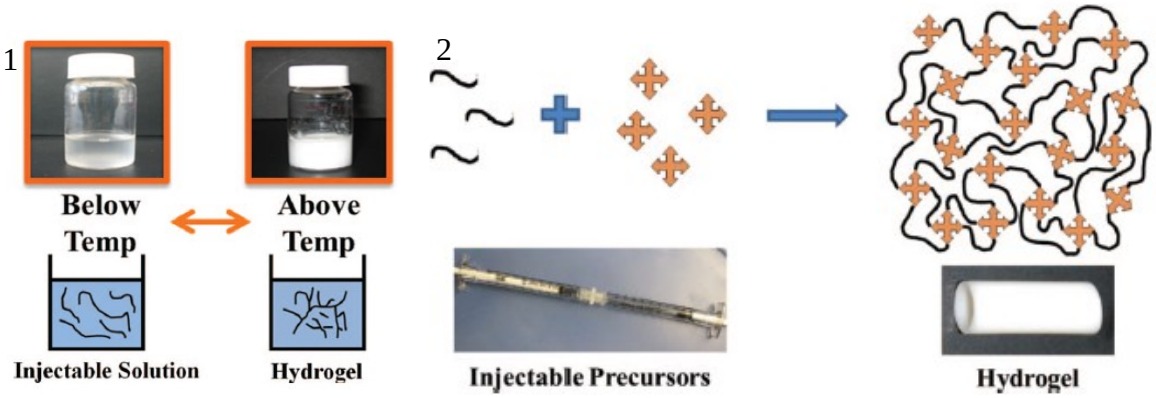

Figure 2.1 Physical crosslink gelation (1) and chemical crosslink gelation (2) *in vivo* ([55] Copyright: The Royal Society of Chemistry, reproduced with permission)

Hydrogels also can be produced from liquid precursors or in solution *in situ* via a chemical reaction by a number of mechanisms, including thermal polymerization, photo-polymerization, or polymer-polymer crosslinking reactions. *In situ* cross-linking is ideal for incorporating a wide variety of biocompatible hydrophilic biomaterials (such as PEG) into an injectable hydrogel. The material must have low enough viscosity to be injectable and yet gel fast after injection to avoid release. Efficient cross-linking is also important for minimizing the toxicity associated with reactive chemical species or leachable small molecules [55].

Compared to physically crosslinked injectable hydrogels, chemically crosslinked ones have more limited applications since they are restricted to certain reactions and types. It is essential for biomedical hydrogels that the chemical environment is kept benign, and to avoid toxic chemicals,

overheating, release of gases, and a change in pH beyond the physiological value. However, the merits of chemically crosslinked hydrogels are obvious: first, the reaction *in situ* reduces the cost for preparation of precursors that could be rather high in the case of physically crosslinked hydrogels. Additionally, chemical reactions might be terminated in a very short period of time and the risk of burst release of enclosed drugs might be lower upon injection. Physical crosslinking can take minutes or even hours for the gelation to occur. Finally, physically crosslinked hydrogels cannot measure up in properties compared to chemically crosslinked ones in regard to their properties, especially as mechanical and rheological features are concerned. Ionic injectable hydrogels bridge the gap between physically and chemically crosslinked ones, although only a few natural polymers can be used as ionic injectable hydrogels.

Hydrogels for drug release and tissue repair

Injectable hydrogels have been explored to serve as scaffolds in tissue engineering that simultaneously allow the transport of cells and nutrients and thus provide a short-term support structure for cell growth. Hydrogels intended as drug carriers are employed to provide greater drug concentrations at a desired target location while both minimizing drug accumulation in other parts of the body as well as potential side-effects. Injectable hydrogels can also be easily delivered into sites that are difficult or inaccessible in surgery [56]. In Figure 2.2 the concept of injectable, degradable polymers for drug delivery is shown.

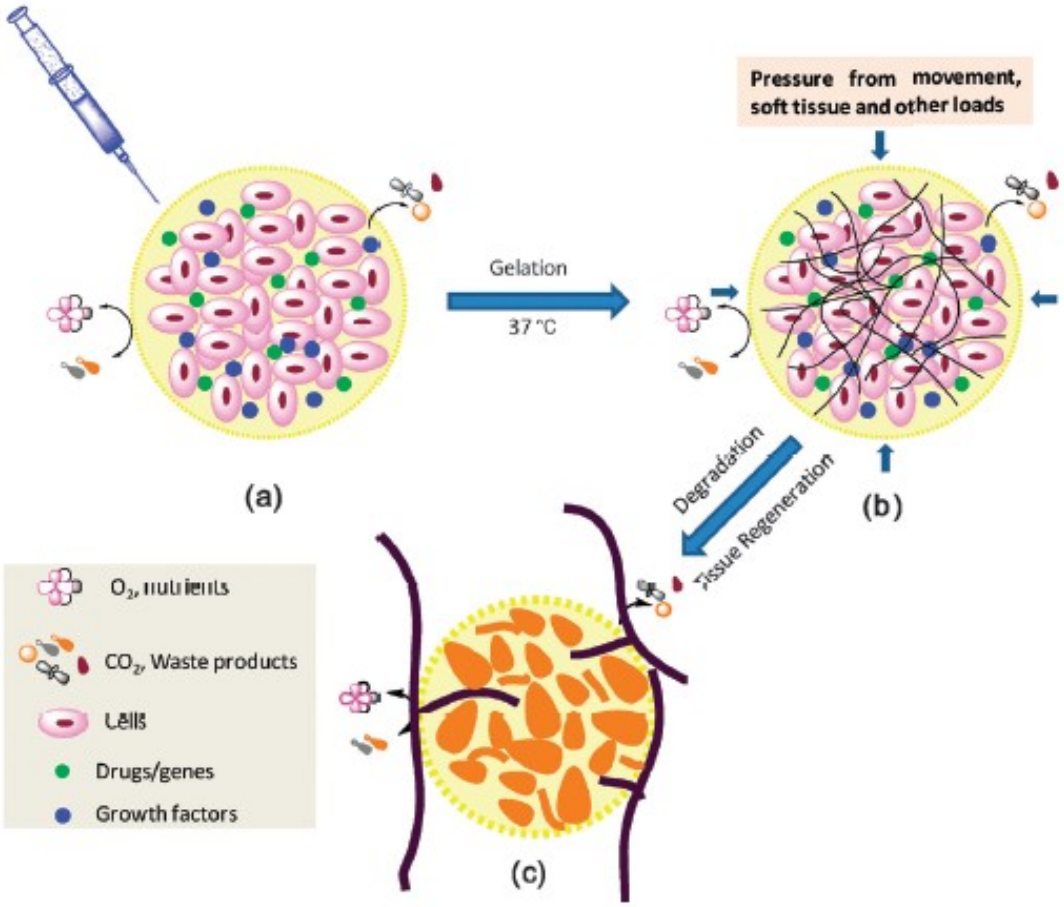

Figure 2.2 Injectable hydrogels for delivery (a) the precursors are mixed with cells, drugs or factors before gelation; (b) injected materials should form hydrogels *in situ*, holding cells or drugs and avoiding initial burst effects; (c) hydrogels degrade in a controlled manner leaving space for newly formed tissue. ([55] Copyright: The Royal Society of Chemistry, reproduced with permission)

In general, some unresolved issues still exist for injectable hydrogels intended for drug delivery. Most hydrogels are too weak to be bearing a load, and some physically crosslinked hydrogels are prone to plastic deformation in response to stress. Also, insoluble drugs can become heterogeneously distributed within the gels, and a significant concentration gradient at the drug

release location could occur. The greatest problem, however, is a frequently observed sudden initial drug release from the hydrogel (burst release). In extreme cases, the drug discharge can come to a complete halt. Burst release is the primary concern for injectable formulations for the reason that slower gelation *in situ* may lead to a loss of drug before the gel had a chance to fully form. Changes in gel volume after gelation, whether caused by degradation or diffusion, can also cause rapid release [55-64]. In the following section, several classes of injectable hydrogels for drug or protein delivery are presented in more detail.

In the study of Kim et al. [56], chitosan/glycerophosphate solutions exhibited complete reversible thermosensitivity in the pH range of 6.4 to 6.8 by a change in hydrogen bonding and other interactions. The properties of this hydrogel were investigated by using ellagic acid release for cancer treatment. The viability of U87 cells and C6 cells were significantly reduced compared to pure chitosan gels after 3 days of incubation. Prolonged release of ellagic acid was achieved by slow enzymatic biodegradation of the gel to control the drug release rate [56]. However, as with other current studies in anti-cancer research, unfortunately cancer cells could not be fully destroyed; instead they were reduced by only a small fraction. With low viability the effectiveness of a cancer treatment cannot be guaranteed. Furthermore, degradation of this material only occurred at a pH value below 7 and thus cannot accommodate a variety of cancer types. However, the novelty of this hydrogel should not be underestimated, and with further studies it might provide an effective delivery system in the future.

In another study [61], a chitosan-based hydrogel has been discussed which has a gelation temperature near body temperature and gels within minutes. Different types of proteins have been enclosed and the release time measured. In this case, it was found that due to the different

molecular sizes and the relatively low solubility of the proteins, the release was not homogeneous. As with other types of injectable hydrogels, the initial burst release of protein seemed to have been a major concern.

Hyaluronic acid (HA) plays an important role in wound healing, cell motility, and angiogenesis as well as in the construction of the extracellular matrix (ECM). It directly affects tissue organization via interactions with cell-surface receptors, promotes the migration of cells, facilitates ECM remodeling, and stimulates the production of collagen type II [57]. Therefore, it has been extensively employed in the biomedical field for drug and gene delivery systems as well as for tissue regeneration.

A PNIPAM-grafted HA injectable hydrogel showed sustained release of riboflavin and fluorescein isothiocyanate (FITC) -labeled bovine serum albumin (BSA-FITC) when the grafting yield of PNIPAM onto the HA backbone had been increased[60]. Aldehyde and hydrazide modified hyaluronic acid led to a hydrazone-crosslinked hydrogel within 30 s, which *in vitro* showed a controlled release of bone morphogenic protein-2 (BMP-2) in up to 28 days. After *in vivo* injection (rat calvarium), a new bone was formed within 8 weeks. The process depended on the amount of loaded bone morphogenetic protein in the gel. This study achieved good results by controlling the amount of grafted synthetic polymer on HA to modify its gel properties. The gel properties can significantly change with the molecular weight of the grafted polymer. Thus, finding the proper length for the grafted chain may be the critical issue for gelation and biodegradation *in vivo*. It does, however, not seem to solve the problem of initial burst release.

Another area of research are hydrogels for potential articular cartilage regeneration. In numerous studies [58], thermosensitive hydrogels on the basis of polyoxyethylene-polyoxypropylene block-

copolymers (poloxamers) have been explored as drug delivery systems and some are commercially available (Pluronic®). A chitosan based Pluronic® (CP) hydrogel was designed as an injectable cell delivery carrier for cartilage regeneration. The CP conjugate was synthesized by grafting Pluronic® onto chitosan using EDC/NHS chemistry. The Sol-Gel transition near body temperature and the mechanical properties of the CP hydrogel suggested that this material has potential as an injectable scaffold for cartilage regeneration [59] with possible commercialization.

Jung et al. [57] explored Pluronic® F-127 derivatives and crosslinked HA hydrogels for sustained release of a chondrogenic growth factor. HA is component of the cartilage fluid and therefore could add biocompatibility and effectiveness. The gel was found to be thermoreversible and biodegradable and in fact could potentially have a positive effect on cartilage repair.

In other studies [55, 63, 64], alginate hydrogels were explored. They were shown to be enzymatically degraded in a controlled and tunable fashion by PLGA-MP with incorporated lyase loaded into alginate [64]. Hydrogels with the encapsulated alginate lyase supported proliferation of neural stem cells and thus could provide the potential microenvironment for neural stem cell culture. Currently, there is a small number of injectable hydrogels that have been commercialized and that undergo the early stages of clinical trial [66-68].

Property driven developments of novel hydrogels

In the previous section studies has been discussed in which hydrogels had been developed with a biomedical goal in mind, such as the design of drug delivery vehicles for the cure of a particular disease. An alternative approach, however, could be to primarily focus on the development of hydrogels that have unique properties and then find a suitable application for these materials. It is well known that the exogenous signals on extracellular matrices in physiological environments

play an important role in cell behavior and cell fate. Therefore, the question can be posed of how to design biomimetic hydrogels with bioactive functions, for instance, through ligands, that are able to respond to cell-secreted signals. Such ligands would then enable proteolytic remodeling or initiate the local recruitment of specific cells by tunable specific interactions [64, 65]. A future injectable hydrogels will react to a specific biomedical need through incorporated groups that are capable of clearly identifying this need.

2.4 ARTIFICIAL EXTRACELLULAR MATRIX (ECM)

The extracellular matrix (ECM) is a part of a multiple cell system which provides binding of and support for surrounding cells. Natural ECM is constituted of a crosslinked mesh of proteins (collagen, elastin and fibronectin) and glycosaminoglycans (proteoglycans, heparin sulfate, keratin sulfate, etc.) (Figure 2.3) [69]. The ECM is crucial for cellular behavior, such as proliferation and growth, survival, change of shape, migration and differentiation. In tissue engineering, as the replacement of natural ECM, artificial ECM must be designed to fulfill these requirements: non-toxicity, desirable degradation rate, sufficient mechanical properties, non-inflammatory and availability to nutrients and growth factors [70].

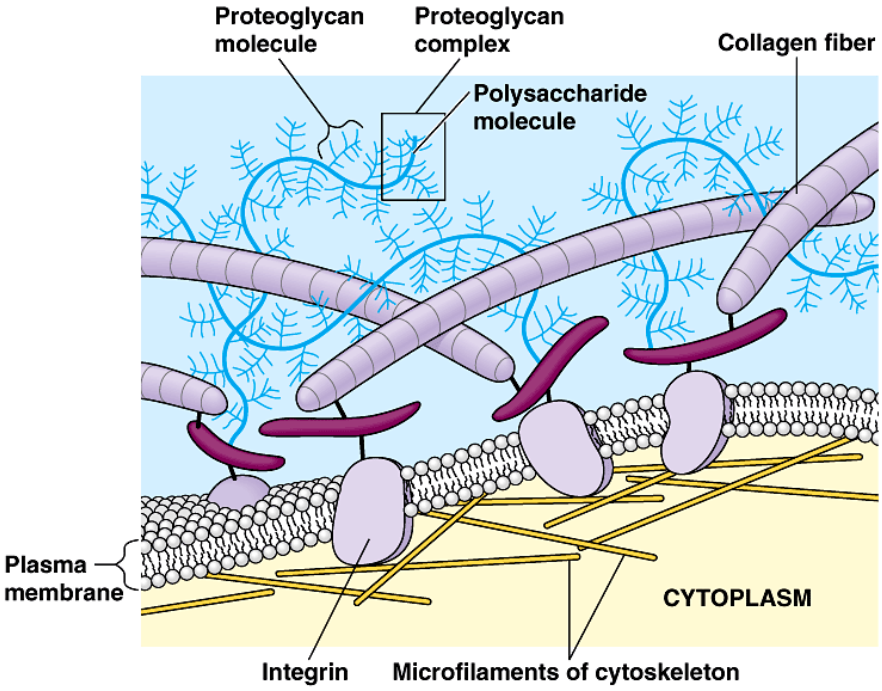

Figure 2.3 Natural ECM structure and components. (Copyright Pearson Education, reproduced with permission)

Artificial ECM can be divided into two categories: naturally derived and synthetic artificial ECM. For naturally derived ECM, selected polymers generally include components of native ECM along with some other polysaccharides and proteins [71]; this type of ECM seems to show superior cell adhesion and more appropriate mimicking of the mechanical properties of tissue. As can be expected, biocompatibility and biodegradability are considerably better for this type than for an ECM derived from synthetic polymers [71]. As synthetic polymers, specially designed homopolymers or copolymers are preferred which are biodegradable and biocompatible. The properties of synthetic polymers are easier to manipulate for differing applications [71], but they may cause severe inflammation when implanted or lack the sites for cell adhesion. Additionally, synthetic polymers may take a relatively long time to degrade in the living body. However, they

are cost-effective alternatives for tissue engineering. A summary of synthetic and naturally derived polymers is presented in Table 2.2.

Table 2.2. Advantages and disadvantages of artificial ECM from natural and synthetic sources ([70] Copyright: Wiley-VCH, reproduced with permission)

Polymers	Biocompatibility	Disadvantages	Biodegradability	Application
Collagen	Minimal cytotoxicity, Mild foreign body reaction, Minimal inflammation	Proteolytic removal of small non helical telopeptites	Bulk, Controllable	Skin; cartilage; bone; ligaments; tendons; vessels; nerves; liver
Hyaluronic acid	Minimal foreign body reaction, No inflammation	Highly viscous solution, Many purification steps after chemical modification	Bulk, 1 h to 1 month	Skin; cartilage; bone; ligaments; nerves; vessels; liver
Alginate	Minimal foreign body reaction, No inflammation	Uncontrollable dissolution of hydrogel	Bulk, 1 day to 3 months	Skin; cartilage; bone; nerves; muscle; pancreas
Chitosan	Minimal foreign body reaction, No inflammation	Uncontrollable deacetylation and molecular weight	Bulk, 3 days to 6 months	Skin; cartilage; bone; nerves; vessels; liver; pancreas
Gelatin	Minimal cytotoxicity, Mild foreign body reaction, Minimal inflammation	Weak mechanical property	Bulk, Controllable	Skin; bone; cartilage; ligaments breast
Fibrin	Minimal cytotoxicity, Mild foreign body reaction, Minimal inflammation	Weak mechanical property	Bulk, Controllable	Skin, bone, cartilage liver, tendons; ligaments; vessels
Silk	Minimal cytotoxicity, Mild foreign body reaction, Minimal inflammation	Inflammation of sericin	Bulk, Controllable	Skin; ligaments; bone; cartilage; vessels; tendons
Poly (lactic acid)	Minimal cytotoxicity, Mild foreign body reaction, Minimal inflammation	Local inflammation, Random chain hydrolysis	Bulk, 24 months	Skin; cartilage; bone ligaments; tendons; vessels; nerves; bladder; liver
Poly (glycolic acid)	Minimal cytotoxicity, Mild foreign body reaction, Minimal inflammation	Local inflammation, Random chain hydrolysis	Bulk, 6–12 months	Skin; cartilage; bone ligaments; tendons; vessels; nerves; bladder; liver

Poly(lacticacid-co-glycolicacid)	Minimal cytotoxicity, Mild foreign body reaction, Minimal inflammation	Local inflammation, Random chain hydrolys	Bulk, 1–6 months	Skin; cartilage; bone ligaments; tendons; vessels; nerves; bladder; liver
Poly (caprolactone)	Minimal cytotoxicity, Mild foreign body reaction, Minimal inflammation	Hydrophobic	Bulk, 3 years	Skin; cartilage; bone; ligaments; tendons vessels; nerves
Poly(propylene fumarate)	Mild inflammation,	Limited mechanical property	Surface erosion, 1months	Bone
Poly (orthoester)s	Minimal foreign body reaction, Minimal inflammation	Weak mechanical property	Bulk several months	Ear; bone; cartilage

Regeneration of tissue may become necessary for a variety of organs with very differing properties, such as liver, cartilage, bone and skin, along with embryo stem cells. Recent research has been focusing on the incorporation of receptor peptides, such as RGD or ASGPR (asialoglycoprotein receptors), to enhance cell adhesion [47, 72]. For liver tissue engineering, chitosan was galactosylated and crosslinked by EDC/NHS, and studied as artificial ECM in a hepatocytes culture. This material showed increased cell adhesion via galactose recognition and ASGPR specific binding with galactose [79]. In recent years, a broad range of glycosylated hydrogels with synthetic polymer (PLGA, PVLA, PET, etc.) backbones have been developed, and a significant improvement in hepatocytes adhesion as well as in albumin excretion was observed. Some of these products showed similarities with collagen modified surfaces [70, 74]. The native ECM components collagen and fibronectin are among the best performing compounds when it comes to hepatocyte tissue engineering. However, the extremely high cost of these proteins limits their application to a few hydrogels or as coating materials [75, 76]. Less expensive natural polymers, such as chitosan, alginate and gelatin derived from collagen, achieved considerably improved performance after grafting with galactose; however with some products (e.g., glycosylated gelatin), the issue of solubility and weak mechanical properties has limited

their application [48, 76]. It has been found that several factors may affect the behavior of hepatocytes, such as distribution and density of the glycosyl grafts, as well as the topology of the created artificial ECM. Ise et al. [77] could show that both an adequate concentration of galactose or lactose along with a well-defined 3-D structure are essential for the successful construction of an artificial ECM [77].

Protein based materials as well as carbohydrate based materials were employed in cartilage tissue engineering in form of hydrogels and/or sponges. The proteins with RGD sequence as receptors, such as collagen and fibronectin, showed specific adhesion to a5b1 integrin [[48, 70, 78]. Collagen (type II), in a sponge shape with proteoglycans (hyaluronic acid or chondroitin sulfate), may form a well-constructed ECM *in vitro* or *in vivo* with chondrocytes, with addition of the transforming growth factor (TGF)-b1 [84]. The chondrocytes differentiation was only found in a 3-D structure and not on a more two-dimensional membrane, which proved that hydrogels or sponges may provide a better environment for tissue culture [79]. In regard to the materials, HA and CS may also proliferate the growth of chondrocytes in a collagen based system. Hyaluronic acid is one of the most important components in cartilage; cell encapsulation and implantation were conducted with chemically modified hyaluronan and a similar morphology as nearby tissue [80]. Furthermore, silk was investigated as a component of artificial ECM. Fibroin, the major component of silk, in conjunction with glycosaminoglycan may achieve comparable cell density in chondrocytes culture [70, 80]. Finally, alginate and chitosan should also be mentioned as candidates for the mimicking of natural glycosaminoglycan with the application in cartilage tissue engineering [70].

The most critical issues in bone tissue engineering are that the scaffolds provide similar mechanical properties to bones and that they disintegrate at a rate that corresponds to the

simultaneous regeneration of cells. Traditionally, metals and ceramics were widely used for their superior mechanical properties, however, these materials have significant disadvantages due to low cell adhesion, mismatched mechanical properties and toxicity [70, 82]. Fibroin and hyaluronic acid, as well as type I collagen might be used in bone tissue engineering with Type I collagen being a major component of natural bone. In order to assemble artificial ECM from collagen, salt leaching and freeze drying were employed [70]. Incorporated with bone morphogenetic protein-2 (BMP-2), fibroin, HA and collagen I provide a favorable biomimetic environment that facilitates growth of new bone from stem/progenitor cells. However, their mechanical properties are poor [83]. Some synthetic polymer composites of collagen/hydroxyapatite and PCL or PLG may better satisfy the criteria of tissue engineering in regard to cell adhesion and improved mechanical properties [84]. It remains a challenge, however, for the artificial ECM to fully regulate the function of cells *in vivo* after implantation. Growth factors as well as physical stimuli add to the picture after implantation. Collagen based composites and polymers with RGD peptide sequences are preferred for the next generation of artificial ECM for bone regeneration [85].

In opposition to bone repair, there are many commercialized artificial ECMs for skin regeneration. Collagen-based Integra®/Apligraf® has been applied for epidermal/dermal replacement. Modified hyaluronic acid (Hyalograft®-3D) as well as fibrin-based products (Bioseed®-S) have been developed for skin repair [86]. The next generation skin tissue engineering is to add more function to engineered skins, in order to better mimic natural skin.

Stem cells may be regulated by artificial ECM in regard to cell behavior, such as cell adhesion, proliferation and differentiation. As it is the case with other types of differentiated cells, the key issues include incorporating factors, creating cell adhesion sites, modulating cells behavior and formation, and providing adequate mechanical properties [70]. Growth factors play an important

role in cells modulation. TGF-b1, FGF-2, BMP and EGF can be incorporated in artificial ECM, and released by diffusion and/or degradation of the artificial ECM. The Gln-Pro-Gln-Gly-Leu-Ala-Lys-NH_2 (QPQGLAK-NH_2) sequence could be introduced into semi-interpenetrate networks for cell adhesion, as well as the RGD sequence [70, 86, 87]. The scale may determine the fate of the cells: macroscale artificial ECM may provide superior mechanical properties but nanoscale enables precise cell behavior control and formation [70, 88].

Reference

1. Friedli, G., Interaction of SWP with bovine serum albumin (BSA).PhD Dissertation, University of Surrey, 1996.
2. Abuchowski, A., Vanes, T., Palczuk, N. C., Davis, F. F., J. Biol. Chem. 1977, 252 (11), 3578-3581.
3. Hoare, T. R., Kohane, D. S. Polymer 2008, 49(8): 1993-2007.
4. Zhang, X. H., Khan, M. M. R., Yamamoto, T., Tsukada, M., Morikawa, H. Intern. J. Biol. Macromol. 2012, *50*, 337-347.
5. Reddy, N., Yang, Y. Biotechn. Progr. 2009, 25, 1796-1802.
6. Paparcone, R., Buehler, M. J. Biomater.2011, 32, 3367-3374.
7. Veronese, F. M., Pasut, G. Drug Discov. Today 2005, 10 (21), 1451-1458.
8. Gayet, J. C., G. Fortier J. Control Release 1996, 38(2-3): 177-184.
9. Gayet, J. C., Fortier, G. J J. Polym. Sci. Pol. Phys. 2001, 39 (24), 3128-3161.

10. Jacksen, J. J. Chromatogr. B. 2010, 878, 1125–1134.

11. Elzoghby, A. O., Samy, W. M, Elgindy, N. A. J. Control Release 2012, 157, 168-182.

12. Naveenraj, S., Anandan, S. J. Photochem. and Photobio. C: Photochemistry Reviews 2013, 1, 1453–1471.

13. Liu, Z., Jiao, Y., Wang, Y., Zhou, C., Zhang, Z., Adv. Drug Deliv. Rev. 2008, 60, 1650–1662.

14. Plesner, B., Fee, C. J., Westh, P., Nielsen, A. D., Eur. J. Pharm. Biopharm. 2011, 79 (2), 399-405.

15. Dror, Y., Ziv, T. Makarov, V., Wolf, H., Admon., A., Zussman E., Biomacromolecules 2008, 9(10), 2749-2754.

16. Kawamura, R., Mishima, M., Ryu. S., Arai, Y., Okose, M., Silberberg, Y. R., Rao, S. R., Nakamura C., Langmuir 2013, 29(21), 6429-6433.

17. Scheibel T. Current Opinion in Biotechnology 2005, 16, 427–433.

18. Woolfson, D., Ryadnov, M. G. Current Opinion in Chemical Biology 2006, 10:559–567.

19. Sill, T. J., von Recum, H.A. Biomaterials 2008 29, 1989-2006.

20. Huemmerich, D., Scheibel, T., Vollrath, F., Cohen, S., Gat, U., Ittah, I. Curr. Biol. 2004, 14, 2070-2074.

21. Tao, H., Kaplan, D. L., Omenetto F. D., Adv. Mater. 2012, 24, 2824–2837.

22. Hu, X., Shmelev, K., Sun, L., Gil, E. S., Park, S. H., Cebe, P., Kaplan, D. L., Biomacromolecules 2011, 12, 1686-1696.

23. Kundu, S. C., Khire, T. S., Kundu, J., Yadavalli, V. K., Soft Matter 2010 , 6 , 2066-2071.

24. Lu, S. Z., Wang, X. Q., Lu, Q., Hu, X., Uppal, N., Omenetto, F. G., Kaplan D. L., Biomacromolecules 2009, 10 , 1032-1042.

25. Meinel, L., Karageorgiou, V., Fajardo, R., Snyder, B., Shinde-Patil, V., Zichner, L., Kaplan, D., Langer, R., Vunjak-Novakovic, G., Ann. Biomed. Eng. 2004, 32, 112-117.

26. Marolt, D., Augst. A., Freed, L. E., Vepari, C., Fajardo, R., Patel, N., Gray, M., Farley, M., Kaplan, D., Vunjak-Novakovic, G., Biomaterials 2006 , 27 , 6138-6149.

27. Jin, H. J., Chen, J. S., Karageorgiou, V., Altman, G. H., Kaplan, D. L. Biomaterials 2004, 25, 1039–1047.

28. Bhumiratana, S., Grayson, W. L., Castaneda, A., Rockwood, D. N., Gil, E. S, Kaplan, D. L., Vunjak-Novakovic, G. Biomaterials 2011, 32, 2812–2820.

29. Sofia, S., McCarthy, M. B., Gronowicz, G., Kaplan, D. L. J. Biomed. Mater. Res. 2001, 54, 139–148.

30. Vauthey, S., Santoso, S., Gong, H., Watson, N., Zhang, S. Proc. Natl. Acad. Sci. USA 2002, 99, 5355-5360.

31. Shao, Z, Vollrath, F., Nature 2002, 418, 741-741.

32. Scheibel, T., Microb. Cell Fact 2004, 3, 14.

33. Huemmerich, D., Helsen, C. W., Quedzuweit, S., Oschmann, J., Rudolph, R., Scheibel, T. Biochemistry 2004, 43, 13604-13612.

34. Boyer R. A. Ind. Eng. Chem. 1940, 32, 1549-1553.

35. Morimoto S. Encyclopedia of Polymer Science and Engineering Supplement II, H. F. Mark, and N. M. Bikales, Eds., Wiley, New York, 1977, p. 159.

36. Reddy, N., Yang, Y. Biotechnology progress, 2009, 25(6), 1796-1802.

37. Thirugnanaselvam, M., Gobi, N., Arun Karthick, S., Fibers and Polymers 2013, 14, (6), 965-969

38. Deng, S., Cheng, J., Guo, X., Jiang, L., Zhang, J. J Polym. Environ. 2014, 22, 17–26.

39. Biehn, G. F.; Cline, E. T. U.S. Pat. 1947, 2,429,214.

40. Shukla, R.; Cheryan, M. Ind. Crops. Prod. 2001, 13, 171-192.

41. Jiang, Q., Yang, Y., J. Biomat. Sci. 2011, 22, 1393–1408.

42. Wang, Y., Chen, L., ACS Appl. Mater. Interfaces 2014, 6, 1709−1718.

43. Whittier, E.O., Gould, S.P., Industrial & Engineering Chemistry 1940, 32(7), 906-907.

44. Traill, D., J. Soci. Dyers Col. 1951, 67(7), 257–270.

45. Yang, Y., Reddy, N., Int. J. Bio. Macrom. 2012, 51, 37– 44.

46. Sudha, T. B., Thanikaivelan, P., Ashokkumar, M., Chandrasekaran, B., Appl. Biochem. Biotechnol. 2011, 163, 247–257.

47. Zheng, W. F., Zhang, W., Jiang, X. Y. Adv. Eng. Mater. 2010, 12: B, 451–B466.

48. Dong, B., Arnoult, O., Smith M. E., Wnek, G. E., Macromol. Rapid Commun. 2009; 30, 539–542.

49. Jiang, Q., Reddy, N., Zhang, S., Roscioli, N. Yang, Y. J. Biomed. Mat. Res. A 2013, 101a(5), 1237–1247.

50. Zhang, M., Liu, Y.,Yi, H., Luan, J., Zhang, Y., Cai, H. Sun, D., The Journal of The Textile Institute, 2014, 105(3), 246-255.

51. de Oliveira Mori C.L.S. et al. Industrial Crops and Products 2014, 52, 298–304.

52. Yao, C., Li, X., Song, T., Li, Y., Pu, Y., Polym Int 2009; 58: 396–402.

53. http://www.cnn.com/2012/07/05/world/europe/qmilch-milk-sustainable-fashion/index.html

54. Overstreet, D. J. J. Polym. Sci. B: Polymer physics, 2012, 50, 881–903.

55. Li, Y. Rodriguesa, J., Tomás H. Chem. Soc. Rev., 2012, 41, 2193-2221.

56. Kim, S., Nishimoto, S. K., Bumgardner, J. D., Haggard, W. O., Gaber, M. W., Yang Y. Biomaterials 2010, 31, 4157-4166.

57. Jung, H. H., Park K., Han, D. K. J. Control Release 2010, 147, 84-91.

58. Escobar-Chávez, J. J. López-Cervantes, M. Naïk, A. Kalia, Y. N. Quintanar-Guerrero, D. Ganem-Quintanar, A. J. Pharm. Pharmaceut. Sci. 2006, 9(3), 339-358.

59. Yu, L., Zhang, Z., Zhang, H., and Ding, J. Biomacromolecules, 2010, 11, 2169-2178.

60. Tan, H., Chu, C. R., Marra, K. G. Biomaterials, 2009, 30, 2499-2506.

61. Van Vlierberghe, S., Dubruel, P. Schacht, E. Biomacromolecules, 2011, 12, 1387-1408.

62. Strehin, I. Nahas, Z. Arora, K., Nguyen, T., Elisseeff, J. Biomaterials, 2010, 31, 2788-2797.

63. Ta, H. T.. Dass, C. R., Larson, I. Choong, F.M., Dunstan, D. E. Biomaterials, 2009, 30, 3605-3613.

64. Jin, R. Teixeira, L. S. Dijkstra, P. J., Karperien, M. Van Blitterswijk, C. A. Zhong, Z. Y. Feijen, J. Biomaterials, 2009, 30, 2544-2551.

65. Kim, J., Kim, I. S., Cho, T. H., Lee, K. B., Hwang, S. J., Tae, G. Noh, I. Lee, S. H., Park, Y. Sun, K. Biomaterials, 2007, 28, 1830-1837.

66. Collin, E. C., Grad, S., Zeugolis, D. I., Vinatier, C. S., Clouet, J. R., Guicheux, J. J. Weiss, P., Alini, M., Pandit, A. S. Biomaterials, 2011, 32, 2862-2870.

67. Pek, Y. S., Kurisawa, M., Gao, S., Chung, J. E. Ying, J. Y. Biomaterials, 2009, 30, 822-828.

68. Zhao, L., Weir, M. D., Xu, H. K. Biomaterials, 2010, 31, 6502-6510.

69. Rosso F, Giordano A, Barbarisi M, Barbarisi A. J Cell Physiol. 2004; 199: 174–180.

70. Kim, B.-S. et al. Progress in Polymer Science 36 (2011) 238–268.

71. Rosso, F., Marino, G., Giordano, A., Barbarisi, M., Parmeggiani, D., Barbarisi, A. J. Cell. Physiol. 2005, 203, 465–470.

72. Wall, D. A., Wilson, G., Hubbard, A. L., Cell 1980, 21, 79–93.

73. Park, I. K., Yang, J., Jeong, H. J., Bom, H. S., Harada, I., Akaike, T., Kim, S. I., Cho, C. S., Biomaterials 2003, 24, 2331–2337.

74. Bhadriraju, K., Hansen, L. K. Biomaterials 2000, 21, 267–272.

75. Sosnik, A., Sefton, M. V. Biomaterials 2005, 26, 7425–7435.

76. Zhao, Y., Xu, Y., Zhang, B., Wu, X., Xu, F., Liang, W., Du, X., Li, R. Tissue Eng. C Methods 2010, 16, 653–659.

77. Ise, H., Sugihara, N., Negishi, N., Nikaido, T., Akaike, T. Biochem Biophys Res Commun 2001, 285, 172–182.

78. Silver, F. H., Freeman, J. W., Seehra. G. P. J. Biomech. 2003, 36, 1529–1553.

79. Awad, H. A., Wickham, M. Q., Leddy, H. A., Gimble, J. M., Guilak, F.. Biomaterials 2004, 25, 3211–3222.

80. Wu, C. H., Ko, C. S., Huang, J. W., Huang, H. J., Chu, I. M. J Mater. Sci. Mater. Med. 2010, 21, 725–729.

81. Diduch, D. R., Jordan, L. C., Mierisch, C. M., Balian, G. Arthroscopy 2000, 16, 571–577.

82. Hulbert, S. F., Young, F. A., Mathews, R. S., Klawitter, J. J., Talbert, C. D., Stelling, F. H. J Biomed. Mater. Res. 1970, 4: 433–456.

83. Kim, J., Kim, I. S., Cho, T. H., Lee, K. B., Hwang, S. J., Tae, G., Noh, I., Lee, S. H., Park, Y., Sun, K. Biomaterials 2007, 28, 1830–1837.

84. Hu, Y., Winn, S. R., Krajbich, I., Hollinger, J. O. J, Biomed. Mater. Res. A 2003, 64, 583–590.

85. Glowacki, J., Mizuno, S. Collagen scaffolds for tissue engineering. Biopolymers 2008, 89, 338–344.

86. Dainiak, M. B., Allan, I. U., Savina, I. N., Cornelio, L., James, E.S., James, S. L., Mikhalovsky, S. V., Jungvid, H., Galaev, I. Y. Biomaterials 2010, 31, 67–76.

87. Kim, S., Healy, K. E., Biomacromolecules 2003, 4, 1214–1223.

88. Oh, S., Brammer, K. S., Li, Y. S., Teng, D., Engler, A. J., Chien, S., Jin, S. Proc. Natl. Acad. Sci. USA 2009, 106, 2130–2135.

CHAPTER 3 BSA FIBERS PREPARED BY DEHYDRATION INTRODUCED AGGREGATION

3.1 INTRODUCTION

The dehydration of mammalian cells in culture results in the formation of structures similar in morphology to amyloidal fibrils.[1,2] Amyloidal fibrils have been known to exist in the human body for decades.[3] They are produced from diverse proteins including Aβ amyloid precursor protein, apolipoprotein A_1, β_2-microglobulin, transthyretin, lysozyme, huntingtin, insulin, calcitonin, asynuclein, prolactin, immunoglobulin light chain, serum amyloid prion, islet amyloid polypeptide, and albumin.[4,5] The ubiquity of the cellular dehydration response in forming fibrous structures was demonstrated in many cell types[2], yet the mechanisms responsible for cellular transformation into fibrillar morphology have not been elucidated. It has been observed that the dehydrated solution of albumin or serum results in the formation of a very similar fibril morphology.[1,2]

The study of amyloidal fibril formation in a single protein solution *in vitro* revealed that many proteins are capable of forming fibrils under specific conditions regardless of their primary sequence.[6] Typically, mature fibrils consist of two to six unbranched protofilaments 2-5 nm in diameter that are associated laterally or twisted together to form larger fibrils with a diameter of 4-13 nm and a characteristic twisted, rope-like appearance.[7] Amyloids in which the β-strands are arranged perpendicular to the fibril axis contain an extended cross-β sheet central core that can be detected using X-ray diffraction.[8-10]

Many proteins have been found to form fibrils *in vitro*, indicating that the tendency to fibrillate is a generic property of the polypeptide chain.[4] The pathways leading to fibril formation, however,

have yet to be fully understood.[11,12] The protein aggregates are thought to arise from interactions that normally occur intramolecularly, but in this case arise in an intermolecular fashion.[13,14] The *in vitro* conditions necessary to induce fibril formation are mediated through accelerating the aggregation of unstable protein conformations, typically at low pH (2.5), high temperature (65°C), high salt content (50 mM NaCl), and/or with protein concentrations of less than 10 mg/mL.[7,8] These conditions are quite different from physiological conditions in blood and tissue environments (i.e., pH 7.4, 37°C, μM divalent anionic salts, more than 100 mg/mL proteins).

In addition to their medical relevance, these aggregated protein fibers have potential industrial applications. For example, products made from protein fibrils are emerging as a novel class of functional bionanomaterials;[15,16] however, scaling up their synthesis from nano- to macroscale to create useful macroscopic materials remains a challenge.[17] Protein fibers from non-traditional sources for textile use or incorporation in fibrous composites have been mentioned in the literature, for instance, fibers made from milk were reported as early as 1938.[18] Yang and Reddy investigated casein fibers regenerated from alkaline solution and cross-linked with citric acid for reduced water-solubility and reasonable mechanical strength.[19] Fibers have also been made from sericin, the adhesive of silk filaments.[20,21,22] Although water-soluble, sericin can be cross-linked with formaldehyde for reduced solubility and used by itself, in composites with other polymers, or electrospun into nanofibrous biomaterials. Fibers made from the corn protein zein were sold as textile fibers (Vicara®) in the 1960s[23] and have different potential applications.[24] Milk fibers as well as soy protein fibers have been commercialized, primarily by Asian companies.[25]

Dehydration-induced protein fibril formation is thought to result from water evaporation and induced conformational changes in protein structure. It could therefore be considered an example of dynamic self-assembly.[26] In this research, aggregation induced by dehydration of bovine

serum albumin (BSA) was investigated to identify the environmental factors governing protein aggregate (i.e., fiber) formation, including the effect of ion types and concentration, pH, protein concentration, and the chemical composition of the solution with the goal of producing novel fibers with sufficient mechanical strength and elasticity for a variety of applications. A small-scale feasibility study was performed to determine whether these BSA fibers could be made into larger assemblies, such as yarns, and dyed with acid dyes similar to traditional protein fibers, such as silk and wool, for a variety of commercial applications.

3.2 EXPERIMENTAL

Materials

Bovine serum albumin (BSA, Probumin®, Life Science Grade) was purchased from Millipore Corporation (Kankakee, Illinois). Dithiothreitol (DTT) was obtained from Sigma and EDC (1-ethyl-3-[3-dimethylaminopropyl] carbodiimide) from Thermo Scientific. All other chemicals (formaldehyde, glutaraldehyde, salts, solvents, etc.) were purchased from VWR and were of the highest purity available.

Production of BSA Fibers

Gram quantity BSA fiber production used 200 mL solution (BSA, 10 mg/mL, 10 mM Na_2SO_4, 45 mM DTT, in Millipore water adjusted to a pH of 4.7 with HCl). The protein solution was filtered and air bubbles were removed. The protein solution was poured onto a 44 cm x 72 cm glass surface; the desired geometry was held by surface tension. The angle of the glass plate was set by adjusting the tilting to front-high and back-low positions with no dislocation of water on the plate. The protein plate was housed in a controlled dehydration environment (Figure 3.1)

where air temperature and humidity were held at 30°C and less than 30%, respectively. Air flow was regulated by a 3-speed WindTunnel (Power Fan, Lasko), air temperature was adjusted by an oscillate air heater (Model 5307, Lasko), and air purity was controlled by filtering the air through a microbial-free Filtrete (Ultra Allergen Air Filter – 1250, 3M). Fibril formation was achieved by pulling air over the protein solution in a near constant laminar flow. The edge of the solution was roughened with the tip of a pipette at the beginning to enhance the nucleation that started fiber growth; dehydration and fibrillation were complete in 7 h.

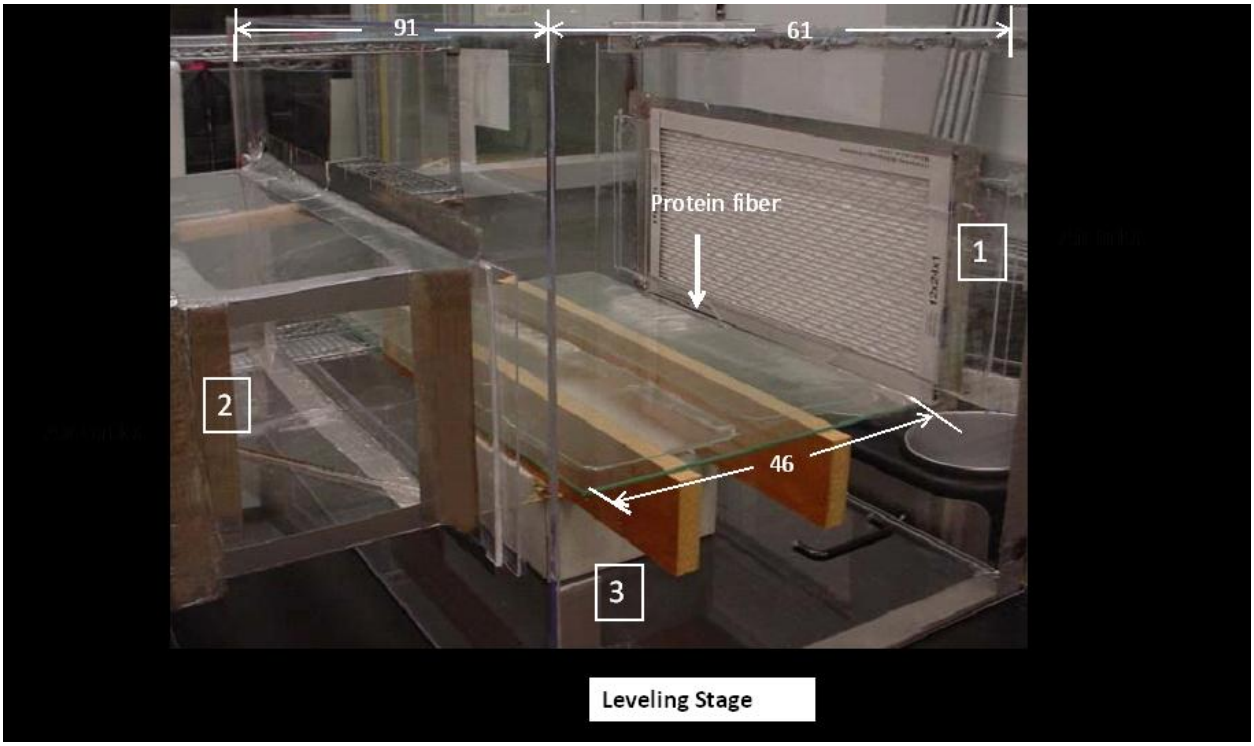

FIGURE 3.1. Dehydration box – side view, with (1) air inlet unit: control of air temperature, humidity and angle of the air-water interface, (2) air outlet unit: control of air flow rate by moving air with a fan at three sets of speed, (3) stage leveling unit: control of the angle of the plate: slight tilt (1^{o}) of plate allows less water in the drying front and more in the back to facilitate fiber elongation. Protein fibers are formed on the surface of a glass plate (arrow). Dimensions in cm.

Cross-linking of Protein β-Sheets by Aldehydes

The glass plate carrying the dried protein sheet was exposed to a 0.1% formaldehyde vapor in methanol overnight at room temperature in a closed environment. The fibers were then released from the glass plate by sonication in acetonitrile for 2 min, or simply scrapped off with a razor blade. Selected batches were additionally cross-linked with 0.1% aqueous glutaraldehyde solution at pH 4 at room temperature overnight. The fibers were repeatedly rinsed with methanol and air-dried. Alternatively, EDC cross-linking was performed by dissolving 1 g EDC in 100 mL methanol/water (90:10) and adding 10 uL of 4N HCl. The BSA fibers were immersed in the solution at room temperature overnight, rinsed with methanol several times and air-dried.

CR Binding

Congo Red (Acros Organics, Geel, Belgium) that binds specifically to protein β–sheets was used to measure the BSA fibril concentration in an ultraviolet-visible (UV-Vis) spectrophotometer (DU series 640; Beckman Coulter Fullerton, CA). All measurements were made in the wavelength range of 200-700 nm in matched quartz cuvettes. Changes in the absorption spectra of CR before and after fibril formation in a solution of 15 μM of both BSA and CR in 10 mM Na_2SO_4 were recorded. The average of results from three experiments was used.

Circular Dichroism

Far- and near-ultraviolet (UV) circular dichroism (CD) spectra were obtained using a JASCO-810 automatic recording spectropolarimeter (Jasco, Tokyo, Japan). Quartz cuvettes with 0.2 cm path length were used. CD spectra were obtained from aliquots taken from protein solutions at

indicated conditions and recorded between 180 and 300 nm at 25°C. The molar ellipticity θ (deg cm^2 $dmol^{-1}$) was calculated from the formula: $\theta = 100\ \theta_{obs}/rlc$, where θ_{obs} is the observed ellipticity in deg, r is the amino acid residue number of the protein, l is the optical path length in cm, and c is the protein concentration in mM. Protein solutions were tested before fibril formation, after mixing with salts, and after being reconstituted after fibril formation. Controls included all compounds except protein for the background CD spectra. The average of eight spectra was used for all data acquisitions.

Structural Analysis with FT-IR Spectroscopy

Fibrils were manually crushed into powder, mixed with pulverized potassium bromide (99% spectroscopy IR grade), and formed into a solid pellet. The pellet was analyzed in absorbance mode on a FTIR (IR Prestige-21, Shimadzu) in the range of 4,000 to 500 cm^{-1}.

Fiber Morphology

The microscopic methods used to investigate the morphology of the fibers were scanning electron microscopy (SEM, Zeiss EVO 50) at 20 kV on gold sputter-coated samples and light microscopy as previously described.[1,2]

Evaluation of Mechanical Properties

The mechanical properties of single fibers were tested with a Dynamics Mechanical Analyzer (RSA3, TA Instrument) measuring tensile strength.[28] Ten individual fibers were measured from each group, and their mechanical strength compared with single cotton fibers (Alabama Yarn Company) and silk fibers (experimental sample, Indonesia). Measurements were taken at room

temperature (22°C) with 10 mm gauge length at 0.2 mm/min tensile speed. Calculation of strength and stress used the ribbon model (cuboids).[28] Young's Modulus was determined by using the stress at 1% strain. Width and thickness were measured by using an optical microscope. The average of three measurements is represented as dimension of individual fiber.

Dyeing of BSA Fibers with Acid Dyes

Formaldehyde cross-linked fibers were dyed with four different Acid Dyes, including C. I. Acid Red 182, C. I. Acid Orange 7, C. I. Acid Violet 12 and C. I. Acid Blue 25. For each dyeing, 0.5 g fibers were immersed in 100 mL aqueous dye bath containing 0.02% (w/w) dye, 0.25% (w/w) Na_2SO_4 at pH 3 and a temperature of 50℃ for 1 h. The fibers were rinsed in 50℃ water and air-dried.

Yarn Formation

Two sets of experimental yarn were made based on 0.2 g and 0.5 g BSA fibers using first an opening machine (Zellweger Uster Rotorring 580) at a rotor speed of 3000 rpm in order to orient the fibers in parallel position. Fibers of 0.2 g were twisted at 9 TPI (twists per inch (2.54 cm)) and fibers of 0.5 g were twisted at 11 TPI. The opened fibers of 25.4 cm length were tested on a twist tester (United States Test CO. INC.) with caliper of 5.08 cm. The twist test was conducted according to the ASTM D1422 standard.

3.3 RESULTS AND DISCUSSION

Production of BSA Fibers

White and soft fiber material was prepared by BSA aggregation (Figs. 2a and b). Individual fibers had an average length of 35 cm and a diameter of 10-20 μm, which amounts to several orders of magnitude larger than typical amyloid fibrils.[29] The formation and quality of the BSA fibrils depended on each component in the solution mixture. Growth of fibrils occurred immediately when the liquid was drying with expanding tips pointing toward the retreating water front. This is consistent with the concept that protein aggregation must occur on the liquid side of the interface for proteins to be sufficiently mobile to stack onto the nascent growing tip. The growth appeared as an organized event (Figure 3.2c). Molecules assembled into fibrils are hypothesized to be in a dynamic equilibrium with a pool of soluble monomers surrounding the growing tip. Fibrils extended from the nascent fine tip while simultaneously widening the maturing fibril by monomer incorporation within β-sheet aggregates. The diameter of a fibril was determined by the local dehydration rate. Slower drying allowed more time for monomers to be incorporated and resulted in fibers with larger diameters. It could be assumed that an equilibrium between globular and aggregated species developed in the evaporating solution that determined the width of each region when dried (Figure 3.2d).

Dehydration of a protein solution removes water molecules required for maintaining protein conformation, resulting in the exposure of internal hydrophobic residues and increased intermolecular interactions. A delicate balance between folded and extended protein conformations is rapidly altered when water evaporation triggers a cascade of events in protein folding that favors an unfolded conformation and results in an ordered aggregation of proteins in cross β–sheets. Inter- and intra-molecular interactions that maintain a protein in its native conformation are replaced by the intermolecular interactions that aggregate monomers into polymers in response to environmental factors.[14,30] In the case of the air-liquid interphase,

proteins extend into β-pleated sheets through intermolecular hydrogen bonds in which neighboring polypeptide chains run in the same direction, forming a parallel β-pleated sheet. As the volume of the protein solution decreases, there is a change from a folded protein conformation to an aggregated protein conformation as a consequence of the different amount of residual water each conformation retains. It was reported that a dehydrated β-sheet structure was found in yeast amyloid-forming peptides with a reduced size.[31] The intermediate state of a partially folded amyloid protein was thought to have a larger volume than its native conformation.[32]

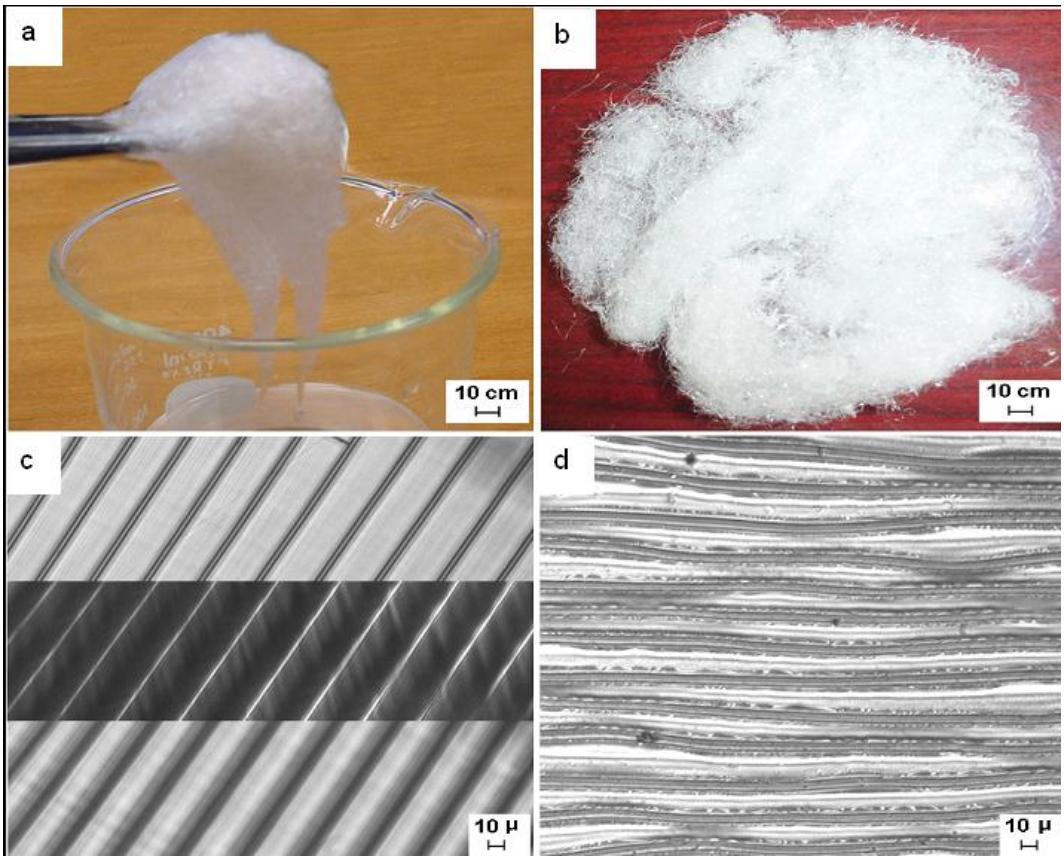

FIGURE 3.2. (a) BSA fibers harvested from glass plate after rinsing in acetonitrile solution; (b) Dried BSA fibers (amount shown is 1 g); c) optical microscopic images (magnification 40) of longitudinal fibers superimposed on the same field with different focal points; top field: b-sheet

aggregates (average width of b-sheet 9 mm), bottom field: globular form (average width 15 mm); (d) optical microscopic side view of b-sheet region with globular regions between b-sheets.

Regions of growth can be observed to drift where the “aggregation regions” along the length of the fibril appear more condensed than the neighboring “globular region” of albumins still in the native conformation (Figure 3.2d). High resolution SEM images of individual fibers revealed that fibers broke off of the large sheet in the middle of an aggregation region (Figure 3.3a) and that each fiber contained two aggregation edges along the fiber axis that have a denser texture than the globular region in the middle (Figure 3.3b). After cross-linking with aldehyde or EDC, these structures were no longer soluble in aqueous solution.

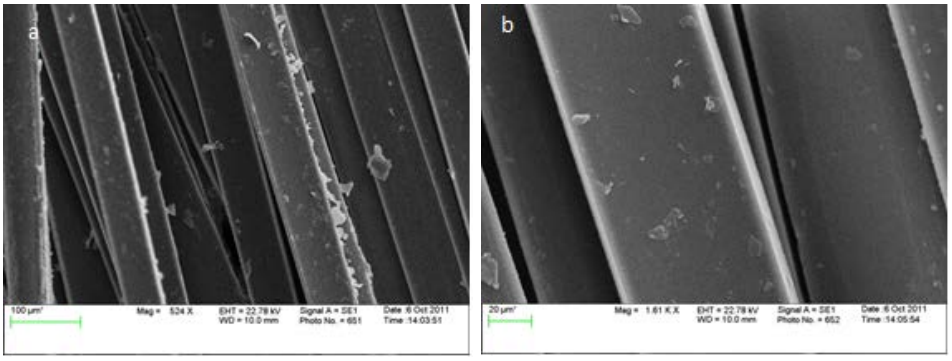

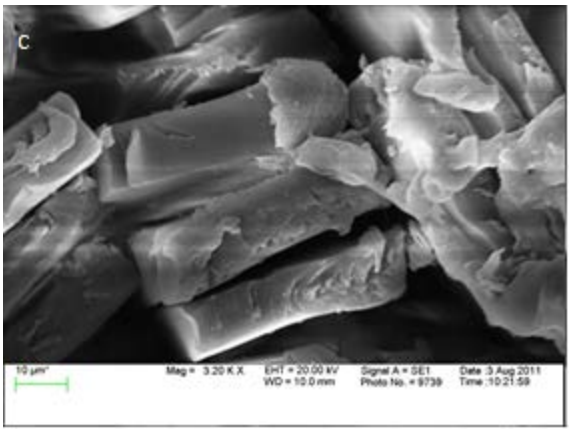

FIGURE 3.3 (a) SEM micrograph of a fibril sheet with aggregated and globular regions; (b) High-resolution SEM image of fibers with globular form in the center and β-sheet regions at both outer edges. (c) SEM images of fibers cross section.

Straight fibrils initially formed at a slow speed, and then the rate increased considerably. The rate of fiber growth, which equaled the rate of drying, was estimated at 1.2 mm/min on average, and was 10^8 faster than that observed for amyloid formation *in vitro* when induced with low pH and high temperature.[7] The rate-limiting step in the protein conformational change seems to be dependent on solvent availability;[30] however, the rate of fibril growth was directly related to the rate of drying, which in turn is affected by air humidity, air flow (speed and volume), temperature, protein and salt concentrations.

Without cross-linking the fibers dissolved in water or 50% methanol but could be reformed when the water was removed with an identical structure and position which indicates that aggregation and fibril formation is a non-covalent and reversible process dependent on water availability. The cycle of fibril formation and dissolution that occurred with dehydration and rehydration was interrupted by adjusting the solution to an acidic pH (< 3), or by removing water from newly formed fibrils with acetonitrile. The type of supporting surface, either a hydrophilic

glass surface or a hydrophobic polyvinyl plastic surface, did not affect fibril growth. Only the rate of fibril formation was slightly higher when a hydrophobic surface was used.

When serum had been dialyzed with a 12 KD membrane, it lost the ability to produce fibrils. However, the addition of a divalent salt (e.g., 10 mM Na_2SO_4) restored its capacity for fibril formation, and star-shaped fibrillar morphology similar to that previously reported for dehydrated "straw" cells[1] was observed. The impact of salt addition on fiber formation from protein solutions was therefore investigated further.

It was found that di- and trivalent anions were essential in promoting fibril formation from a pure BSA solution while monovalent anions or cations were not capable of inducing fibril genesis. Of these salts, Na_2SO_4 proved to be the most effective for fibril formation (in terms of fibril quantity) at a concentration of 10 mM, followed by Na_2HPO_4/NaH_2PO_4, $NaHCO_3$ and finally KIO_3(100:15:2:1). At higher salt concentrations (50-100 mM), $Na_2SO_4$and Na_2HPO_4/NaH_2PO_4 became equally effective, while the other salts still resulted in less fiber formation. Ammonium sulfate, commonly used for salting out during protein purification, was not as effective as Na_2SO_4 for BSA fibril formation. Based on other studies,[33,34] Na_2SO_4 increases solvent surface tension and decreases the solubility of protein molecules (salting out), resulting in strengthened hydrophobic interactions.

The mechanism of the Hofmeister series[35] in salting out protein is not entirely clear, as multiple interactions may play a role in initiating BSA fibril growth during dehydration. Sulfate ions bind to protein at low concentrations and change the overall ionic interaction at high concentrations.[36] As water evaporates, the concentration of sulfate ions increases, the repulsive forces turn into attractive forces and the hydrophobic interactions become dominant. Although NH_4^+ is a larger ion than Na^+ in salting out protein, NH_4^+ was not as effective as Na^+ in initiating dehydration-

induced fibril growth, which suggests that the mechanism is influenced by various complex factors.

Fibril formation in BSA solutions not only depends on the proton concentration but also on the pH value of the solution. In tissue, the physiological pH is effectively buffered at around 7.4, which corresponds to a low rate of fibril formation of a protein solution *in vitro*. Under slightly acidic conditions, fibrils were produced with a texture and morphology somewhat different from those at basic pH. A further increase in acidity to pH<3.5 resulted in complete inhibition of fibril formation and finally caused the protein to denature. At basic pH (>8) BSA solutions produced dramatically more, but less mechanically stable, fibrils with a peak of fibril formation observed at pH 9.0. Although a high pH value increased the solubility for most compounds, the effect could be interpreted as base-catalyzed fibril formation. Hydrogen bonds stabilize alpha in the stabilization of α-helical structures; however, these protons would preferentially stabilize globular conformation over extended cross β-sheets.

At the isoelectric point of BSA (pH 4.7), the anionic repulsion force between neighboring fibrils is lessened. At this pH, the fibril density was effectively increased, the individual fibril diameter reduced, and the conversion rate and yield were clearly enhanced. Addition of 45 mM DTT increased the fibril density further and shortened the distance between neighboring fibrils, thus further increasing the conversion rate and yield. DTT functions by chemically reducing BSA disulfide bonds formed from 36 cysteine residues to create a more open and linear structure, easing β-sheet formation with tight packaging into fibrils. Fibers formed at the isoelectric point showed the best mechanical properties and were studied more in detail.

Additional important factors affecting fiber formation included air flow rate and temperature during dehydration. It was found that a high constant air flow was required in order to produce

long and dense fibrils. Slowing the air flow resulted in more amorphous aggregates with less density and more random orientation. Slow air flow also required a longer time (typically overnight) to dry a layer of protein solution at a 3 mm depth.

The optimum temperature for fibril growth was determined to be 30°C. Maintaining this temperature was important since water evaporation cooled the solution and also impacted protein aggregation in fiber formation. With all conditions and steps optimized, the final yield was at 80% (fiber weight/initial BSA weight).

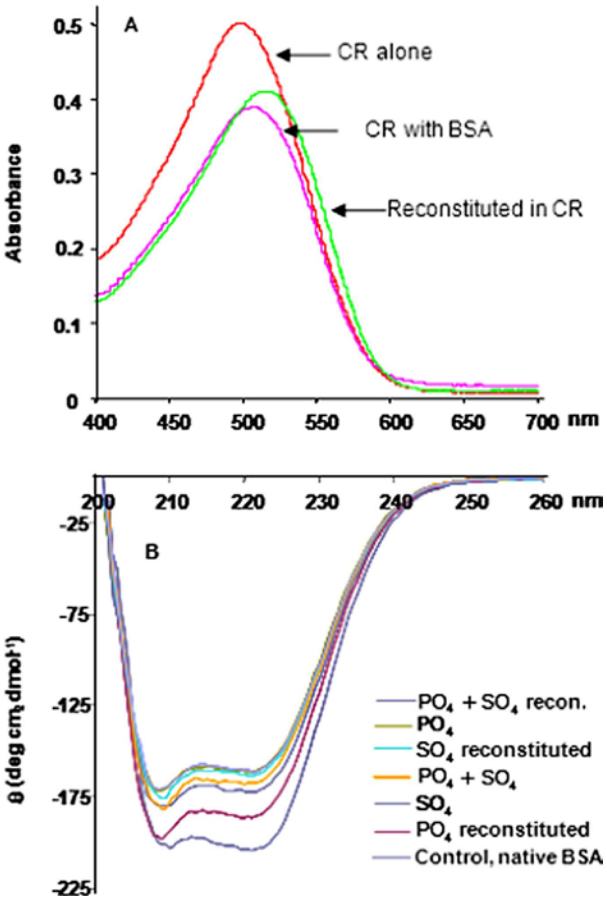

Figure 3.4 (a) BSA-derived fibers showing red-shifted Congo Red absorption spectra (concentration 15 mM); (b) CD-spectra of BSA solutions before and after fiber formation and subsequent reformation.

Confirmation of beta-sheet structure in BSA fiber

Data collected from FT-IR spectroscopy of fibrils showed a peak at 1633.41 cm^{-1} indicating β-sheet structure. The peak for anti-parallel β-sheet (between1675–1695 cm^{-1}) was absent, suggesting that the strands within a β-sheet were parallel.[31]

Congo Red (CR) absorption can show the β-sheet structure of a protein.[37] BSA fibrils stained with CR had an absorption shift to longer wavelengths (data not shown), confirming the presence of proteins with a β-sheet conformation when aggregated from solution. The comparison of reconstituted BSA fibrils stained with CR (15 μM) with pure CR as the control indicated that fibrils prior to their disintegration were bound to CR causing the observed shift in the spectrum.

XRD diffraction of fibrils consisting roughly of aggregated (2/3) and globular BSA (1/3), and of fibrils in which the globular portion had been removed, showed two diffraction peaks at 3.6 and 3.2 Å corresponding to side chain amides facing the internal cavity and the repeat of amino acids in a parallel β-sheet.[9] The strand orientation for the stacked sheets was found to be perpendicular to the fiber axis. The meridional diffraction peaks appeared at 4.7 Å. The equatorial diffraction peaks at approximately 10 Å correspond to inter-strand separation in a β-sheet and inter-sheet separation, respectively. These peaks were absent after dehydration-induced fibril formation which could have been the consequence of water removal.

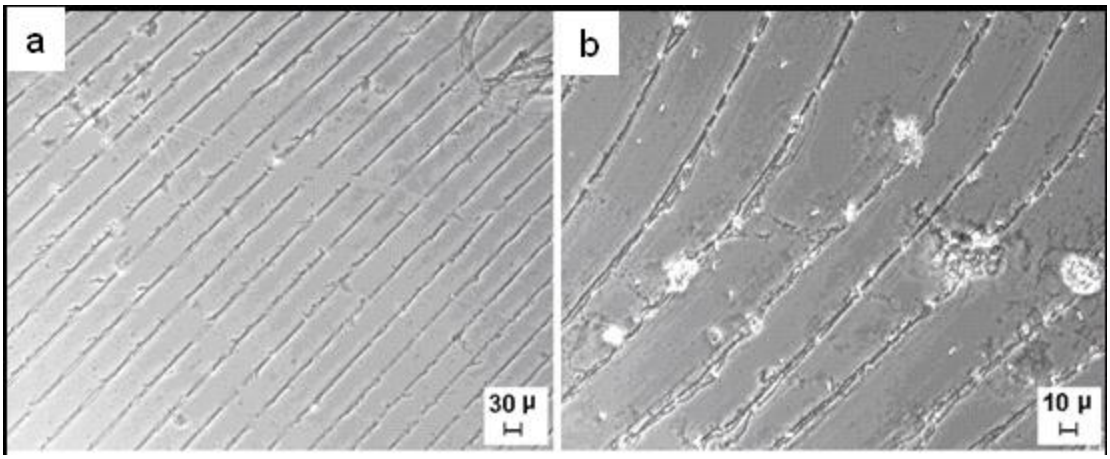

FIGURE 3.5 Light microscopic image of a BSA aggregates after removal of the globular regions by briefly washing in 65°C water (a) magnification x 10; (b) magnification x 20.

The macroscopic β-strand aggregation resulting in fiber formation is hypothesized to be arranged perpendicularly to the fibril axis in a twisted pattern, with layers of monomers stacking onto each other, their hydrophobic residues facing outside at the air-solid interface.[38] This outward exposure of hydrophobic residues gives these fibers a smooth touch to human skin, while hydrophilic residues face inside. The hollow space in the middle of the fiber is available for holding or transporting water when rehydrated.

Fibers Made of Pure Cross β-sheet Regions

Before formaldehyde cross-linking, fibrils could be dissolved in aqueous solution and reformed upon dehydration. CD-spectra and far-UV spectrometry supported the reversible transition (data not shown). Since CR-derived fluorescence intensity is a measure of fibril concentration, the observation of CR intensity before and after hydration suggests that most fibrils were in the form of globules in solution after rehydration (Figure 3.4). The formation of fibrils through assembly of protein β–sheets was reversible up to 65°C, beyond which cross β–sheets are no longer

soluble indicating an irreversible free-energy barrier in the protein folding pathway that exists once proteins are sufficiently heat-denatured.

Aggregated regions could be separated from globular regions based on solubility differences in hot water. When dried BSA was briefly immersed in water of 65°C, the aggregated structure was preserved (Figure 3.5a and b) while globular albumins completely dissolved. Granules of sizes less than 1 μm could be identified in cross β-sheets. The diameter of aggregated regions varied. Pure cross β-sheet regions took the shape of either a flat ribbon or a more tubular form, indicating that variations in protein aggregation existed. The yield of these fibers however was rather small and the fibers too short and too brittle for any practical application.

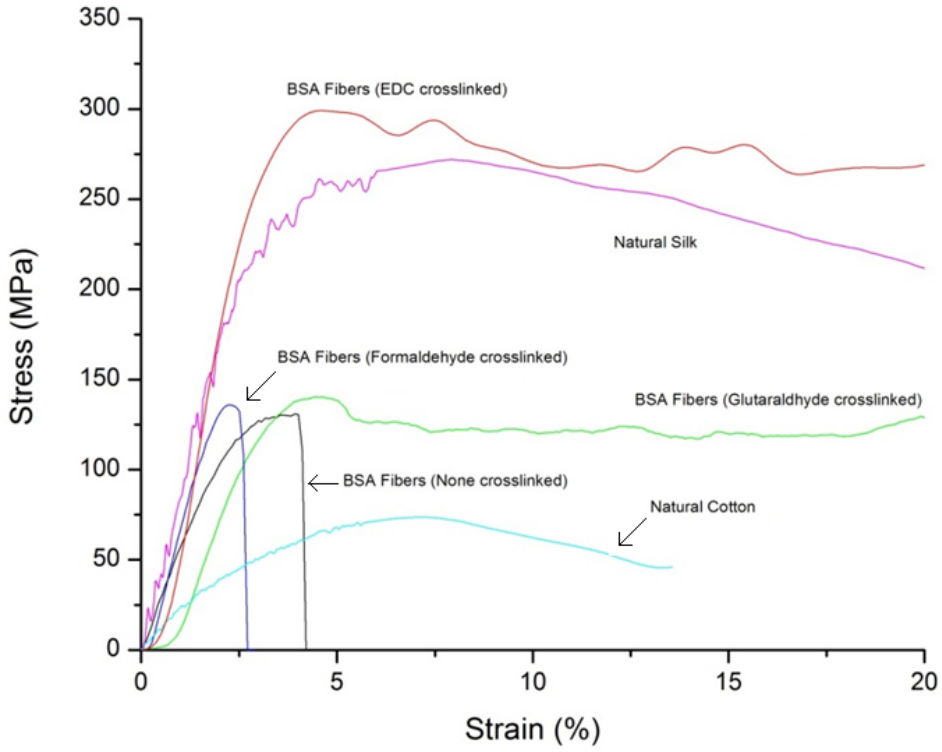

Figure 3.6 Representative stress-strain plot of crosslinked BSA fibers, cotton and silk.

Mechanical Properties of BSA Fibers

The mechanical properties of BSA single fibers were tested with a Dynamical Mechanical Analyzer (DMA) and were compared to those of single fibers of cotton and silk (Table 2). As mentioned above, fibers were clearly higher in strength and much stiffer with comparable elongation if produced at the isoelectric point of BSA (pH 4.7). A second crosslinking with glutaraldehyde further increased the yield strength by approximately 12% at almost unchanged Young's modulus. The failure strain of the fibers, however, dramatically increased to over 30%. If EDC was used as the second crosslinking agent instead of glutaraldehyde, the fiber Young's modulus could be improved by a factor of 160%, compared to untreated BSA fibers. Unfortunately, the yield strength of different fibers strongly varied as indicated by the fairly high standard deviations. While yield strength was variable, these fibers were higher in strength, modulus and failure strain. They almost reached the yield strength of silk fibers and far exceeded cotton single fiber strength, toughness and extensibility. The crosslinking section may have strong impact on the mechanical properties of fibers. Formaldehyde with shorter molecular chain and longer glutaraldehyde only crosslink the lysine residue between BSA molecules, which resulted in limited improvement on mechanical properties. However, EDC allowed denser crosslink via amino and hydroxyl groups which leads to high tensile strength and modulus.

Specimen	Yield Strength (MPa)	Young's Modulus (GPa)	Failure Strain (%)
BSA fiber at pH 6**,** crosslinked with formaldehyde	61±16	2.71±0.6	3.6±1.4
BSA fiber at pH 4.7, crosslinked with formaldehyde	132±30	5.31±2.0	3.9±1.6

BSA fiber at pH 4.7, crosslinked with glutaraldehyde	148±4	5.72±0.3	>30[a]
BSA fiber at 4.7, crosslinked with EDC	214±97	8.26±4.3	>30 [a]
Cotton single fiber	77±7	2.12±0.4	13.8±3.3
Silk single fiber	233±88	4.78±2.0	>30 [a]

[a]Data exceeded test limitation

TABLE 3.1 Mechanical properties of individual single BSA fibers in comparison of cotton and silk

Applications of BSA Fibers

The formation of fibrils from a defined protein solution on a glass surface may be a model for protein aggregation studies. Many proteins/peptides are known to form fibrils when soluble globular forms are destabilized,[31,42] thereby favoring partial unfolding and culminating in the formation of an amyloidogenic intermediate.[43,44] The influence of pH, protein concentration, water activity, and/or presence of divalent anions could affect the outcome of aggregation collectively,[45] or any one of these factors could impact aggregation dynamics. Therefore, a better understanding of protein aggregate biogenesis could contribute to the rational design of improved pharmaceuticals.

Varying the conditions that lead to protein aggregation has demonstrated that protein fibers can be produced in a useful size and quantity. Long fibers may be further developed for the production of novel, high-value materials with commercial utility. For instance, BSA fibers have sufficient strength and durability to be incorporated in sustainable textile composites, used as filter materials or for textile applications, to name a few potential applications.

To explore potential commercialization and to further illustrate practical versatility, it is essential that fibrous products accept colorants and form assemblies larger than single fibers. Therefore, a small-scale feasibility study was performed that included coloration experiments with BSA fibers with a number of acid dyes that are normally used for protein fibers as colorants (Figure 3.7). Further, simple experiments towards yarn formation at two different twist levels were also carried out (Figure 3.8). The products of these experiments proved to be very promising and their properties will be explored in more detail in future research.

FIGURE 3.7 BSA fibers dyed with commercially available acid dyes (left to right: C.I. Acid Red 182, C.I. Acid Orange 7, C.I. Acid Blue 12, C.I. Acid Violet 12).

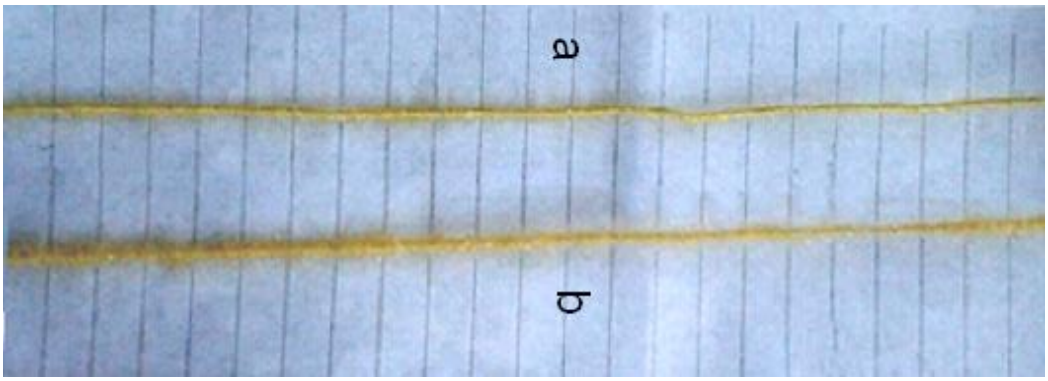

FIGURE 3.8 Assembly of BSA fibers into yarns: (a) 25.4 cm long BSA yarn made from 0.2 g fiber by twisting at 9 TPI (twists per inch (2.54 cm)), (b) 25.4 cm long yarn made from 0.5 g fiber by twisting at 11 TPI.

3.4 CONCLUSIONS

Fibers of good mechanical strength were made by controlled dehydration of BSA solution via an aggregation/self-assembly mechanism of stacking monomers when the forces maintaining a folded native state were removed during dehydration. Protein assembly at the air-liquid interface formed a tightly packed β-sheet fibril. Fibers formed at the isoelectric point of BSA and in the presence of Na_2SO_4 showed enhanced mechanical properties compared to fibers produced at other pH values. Formaldehyde cross-linking rendered the fibers insoluble in water. Additional cross-linking with glutaraldehyde or EDC further improved the mechanical properties of the fibers to the level of silk or better. BSA fibers were smooth and white and easily accepted conventional acid dyes. The fibers could be twisted into a yarn-like assembly and show potential as novel fibers for textile applications.

REFERENCES

1. Wu, Y.; Henry, D.; Heim, K.; Tomkins, J.; Kuan, C.-Y., *BMC Cell Biology* **2008**, *9*, 26.

2. Wu, Y.; Laughlin, R. C.; Henry, D. C.; Krueger, D. E.; Hudson, J. S.; Kuan, C.-Y.; He, J.; Reppert, J.; Tomkins, J. P., *BMC Cell Biology* **2007**, *8*, 36.

3. Puchtler, H.; Sweat, F. A., *J. Histochem. Cytochem*. **1966**, *14*, 123-134.

4. Sacchettini, J. C.; Kelly, J. W. *Nat. Rev. Drug Discov*. **2002**, *1*, 267-275.

5. Chiti, F.; Dobson, C. M. *Annu. Rev. Biochem.* **2006**, *75*, 333-366.

6. Dobson, C. M., *Nature* **2003,** *426*, 884-890.

7. Juarez, J.; Taboada, P.; Mosquera, V. *Biophysical Journal* **2009**, *96*, 2353-2370.

8. Munishkina, L. A.; Fink, A. L.; Uversky, V. N. *J. Molec. Biol.* **2004,** *342*, 1305-1324.

9. Perutz, M. F.; Finch, J. T.; Berriman, J.; Lesk, A. *PNAS* **2001**, *99*, 5591-5595.

10. Perutz, M. F.; Johnson, T.; Suzuki, M.; Finch, J. T. *PNAS* **1994**, *91*, 5355-5358.

11. Jahn, T. R.; Radford, S. E. *Arch. Biochem. Biophys.* **2008,** *469*, 100-117.

12. Kad, N. M.; Myers, S. L.; Smith, D. P.; Smith, D. A.; Radford, S. E.; Thomson, N. H. *J. Mol. Biol.* **2003,** *330*, 785-797.

13. Ashcroft, A. E., *J. Amer. Soc. Mass Spectrom.* **2010**, *21*, 1087-1096.

14. Uversky, V. N.; Segel, D. J.; Doniach, S.; Fink, A. L. *Proc. Natl. Acad. Sci. USA* **1998**, *95*, 5480-5483.

15. Oppenheim, T. W.; Knowles, T. P. J.; Lacour, S. P.; Welland, M. E. *Acta Biomater.* **2010,** *6*, 1337-1341.

16. Sweers, K.; Werf, K. v. d.; Bennink, M.; Subramaniam, V., *Nanoscale Res. Lett.* **2011**, *6*, 270.

17. Knowles, T. P. J.; Oppenheim, T. W.; Buell, A. K.; Chirgadze, D. Y.; Welland, M. E., *Nature Nanotechnol.* **2010,** *5*, 204-207.

18. R.H.O. *J. Franklin Inst.* **1938**, 225, 620-621.

19. Yang, Y.; Narendra, R. *Intern. J. Biol. Macromol.* **2012**, *51*, 37-44.

20. Whittier, E. O.; Gould, S. P. *Ind. Eng. Chem.* **1940**, *32*, 906-907.

21. Zhang, X. H.; Khan, M. M. R.; Yamamoto, T.; Tsukada, M.; Morikawa, H. *Intern. J. Biol. Macromol.* **2012**, *50*, 337-347.

22. Zhang, Y.-Q. *Biotechn. Adv.* **2002**, *20*, 91-100.

23. Seymore, R. B. InThe Encyclopedia of Chemistry; Clark, G. L., Ed.; Reynold N.Y., **1966**, pp 848-849.

24. Shukla, R.; Cheryan, M. *Indust. Crops . Prod.* **2001**, *13*, 171-192.

25. Reddy, N.; Yang, Y. *Biotechn. Progr.* **2009,** *25*, 1796-1802.

26. Whitesides, G. M.; Grzybowski, B. *Science* **2002**, *295*, 2418-2421.

27. Sutherland, B. W.; Toews, J.; Kast, J. *J. Mass Spectrom.* **2008**, *43*, 699-715.

28. Paparcone, R.; Buehler, M. J. *Biomater.* **2011**, *32*, 3367-3374.

29. Shammas, S. L.; Knowles, T. P. J.; Baldwin, R. L.; MacPhee, C. E.; Welland, M. E.; Dobson, C. M.; Devlin, G. L. *Biophys. J.* **2011**, *100*, 2783-2791.

30. Myers, S. L.; Thompson, N. H.; Radford, S. E.; Ashcroft, A. E., *Rapid Commun. Mass Spectrom.* **2006**, *20*, 1628-1636.

31. Balbirnie, M.; Grothe, R.; Eisenberg, D. S. *PNAS* **2001**, *98*, 2375-2380.

32. White, D. A.; Buell, A. K.; Knowles, T. P. J.; Welland, M. E.; Dobson, C. M. *J. Amer. Chem. Soc.* **2010**, *132*, 5171-5175.

33. Thomas, A. S.; Elcock, A. H., *J. Amer. Chem. Soc.* **2007**,*129*, 14887-14898.

34. Zangi, R.; Hagen, M.; Berne, B. J. *J. Amer. Chem. Soc.* **2007**, *129*, 4678-4686.

35. Hofmeister, F. *Arch. Exp. Pathol. Pharmakol.* **1888**, *24*, 247-260.

36. Collins, K. D. *Biophys. J.* **1997**, *72*, 65-76.

37. Carter, D. B.; Chou, K.-C. *Neurobiol. Aging* **1998**, *19*, 37-.

38. Xu, Z.; Paparcone, R.; Buehler, M. J. *Biophys. J.* **2010**, *98*, 2053-2062.

39. Paparcone, R.; Cranford, S. W.; Buehler, M. J. *Nanoscale* **2011**, *3*, 1748-1755.

40. Metz, B.; Kersten, G. F.; Hoogerhout, P.; Brugghe, H. F.; Timmermans, H. A.; De Jong, A.; Meiring, H.; Ten Hove, J.; Hennink, W. E.; Crommelin, D. J.; Jiskoot, W., J. Biol. Chem. **2004**, 279, 6235.

41. Chen, L.; Liu, G.; Wang, Q.; Hou, W. *IEEE EMB* **2010**, 2377-2381.

42. Reches, M.; Porat, Y.; Gazit, E. *J. Biol. Chem.* **2002**, *277*, 35475-35480.

43. Jarrett, J. T.; Lansbury Jr, P. T. *Biochem.* **1992**, *31*, 12345-12352.

44. Lomakin, A.; Teplow, D.B.; Kirschner, D.A.; Benedek, G.B. *Proc. Natl Acad. Sci. USA* **1997**, *94*, 7942-7947.

45. Vetri, V.; D'Amico, M.; Foderà, V.; Leone, M.; Ponzoni, A.; Sberveglieri, G.; Militello, V., Arch. Biochem. Biophys. **2011**, 508, 13-24.

CHAPTER 4 INJECTABLE HYDROGELS FROM BSA AND PEG

4.1 INTRODUCTION

Biopolymeric thermoresponsive gels with a Sol-Gel transition at body temperature have been the recent focus of biomedical research[1]. These gels have a great potential for drug delivery reservoirs while being injectable at a specific location of need [2-6]. It is a challenging task to create such a gel that additionally fulfills nontoxicity requirements, disintegrates without cytotoxicity of the resulting products in a controlled manner and releases drugs within a useful time frame.

In general, hydrogels can be defined as materials that form three-dimensional molecular networks capable of holding large amounts of water. They are considered thermoresponsive when a temperature change functions as the stimulus to perform a desired task, e.g., swelling and collapse[7]. Stimuli-sensitive hydrogels have found extensive interest as drug delivery vehicles[8]. The most recent focus of research has been directed towards hydrogels for which the aqueous precursor is a fluid at room temperature and a gel at body temperature. This behavior could make it possible to form a hydrogel *in-situ* upon injection via *in vivo* crosslinking[9] or by other mechanisms[1] - as opposed to a pre-formed hydrogel - and therefore well adjust to a required defect geometry. For biomedical applications as for tissue repair, it is adamant that the gelation to be conducted under mild conditions and without the use of toxic chemicals, and that the generation of excessive heat or the release of gaseous by-products to be avoided as it could adversely affect tissue. Suitable materials also require biocompatibility, biodegradability, and homogeneous dispensation of loaded drugs or cells.

For thermoresponsive hydrogels, both natural and synthetic polymers have been explored. Among synthetic polymers, a fairly large number of poly(N-isopropyl acrylamide)

(poly(NIPAAM))-based systems have been investigated for their Sol-Gel behavior[10-11] and efforts have been reported to adjust their lower critical solution temperature (LCST) to the physiologically interesting range by modification of the gel architecture, crosslinking and/or copolymerization with natural or synthetic compounds[12-13]. Block copolymeric networks have also been formed based on polyesters, for instance, polylactide (PLA) and poly-lactide-co-glycolide (PLGA)[14-16], frequently with poly(ethylene glycol) (PEG) as a copolymer[17-20]. Synthetic injectable hydrogels, however, may cause more severe immunologic reactions than natural polymer based materials and show a lower degradation rate[21-22].

As natural polymers, polysaccharide-based hydrogels have been studied such as chitosan, xylan, hyaluronic acid, and alginate [23-24], as well as protein (gelatin, collagen, fibrinogen and bovine serum albumin (BSA)) [21-22, 25] and synthetic polypeptide-based ones (e.g., poly(L-glutamates[20]). Direct reaction of PEG or PEG derivatives (aldehydes, carboxylates, carbonates and thiols) with the base polymer have also frequently been used in an attempt to adjust the LCST closer to the desired range[26-33]. The addition of PEG increases the hydrophilicity of the base polymers and their overall molecular weight. PEG with higher molecular weight increases the repulsion of the modified BSA to the phospholipids of the cell membrane, thus, lowering the interaction with cells[19, 21, 29, 33].

Some of the synthetic thermoresponsive hydrogel products have already been approved by FDA for medical applications (e.g., Pluronic™, ReGel™)[3, 5, 34] and most of them can be degraded by metabolic enzymes[34]. However, the complexity of the reaction, the toxicity of some of the reactants, and the low solubility of hydrophobic drugs in the hydrogel still present significant drawbacks[29-33]. Polypeptide or protein-based PEGylated hydrogels generally exhibit superior

performance in drug delivery and tissue engineering[20], especially BSA with hydrophobic pockets for hydrophobic drug binding.

The motivation for this research was to develop a simplified approach to create a PEG-grafted BSA hydrogel, using low-molecular weight PEG simultaneously as a reactant and dispersion medium. The desired Sol-Gel transition of this hydrogel should be in the range of the body temperature so that the hydrogel could potentially be injected. It was assessed whether the chain length of PEG with molecular weight 200 or 400, directly grafted via esterification of the acidic BSA residues, could have a distinct effect on the Sol-Gel transition. Finally, the attempt was made to preserve the secondary/tertiary structure of BSA during and after the reaction, so that the resultant BSA-PEG would be able to hold small molecules for potential drug delivery. Such a thermoresponsive hydrogel could serve as a drug carrier as well as a model platform for other protein-based hydrogels.

4.2 EXPERIMENTAL

Materials and Chemicals

BSA was purchased from Sigma-Aldrich (St. Louis MO); PEG200, PEG400, diethyl ether and ethanol were obtained from Alfa Aesar (Ward Hill, MA) and 98% sulfuric acid from EMD (Gibbstown, NJ). 5-FU (5-fluorouracil) was also purchased from Sigma-Aldrich (St. Louis, MO). Trypsin (1:250, tissue culture grade) and phosphate buffered saline (PBS) were obtained from Amresco (Solon, OH).

Preparation of BSA-PEG precursor

The procedure used to make the hydrogel precursors was roughly adapted from Chen et al., 2011[20]: 0.5 g BSA were suspended in 20 mL PEG (molecular weights 200 and 400,

respectively), and 0.5 mL sulfuric acid (98%) was added drop-wise. The reaction was conducted overnight at room temperature. The product was separated by precipitation in a 1:1 mixture of ethanol and diethyl ether and centrifuged at 5000 rpm for 10 min. The obtained solid product was dissolved in 20 mL 50 mM phosphate buffer saline (PBS) at pH 7.4, and separated from trace amounts of unreacted PEG by centrifugal ultrafiltration (Amicon Ultra-15, MWCO 30KDa, EMD Millipore, Billerica, MA). Ultrafiltration was repeated three more times with deionized (DI) water. The obtained BSA-PEG precursor was pre-frozen at -18°C and dried by lyophilization. The yield of purified product was 76.9% for BSA-PEG200 (0.4g) and 57.3% for BSA-PEG400 (0.32g).

Gelation

For the gelation experiments 0.5 g BSA-PEG precursor (PEG molecular weights 200 and 400, respectively) was dissolved in 10 mL 50 mM PBS (pH 7.4) and the solution brought to a concentration of 15% (wt) (3.3 g) using centrifugal ultrafiltration at 5000 rpm. Precursor solution was filled in individual vials and heated in a water bath to various temperatures (25, 30, 35, 37 and 40°C) for 30 min. If gelation did not occur under these conditions, the concentration was increased until the precursor gelled and the mass was determined by weighing the sample vials. The Sol-Gel transition concentration of the formed hydrogel was calculated by the following equation (eq. 1)

$$W = \frac{m'}{m} \times 100\% \qquad (1)$$

The mass (g) of the hydrogel at gelation is m, and m’ is the mass of hydrogel precursor (0.5g); W is the hydrogel precursor weight percentage at Sol-Gel transition.

A tubular polyacrylamide mold of 10 mm inner diameter and 4 mm depth was prepared into which the precursor gel was injected. The mold was pre-heated to a set temperature for the gelation experiments and the gelling ability of the precursor studied under these conditions.

Drug Delivery

Drug loading capacity of BSA-PEG200 and BSA-PEG400 solution, respectively, was evaluated by the following method: 1 mg/mL 5-FU solution in 50 mM PBS at pH 7.4 was mixed with different molar ratios of BSA to 5-FU (100, 200, 300 and 400). BSA-PEG and 5-FU were incubated at 40°C for 2 h, and separated by ultrafiltration (Amicon Ultra-15, MWCO 30KDa, EMD Millipore, Billerica, MA)[36]. Separated 5-FU solution concentration was used to determine the drug loading ratio by the following equation (eq. 2):

$$R = R' * \frac{C_i - C_f}{C_i} \qquad (2)$$

Here, R is the loaded 5-FU to BSA molar ratio, C_i is the initial 5-FU concentration (1 mg/mL) and C_f is the concentration of separated 5-FU determined by UV-Vis, R' is the incubated-BSA to 5-FU molar ratio. Release of 5-FU was determined by a discontinuous method[17]. Each type of hydrogel (0.5 g) was sealed in an individual dialysis tube (MWCO 30kDa) and exposed to 50 mL 50 mM PBS at pH 7.4, with native BSA gelled at 70°C as the control sample. For UV-Vis spectroscopic examination, 4 mL of the solution were used and 4 mL 50 mM fresh PBS were added to maintain the total volume.

Degradation

Degradation experiments were performed with 15% BSA-PEG200 and BSA-PEG400 hydrogels, respectively. Each sample contained 1 g hydrogel enclosed in 20 mL vials and heated to 40°C; 10 mL 0.05 M PBS (pH adjusted to 8) with 10 unit/mL trypsin (BSA : trypsin=1:50 in mole

ratio) were added to the vials. The control sample only contained hydrogels in 10 mL 0.05 M PBS (no trypsin). The vials were kept in 37°C in a water bath and stirred. Vials were weighed before the degradation process was started. After every 12 h, 10 mL solution was removed from the vials and the same volume (10 mL) PBS added. The vials were weighed at every interval. The degradation test was conducted for seven days.

Characterization

Fourier Transform Infrared spectroscopy (FT-IR) was conducted using a Thermo Scientific Nicolet 6700 FT-IR spectrometer for the chemical characterization of the products; the wave number range was set at 4000 to 400 cm^{-1} over 32 scans with a resolution of 4 cm^{-1}. IR (ATR): ν = 3270 (m), 2939 (w), 2890 (w), 1623 (s, amine I), 1540 (m, amine II) 1187 (s, C-N), 1083 (s, C-O) cm^{-1}.

A Bruker Microflex LT MALDI-TOF mass spectrometer and control software from Bruker Daltonics were utilized to estimate the molecular weight. The range for the MALDI-TOF test was 20-250 kDa. Sinapic acid and native BSA protein were used as matrix.

^{1}H-NMR spectroscopy was conducted on a Bruker 400MHz spectrometer to determine the molecular structure and estimate the PEGylation ratio. Samples were dissolved in 0.5 mL deuterium oxide and water was used as reference. ^{1}H NMR (400 MHz, D_2O, δ): 7.20 (m, 2H; ArH), 4.70 (m, 1H, CH), 3.59 (m, 4H; OCH_2CH_2), 2.87 (m, 2H; NH_2), 1.53 (m, 2H; CH_2), 0.75 (m, 3H; CH_3) ppm.

UV-Vis was carried out on a Thermo Scientific Genesys 6 spectrometer to quantify the 5-FU to BSA ratio. Quartz cuvettes with 10 mm path length were used. UV-Vis (0.05M PBS, pH=7.4): $\lambda_{max}(\varepsilon)$ = 280 (3443824 $M^{-1}cm^{-1}$, BSA), 266 nm (7070, $M^{-1}cm^{-1}$, 5-FU).

Circular dichroism (CD) spectra were obtained by using a JASCO-810 spectropolarimeter (Jasco, Tokyo, Japan) with collecting wavelength ranges from 180 to 300 nm to investigate the secondary and tertiary structure of hydrogel protein moieties. Quartz cuvettes with 0.2 mm path length were used, and the average molecular weight of BSA residues was considered to be 114 g/mol[37, 38]. Samples were dissolved in 0.05 M PBS at pH 7.4 with a concentration of 1 mg/mL. Protein moiety ellipticity was determined by equation (3):

$$\theta = 114\theta_\lambda / 10dc \qquad (3)$$

where θ_λ is the observed ellipticity, d is the light path and c the concentration. Prior to CD analysis, SDS-PAGE was used to confirm the presence of protein; UV-Vis evaluations were performed to determine the solution concentration.

A Carl Zeiss EVO 50 scanning electron microscope (SEM) at 20 kV scanning voltage was used to examine the morphology of dried hydrogels at microscale. Gold coating was applied by a sputter coater prior to imaging. The hydrogels were frozen in liquid nitrogen and dried in a freeze dryer. A Carl Zeiss EM 10 transmission electron microscope (TEM) at 60 kV scanning voltage was used for observation of aggregate sizes. 10 μL 1% and 15% BSA-PEG solutions were placed on a 300 mesh copper grid on filter paper to prepare a thin film. The copper grid was frozen with liquid nitrogen and dried in a freeze dryer.

Rheology tests were performed on a TA Instrument AR2000 Rheometer with a 60 mm diameter flat plate at 0.05 mm gauge by frequency sweeping oscillatory method with 0.1 to 100 Hz frequency. Both the 15% hydrogel precursors and the resultant hydrogels were tested at optimized gelation temperature.

4.3 RESULTS AND DISCUSSION

PEGylation of BSA

BSA and liquid, low molecular weight PEG was reacted with sulfuric acid as the catalyst to form a translucent hydrogel precursor. At room temperature the product precursors showed excellent solubility in both DI water and PBS of pH 7.4 (Figure 4.1), irrespective of the molecular weight of PEG (200 or 400) and the grafting ratio. Successful grafting was verified by FT-IR with the 1083 cm^{-1} absorption peak of the repeat units of PEG.

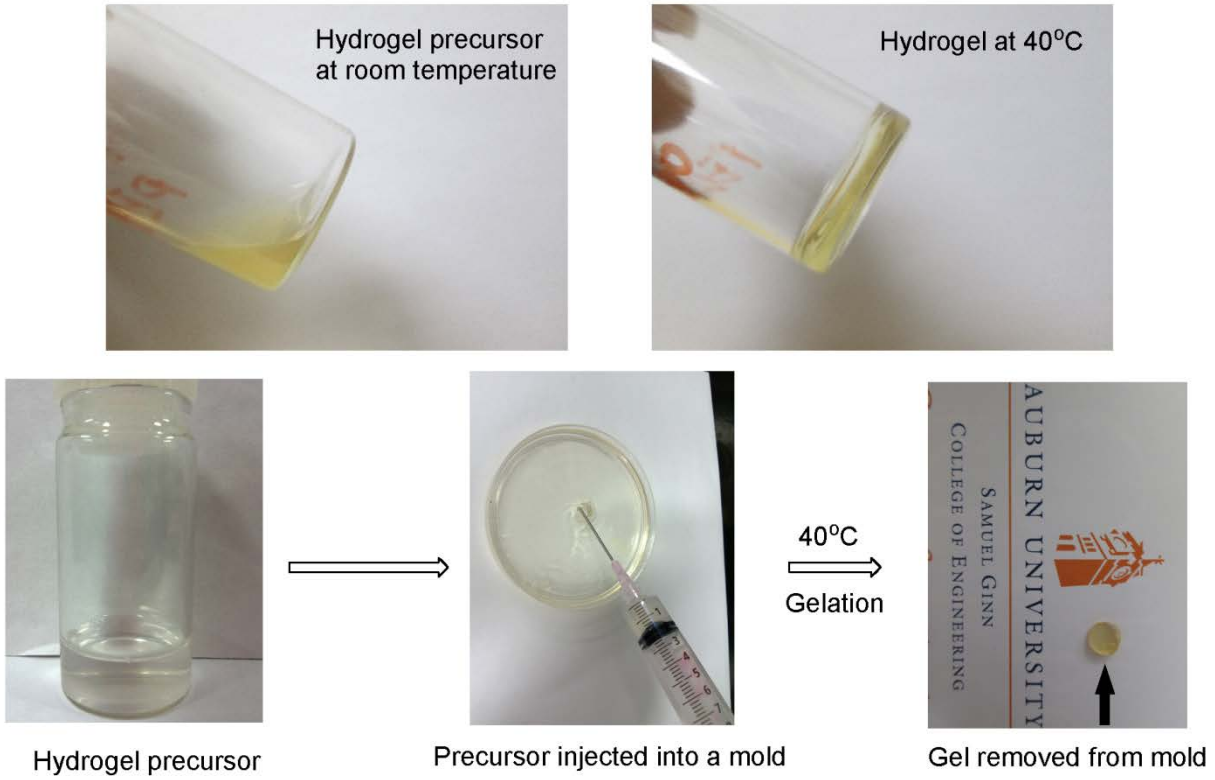

FIGURE 4.1 Precursor (in 0.05 M PBS, pH=7.4) was liquid at room temperature and a hydrogel was obtained with heating to 40°C.

PEG reacted with a fraction of the 96 acidic residues of BSA (glutamic acid (Glu) and aspartic acid (Asp)) by formation of covalent bonds via a single-step reaction. This reaction constitutes an esterification in which PEG can serve as both the reactant and the dispersion medium for BSA. Grafting low molecular weight PEG contributes to product solubility by adding ethylene

oxide units to the protein. Further, the hydrophilicity of BSA is considerably impacted because each ethylene oxide group could theoretically trap three water molecules by hydrogen bonds[26]. With PEGylation of the BSA protein the formation of aggregates becomes possible through short, more hydrophilic PEG tails oriented towards water and away from the relatively hydrophobic BSA moiety in different arrangements (Figure 4.2).

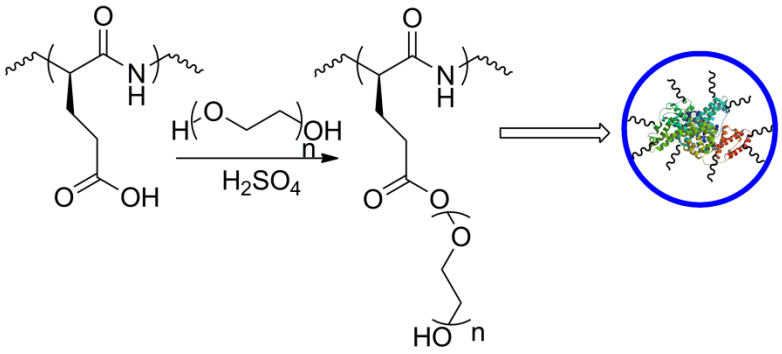

FIGURE 4.2 Schematic of the synthesis and formation of a potentially injectable hydrogel: precursor synthesized from BSA and PEG.

The average molecular weight and grafting ratio of BSA-PEG were determined from the mass spectra (Figure 4.3). As shown in Table 1, the average molecular weight of BSA-PEG200 was 69.1 kDa, and for BSA-PEG400 73.7 kDa. There were an average of 13 mole PEG200 and 18 mole PEG400 grafted to each mole BSA involving approximately one fifth of its acidic residues (Asp and Glu, see H^1-NMR spectra in Figure 4.5). Most of acidic residues on the surface of globular BSA were grafted. The mass spectra did not indicate the formation of any significant amounts of BSA dimers, trimers or oligomers nor any major damage to BSA from the acid catalysis during the PEGylation reaction.

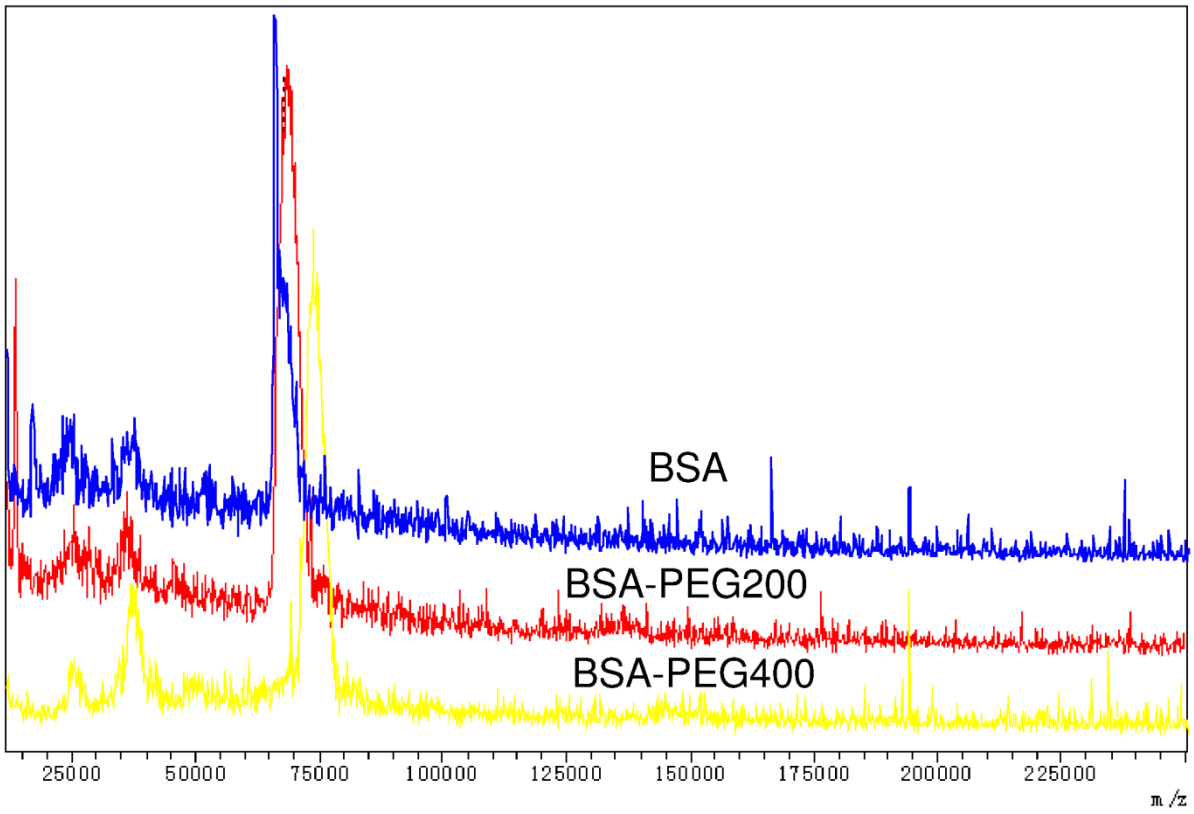

FIGURE 4.3 MALDI-TOF mass spectra of BSA, BSA-PEG200 and BSA-PEG400.

TABLE 4.1 Molecular weight of BSA-PEG200 and BSA-PEG400 determined from MALTI-TOF mass spectra.

Sample	Mn (kDa)	Standard Deviation (kDa)	Grafting Ratio*
BSA-PEG200	69.1	2.53	13
BSA-PEG400	73.7	1.26	18

*Determined with BSA molecule weight 66,462Da

The CD spectra of the samples, with native BSA as the control, showed the characteristic peaks at 210 nm and 225 nm that indicate alpha-helical structure which was predominant in the secondary and tertiary structure of the native protein. The ellipticity of all the samples was in the same range (Figure 4.4), which revealed that the secondary and tertiary structure of BSA was indeed preserved throughout the reaction. This result was also confirmed by FT-IR spectra. The

band at 1623 cm^{-1} for the amino group absorption remained unchanged. Only a limited number of BSA amino acid residues were esterified under the experimental conditions (Table 1), while others remained unreacted. Thus, the majority of native secondary structure of BSA was not affected by the PEGylation reaction.

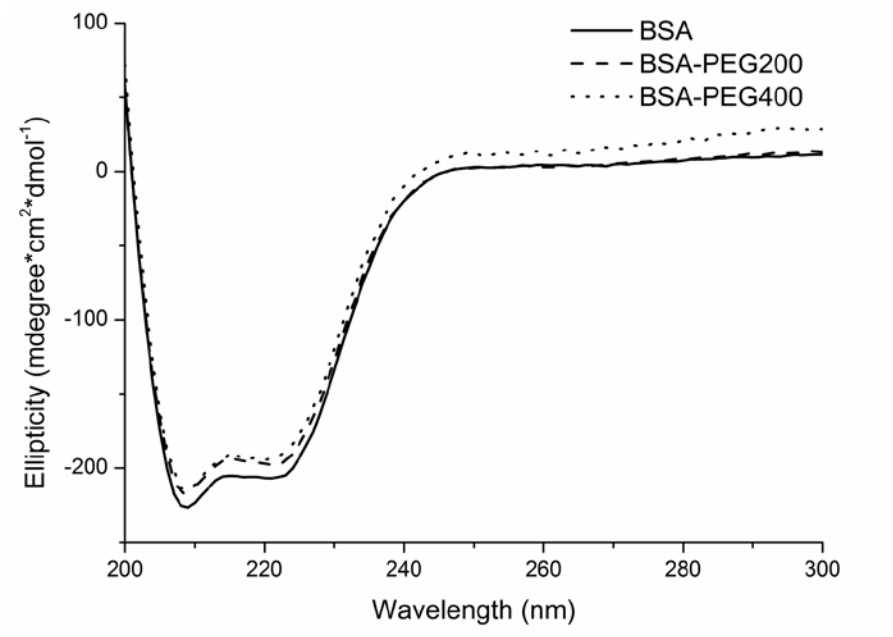

FIGURE 4.4 CD spectra of the BSA as control, BSA-PEG200 and BSA-PEG400 dissolved in 0.05 M PBS at pH 7.4.

The proton NMR spectra in Figure 4.5 support that PEG grafting has been accomplished by exhibiting a strong peak for ethoxyl groups at δ 3.59. The PEG grafting ratio can be approximated by integrating the peak intensity ratios of the aromatic groups (δ 7.15) to ethoxyl groups. As mentioned above, the PEG200 and PEG400 only reacted with acidic residues (Asp and Glu) of BSA, which is reflected by unaffected amino groups (Lys, Asn and Gln). The integrated peak intensity ratio of acidic residues to aromatic groups resulted in similar PEGylation ratios as obtained from mass spectra (Figure 4.3).

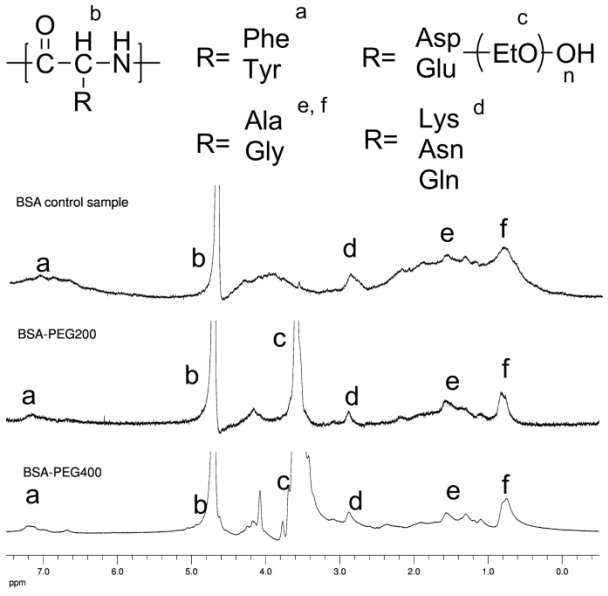

FIGURE 4.5 H^1-NMR spectra of BSA-PEG200 and BSA-PEG400.

Sol-Gel Behavior

The lower critical solution temperature (LCST) determines the solubility of a polymer (hydrogel) in a solvent (water) and thus its Sol-Gel behavior. The gelation of unmodified BSA at physiological pH occurs at around 80°C[39]. If polypeptides are reacted with PEG, the LCST can be lowered and the length of the PEG chains and the ratio of PEG grafting may have an effect on the LCST[12, 20, 40].

As shown in Figure 4.1, synthesized hydrogel precursors were liquid at room temperature, and the gelation of condensed hydrogel precursors occurred when heated up to 40°C. When injected into a preheated polyacrylamide mold, soft yellowish gels could be formed that completely filled the shape of the mold within minutes.

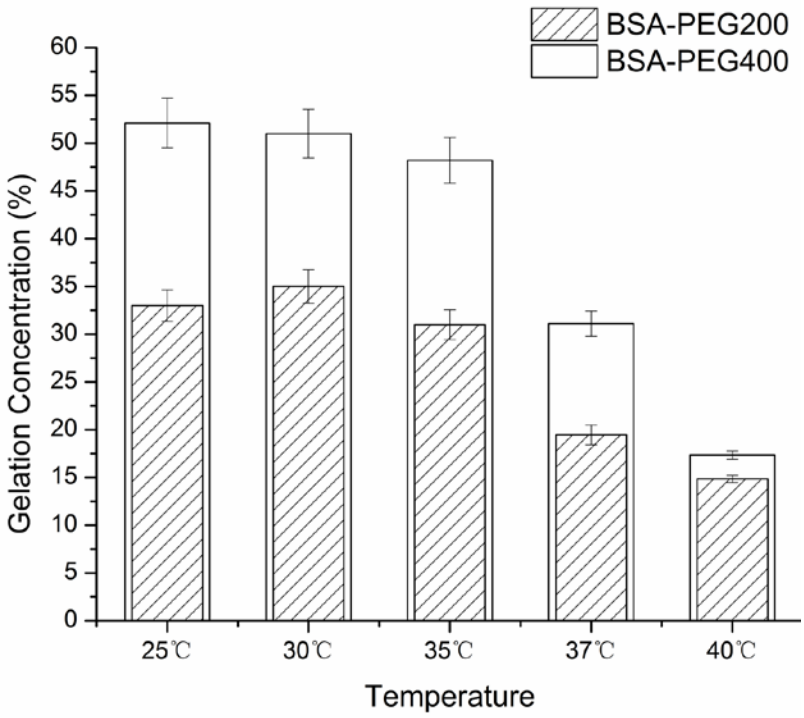

FIGURE 4.6 Temperature dependent Sol-Gel transition concentrations of BSA-PEG200 and BSA-PEG400.

Although PEG grafting only occurred at a limited number of residues in BSA and the molecular weight of PEG was low, it was surprising to find a significant difference of the temperature and concentration dependent behavior of the BSA-PEG precursors relative to the molecular weight of PEG (Figure 4.6). At 30°C and below, fairly high Sol-Gel transition concentrations were observed: for BSA-PEG400 concentrations of over 50% and for BSA-PEG200 over 35% were necessary to form a gel. It seems that in the low molecular weight range of PEG (200 and 400) the impact of the chain length on the LCST does have a more pronounced effect than at longer chain lengths (MW>3000 DA) as reported in other research[40]. Therefore, for BSA-PEG200 lower amounts of precursor were required for a gel to form than for BSA-PEG400. It could be argued that inter- and intramolecular hydrogen bonds usually supporting the BSA backbone

structure, switch to intramolecular H-bonds with water upon PEGylation as has been hypothesized with PEG-grafted glutamates[20], which would explain the water solubility of the grafted derivatives. This effect might be more pronounced the shorter the PEG molecular chain. Approaching the temperature range of 37-40°C, Sol-Gel transition concentrations considerably dropped and the difference between PEG200 and PEG400 almost disappeared; both hydrogels could be formed at a concentration of 15% at 40°C. Above 45°C the hydrogel precursors were unable to produce a gel. Instead, a slurry and finally, a brownish-white precipitate formed.

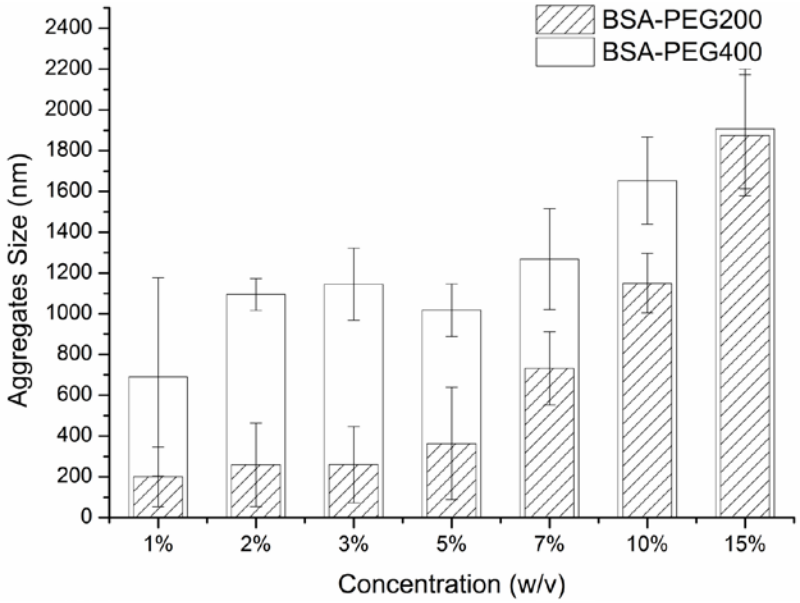

FIGURE 4.7 Particle size of BSA-PEG200 and BSA-PEG400 aggregates in 0.05 M PBS (pH 7.40).

At low precursor concentrations aggregate sizes were relatively small (Figure 4.7; approximately 200 nm in the case of BSA-PEG200) and almost spherical (Figures 4.8 a, b); larger agglomerates were formed with increasing concentration. The variation in shape and size was greater in the case of BSA-PEG400 (Figure 4.8b). At 15% both BSA-PEG gels appeared to have similar aggregate sizes that were by about a factor of 10 larger than at 1% (Figure 4.7). In Figure 8 c, the

TEM of the BSA-PEG200 precursor is displayed; upon heating to 40°C, the visual appearance of the gel corresponds to the one shown in Figure 4.1 (upper right-hand corner).

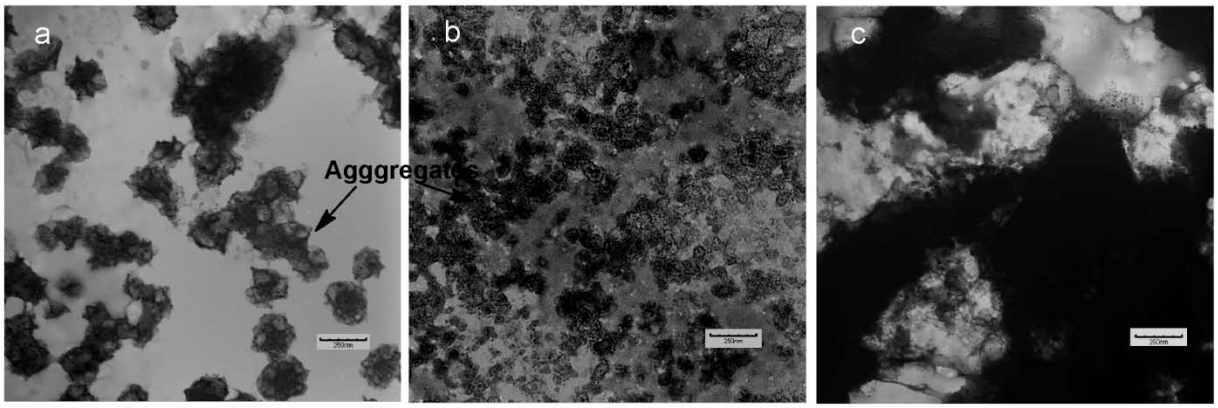

FIGURE 4.8 TEM images of (a) BSA-PEG200 aggregates at 1% in PBS; (b) BSA-PEG400 aggregates at 1% in PBS; (c) BSA-PEG200 aggregates at 15% in PBS.

The morphology of the dried hydrogel was studied by scanning electron microscopy (SEM, Figure 4.9). The dry gels showed a structure with relatively large pores but seemed to be surprisingly compact after the water had been removed by lyophilization, leaving a BSA-PEG skeleton. Since water is the major constituent of a hydrogel, a more porous microarchitecture could have been expected.

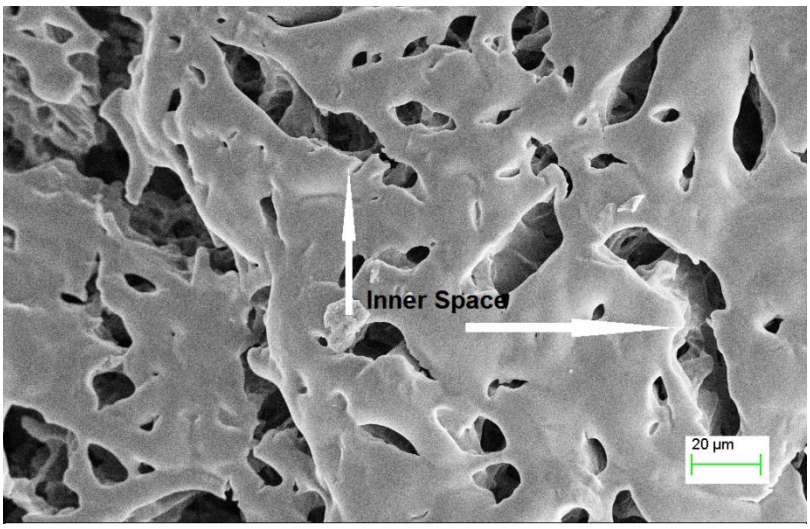

FIGURE 4.9 SEM image of dried BSA-PEG200 hydrogel with porous inner space.

A rheology study was performed to compare the viscoelastic behavior of the hydrogels and their precursors. The results are shown in Figure 4.10. The hydrogel precursors (delta symbols) showed a slight response with low values for the storage (G') and loss modulus (G"). For both BSA-PEG200 and BSA-PEG400 hydrogels (square symbols) G' increased by a factor of approximately 10 and G" by a factor of about 4 when gelation occurred at 40°C. The hydrogels formed with a very low G' value (2 kPa) under the test conditions. The G'/G" ratios for BSA-PEG200 and for BSA-PEG400 hydrogels were around 6-7 at 1Hz frequency, which indicates that the hydrogel precursors transformed to materials of higher consistency.

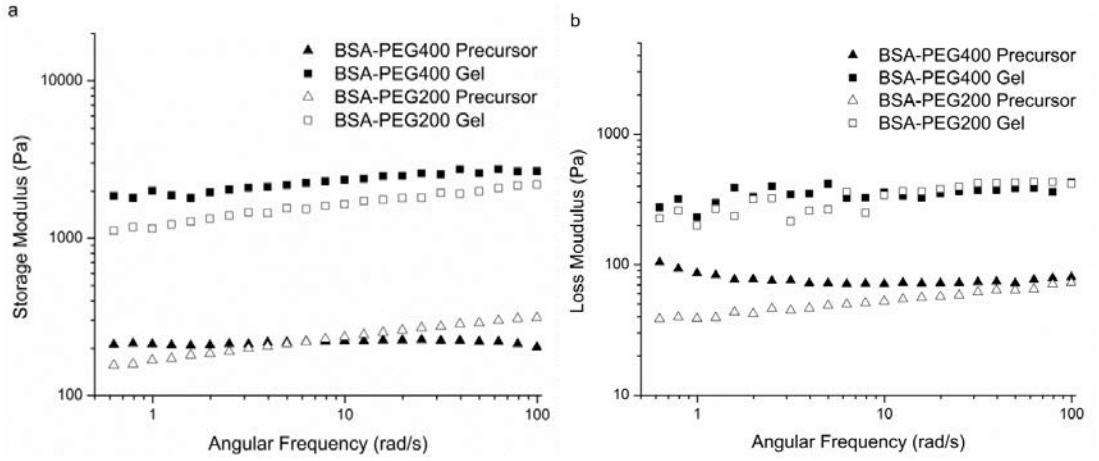

FIGURE 4.10 Rheologic properties of PEGylated BSA hydrogels and precursors at 40°C: (a) storage modulus; (b) loss modulus.

Drug delivery

Drug loading experiments were performed using 5-fluorouracil (5-FU), a common anti-cancer drug [41], to illustrate that the capability of BSA-PEG gels to carry small drug molecules has been preserved, at least to a certain extent (Figure 4.11). Drug loading of 5-FU onto native BSA showed to follow a linear course; it was found to be lower by a factor of four for both BSA-PEG

hydrogels compared to BSA, but also close to linear (R^2=0.97 for BSA-PEG200 and R^2=0.90 for BSA-PEG400). Mass spectra and H^1-NMR experiments had shown that PEG reacted with approximately one fifth of the amino acid residues in BSA (Glu and Asp; Figures 4.3 and 4.5). Thus, it can be assumed that some of the amino acids responsible for interaction with 5-FU were occupied by PEG grafts which lowered the affinity of hydrophobic drugs. The difference in molecular weight of PEG proved to be insignificant in this case. However, it is important to state that the incorporation of 5-FU did not affect the Sol-Gel transition behavior of either BSA-PEG hydrogel.

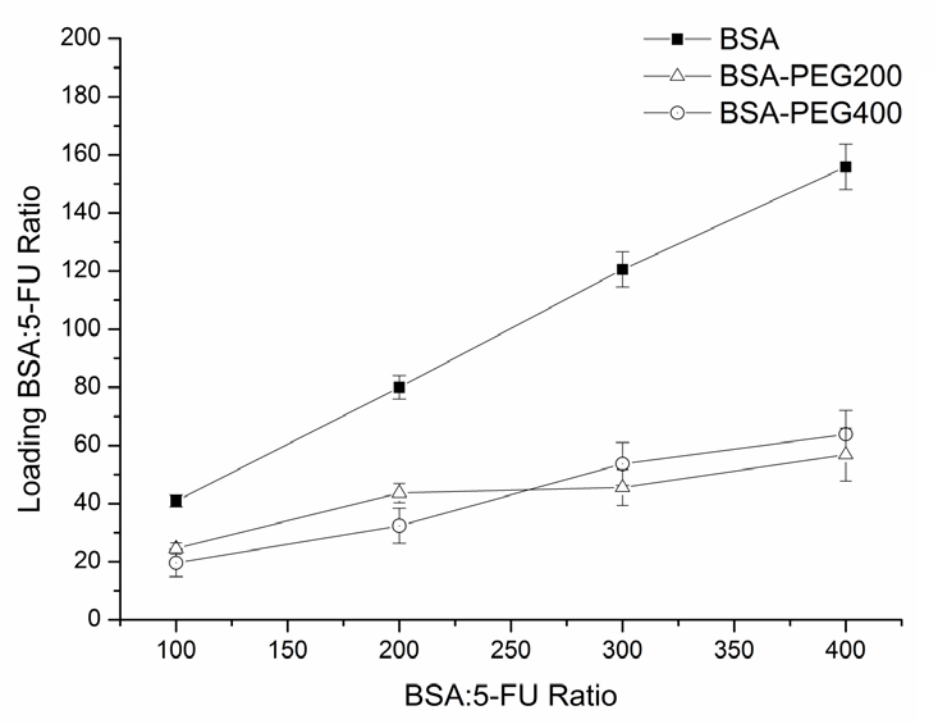

FIGURE 4.11 5-FU loading profile onto BSA-PEG hydrogels and native BSA.

The release profiles of 5-FU for BSA and BSA-PEG gels are shown in Figure 4.12. From both BSA-PEG200 and BSA-PEG400 less 5-FU was discharged into PBS buffer solution compared to native BSA. Both PEGylated hydrogels still contained almost 50% of the drug after 48 h exposure to the release medium, while the BSA control had liberated approximately 90% of the

drug. Thus, although the PEGylated hydrogels could hold less of the drug overall (Figure 4.11), they initially freed a lower amount of 5-FU than BSA and therefore might be considered for future drug carrier applications with sustained release capabilities.

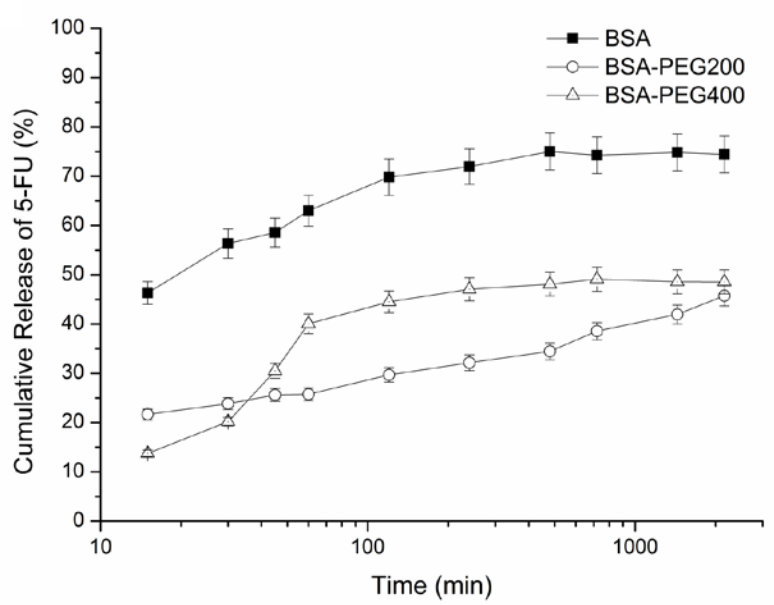

FIGURE 4.12 5-FU discontinuous release profiles in 0.05 M PBS at pH 7.4.

Biodegradation studies

Biodegradation experiments *in vitro* of the hydrogels were conducted to evaluate their stability and degradability in PBS buffer solution at pH 8. From Figure 4.13 it can be seen, that both BSA-PEG200 and BSA-PEG400 hydrogels experienced a steady weight loss even without the addition of trypsin, a metabolizing enzyme; overall, after 144 h over 50% of the hydrogels were still left intact. It is likely that the BSA-PEG hydrogel aggregates slowly collapsed and disintegrated as the buffer solution eroded their three-dimensional arrangement. Trypsin clearly expedited the degradation of the hydrogels and led to rapid disintegration within less than 50 h, faster in the case of BSA-PEG400 than with BSA-PEG200. These observations indicate that modifying BSA with PEG grafts - though only to a fairly small extent and with just short graft

lengths - led to enhanced hydrophilicity and susceptibility to biodegradation. These results could play an important role in drug delivery applications where the drugs were to completely be dispensed over a relatively short time frame.

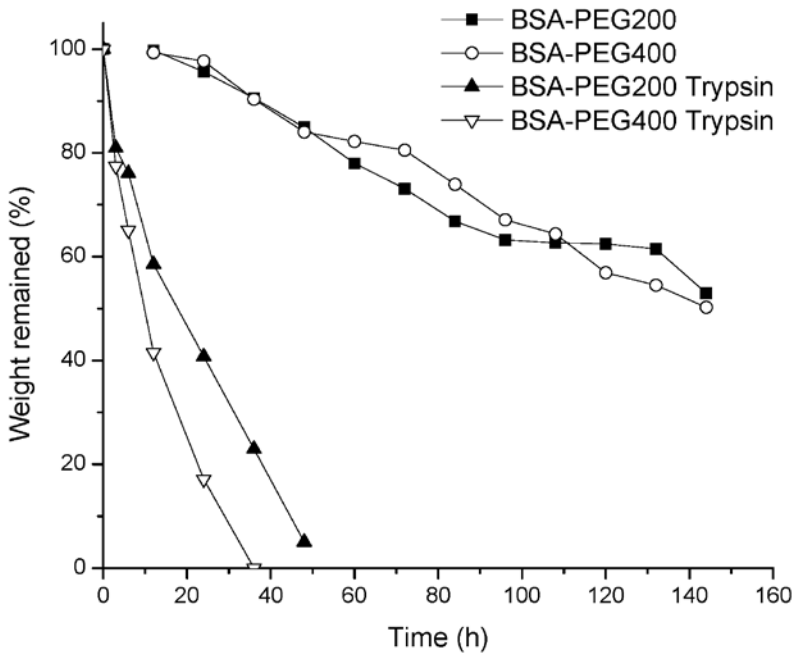

FIGURE 4.13 Biodegradation of BSA-PEG hydrogels at pH 8 without trypsin (square and round symbols) and with trypsin (triangular symbols).

4.4 CONCLUSIONS

In this work, a novel approach was introduced to synthesize a grafted BSA hydrogel via esterification of approximately one fifth of the acidic residues in BSA with PEG200 and PEG400, respectively. Grafting ratios of the BSA-PEG derivatives were determined by MALDI-TOF mass spectrometry and H^1-NMR spectroscopy. It was possible to form BSA-PEG hydrogels with interesting Sol-Gel transition behavior in the range of body temperature: with decreasing concentration and temperatures increasing from 25°C to 37-40°C, small spherical precursor assemblies formed into larger aggregates within minutes. The Sol-Gel transition concentration

for both BSA-PEG200 and BSA-PEG400 hydrogels was 15%. The chain length of the PEG grafts only played a role in the lower concentration range and at temperatures less than 35°C. Due to the overall relatively low grafting ratios, the secondary and tertiary structure of BSA could be preserved in the BSA-PEG hydrogels. The hydrogels were capable of holding a small drug molecule, such as 5-FU by hydrophobic pockets and charges. The release profile for 5-FU into buffer solution showed that the hydrogels could slow the release compared to native BSA. The hydrogels exhibited biodegradability, especially in the presence of a metabolizing enzyme. In future biomedical applications, BSA-PEG hydrogels could function as interesting drug delivery vehicles which, due to their Sol-Gel transition behavior, might even be considered for injectable alternatives. With the observed gelation conditions they might also perfectly fit the environment of a tumor (temperature slightly higher than normal body temperature) and the gels could provide a reservoir for sustained release of an anti-cancer drug.

REFERENCES

1 Buwalda, S. J.; Boere, K. W.M.; Dijkstra, P. J.; Feijen, J.; Vermonden, T.; Hennink, W. E. Hydrogels in a historical perspective: From simple networks to smart materials, *J Control Release*, In Press.

2 Yaszemski, M. J.; Trantolo, D. J.; Lewandrowski, K. -U.; Hasirci, V.; Altobelli, D. E.; Wise, D. L. *Tissue Engineering and Novel Delivery Systems*, Marcel Dekker, New York, **2004**

3 Li, Y. L.; Rodrigues, J.; Tomas, H. Injectable and biodegradable hydrogels: gelation, biodegradation and biomedical applications, *Chem. Soc. Rev* **2012,** *41* (6), 2193-2221.

4 Macaya, D.; Spector, M. Injectable hydrogel materials for spinal cord regeneration: a review, *Biomed. Mater.* **2012,** *7* (1) 1-22.

5 Overstreet, D. J.; Dutta, D.; Stabenfeldt, S. E.; Vernon, B. L. Injectable hydrogels, *J Polym. Sci. Part A: Polym. Phy.* **2012,** *50* (13), 881-903.

6 Park, M. H.; Joo, M. K.; Choi, B. G.; Jeong, B. Biodegradable Thermogels, *Acc. Chem. Res* **2011,** *45* (3), 424-433.

7 Bawa, P.; Pillay, V.; Choonara, Y.E.; du Toit, L.C. Stimuli-responsive polymers and their applications in drug delivery, *Biomed Mater*, **2009,** 4, 1–15.

8 Klouda, L.; Mikos, A. G. Thermoresponsive hydrogels in biomedical applications, *Eur. J. Pharm. Biopharm.* **2008**, 68 (1), 34-45.

9 Teixeira, L. S.; Feijen, J.; van Blitterswijk, C. A.; Dijkstra, P.J.; Karperien, M. Enzyme-catalyzed crosslinkable hydrogels: Emerging strategies for tissue engineering, *Biomaterials,* **2012**, 33, 1281–1290.

10 Schild, H.G. Poly(N-isopropylacrylamide): experiment, theory and application, *Prog. Polym. Sci*, **1992**, 17, 163–249.

11 Schmaljohann, D. Thermo- and pH-responsive polymers in drug delivery, Adv. Drug Delivery Rev. **2006**, 58(15), 1655-1670.

12 Ward, M. A.; Georgiou, T. K. Thermoresponsive polymers for biomedical applications, *Polymers*, **2011**, *3*(3), 1215-1242.

13 Hatefi, A.; Amsden, B. Biodegradable injectable in situ forming drug delivery systems, *J Control Release* **2002**, 80, 9-28.

14 Kan, P.; Lin, X.Z.; Hsieh, M. F.; Chang, K. Y. Thermogelling emulsions for vascular embolization and sustained release of drugs, *J. Biomed. Mater. Res. Part B* **2005**, 75B, 185-192.

15 Meenach, S. A.; Anderson, K. W.; Hilt, J. Z. Synthesis and characterization of thermoresponsive poly(ethylene glycol)-based hydrogels and their magnetic nanocomposites, *J. Polym. Sci. Part A* **2010**, 48, 3229-3235.

16 Yu, L.; Chang, G.; Zhang, H.; Ding, J. Temperature-induced spontaneous sol–gel transitions of poly(D,L-lactic acid-co-glycolic acid)-b-poly(ethylene glycol)-b-poly(D,L-lactic acid-co-glycolic acid) triblock copolymers and their end-capped derivatives in water, *J Polym. Sci. Part A: Polym. Chem.* **2007**, 45: 1122–1133.

17 Alexander, A.; Ajazuddin, J.; Khan, S.; Saraf, S. Poly(ethylene glycol)–poly(lactic-co-glycolic acid) based thermosensitive injectable hydrogels for biomedical applications, *J Control Release*, **2013**, 172 (3), 715-729.

18 Luzon, M.; Boyer, C.; Peinado, C.; Corrales, T.; Whittaker, M.R.; Tao, L.; Davis, T.P. Water-soluble, thermoresponsive, hyperbranched copolymers based on PEG-methacrylates: synthesis, characterization, and LCST behavior, *J Polym. Sci. Part A Polym. Chem.* **2010**, 48, 2783–2792.

19 Hoare, T. R.; Kohane, D. S. Hydrogels in drug delivery: progress and challenges, *Polymer* **2008**, 49(8): 1993-2007.

20 Chen, C. Y.; Wang, Z. H.; Li, Z. B. Thermoresponsive polypeptides from pegylated poly-L-glutamates, *Biomacromolecules* **2011**, 12 (8), 2859-2863.

21 Jonker, A. M.; Lowik, D.; van Hest, J. C. M. Peptide- and protein-based hydrogels, *Chem. Mat.* **2012**, 24 (5), 759-773.

22 Oss-Ronen, L.; Seliktar, D. Polymer-conjugated albumin and fibrinogen composite hydrogels as cell scaffolds designed for affinity-based drug delivery, *Acta Biomater* **2011**, 7 (1), 163-170.

23 Pahimanolis, N.; Sorvari, A.; Dang Luong, N., Seppälä, J. Thermoresponsive xylan hydrogels via copper-catalyzed azide-alkyne cycloaddition, *Carbohydrate Polymers*, **2014**, 102, 637-644.

24 D'Este, M.; Alini, M.; Eglin, D. Single step synthesis and characterization of thermoresponsive hyaluronan hydrogels, *Carbohydrate Polymers*, **2014**, 90 (3), 1378-1385.

25 Chen, T.; Embree, H.D.; Brown, E.M.; Taylor, M.M.; Payne, G.F. Enzyme-catalyzed gel formation of gelatin and chitosan: potential for in situ applications, *Biomaterials*, **2003**, 24, 2831–2841.

26 Abuchowski, A.; Vanes, T.; Palczuk, N. C.; Davis, F. F. Alteration of Immunological Properties of Bovine Serum-Albumin by Covalent Attachment of Polyethylene-Glycol, *J Biol. Chem.* **1977**, 252 (11), 3578-3581.

27 Gayet, J. C.; Fortier, G. High water content BSA-PEG hydrogel for controlled release device: Evaluation of the drug release properties, *J Control Release* **1996**, 38 (2-3), 177-184.

28 Castelletto, V.; Krysmann, M.; Kelarakis, A.; Jauregi, P. Complex formation of bovine serum albumin with a poly(ethylene glycol) lipid conjugate, *Biomacromolecules* **2007**, 8 (7), 2244-2249.

29 Plesner, B.; Fee, C. J.; Westh, P.; Nielsen, A. D. Effects of PEG size on structure, function and stability of PEGylated BSA, *Eur. J Pharm. Biopharm.* **2011**, 79 (2), 399-405.

30 Shakya, A. K.; Sami, H.; Srivastava, A.; Kumar, A. Stability of responsive polymer-protein bioconjugates, *Prog. Polym. Sci.* **2010**, 35 (4), 459-486.

31 Hamley, I. W.; Krysmann, M. J. Effect of PEG crystallization on the self-assembly of PEG/peptide copolymers containing amyloid peptide fragments, *Langmuir* **2008**, 24 (15), 8210-8214.

32 Zarafshani, Z.; Obata, T.; Lutz, J. F. Smart PEGylation of Trypsin, *Biomacromolecules* **2010**, 11 (8), 2130-2135.

33 Veronese, F. M.; Pasut, G. PEGylation, successful approach to drug delivery, *Drug Discov Today* **2005**, 10 (21), 1451-1458.

34 Elstad, N. L.; Fowers, K. D. OncoGel (ReGel/paclitaxel) — Clinical applications for a novel paclitaxel delivery system, *Adv. Drug Delivery Rev.*, **2009**, 61 (10), 785-794.

35 Lin, Z.; Gao, W.; Hu, H.; Ma, K.; He, B.; Dai, W.; Wang, X.; Wang, J.; Zhang, X.; Zhang, Q.; Novel thermo-sensitive hydrogel system with paclitaxel nanocrystals: High drug-loading, sustained drug release and extended local retention guaranteeing better efficacy and lower toxicity, *J Control Release*, **2014**, 174, 161-170.

36 Li, X. Y.; Li, T. H.; Guo, J. S.; Wei, Y.; Jing, X. B.; Chen, X. S.; Huang, Y. B.: PEGylation of bovine serum albumin using click chemistry for the application as drug carriers *Biotechnol. Prog.* **2012**, 28(3), 856-861.

37 Kelly, S. M.; Jess, T. J.; Price, N. C.: How to study proteins by circular dichroism, *Biochimica et Biophysica Acta* **2005**, 1751, 119 – 139.

38 Wu, Y.; Wang, K.; Buschle‐Diller, G.; Liles, M. R. Fiber formation by dehydration‐induced aggregation of albumin. *J App. Polym. Sci.* **2013**, *129*(6), 3591-3600.

39 Barone, G.; Giancola, C.; Verdoliva, A. DSC studies on the denaturation and aggregation of serum albumins. *Thermochimica acta* **1992**, *199*, 197-205.

40 Lutz, J.-F.; Hoth, A. Preparation of ideal peg analogues with a tunable thermosensitivity by controlled radical copolymerization of 2-(2-methoxyethoxy)ethyl methacrylate and oligo(ethylene glycol) methacrylate, *Macromolecules* **2005**, 39, 893-896.

41 Hedley, D.; Ogilvie, L.; Springer, C. Carboxypeptidase G2-based gene-directed enzyme–prodrug therapy: a new weapon in the GDEPT armoury, *Nature Rev. Cancer* **2007**, 7, 870-879.

CHAPTER 5 GLYCOSYLATION BSA EXTRACELLULAR MATRIX MIMICKING SCAFFOLD

5.1 INTRODUCTION

Artificial scaffold materials that can mimic the extracellular matrix (ECM) are the future material resources in tissue engineering. They are required to provide a functional network for appropriate cell interactions and stabilize newly developed tissue, while serving as a nurturing reservoir for molecules such as growth factors[1-4]. In order to achieve these goals, artificial ECM must be designed to be biocompatible, non-toxic, non-immunogenic, biodegradable, and highly porous but at the same time show adequate mechanical properties[2-4]. Numerous materials have been investigated to obtain artificial ECM. Compared to synthetic polymer scaffolds, naturally derived ECM components containing polysaccharides have the advantage of good cell adhesion, desired mechanical properties, minimized foreign body reaction, and lower risk of causing inflammation[5-6].

Natural biopolymers, such as collagen, hyaluronic acid, fibronectin, chitosan, alginate and silk, have been used as scaffold materials in research. Artificial ECM was created by incorporating natural ECM proteins to enhance cell adhesion[7-8]. Proteins with RGD sequence, such as collagen and fibronectin, showed cell adhesion via attachment of integrin[9]. Collagen (type II), in a sponge shape with proteoglycans (hyaluronic acid or chondroitin sulfate), may have formed well-constructed ECM *in vitro* or *in vivo* with chondrocytes[10-11]. Fibroin and hyaluronic acid, as well as type I collagen might be used in bone tissue engineering[12]. Together with the bone morphogenetic protein-2 (BMP-2), these materials can provide a biomimetic environment that facilitates the growth of new bone from stem/progenitor cells[13]. However, the cost of high performance artificial ECM materials, like those based on collagen, hyaluronic acid or fibronectin, can be high[14].

Efforts have been made to finding cost effective ECM materials with enhanced functions. Synthetic materials as well as natural polymers were grafted with RGD or ECM protein mimicking peptides, to enhance cell adhesion[14-16]. The RGD sequence grafted onto polylactic acid films has achieved rapid adhesion of osteogenic precursor cells and proliferated cell growth[16]. RGD was also grafted as pendant in a PEG based hydrogel to encapsulate human mesenchymal stem cells (hMSCs)[17]. The cost for these synthesized peptide products is comparatively low for those hybrids with synthetic polymers; the stability of these peptides, however, was found inadequate and the products were susceptible to degradation[18]. Cyclic structures of the peptides were introduced to improve the stability was also investigated. Low in yield in reaction, the application of those peptides is limited[18].

In other research, mono-, oligo- and polysaccharides (e. g. hyaluronic acid, alginate or galactose) have been employed as the ligands or the grafts for tissue engineering materials. It was found that galactose may serve as asialoglycoprotein receptor (ASGPR) for hepatocytes[19-20]. Alginate combined with galactosylated chitosan may have easily formed stable hydrogels with improved cell adhesion[21]. Although some of the ECM mimics that contained polysaccharide components are still expensive, the cost of polysaccharide and galactosylated polymers is significantly lower than purely protein based materials. Polyethylene glycol (PEG) is a biocompatible polymer and has been applied for modification of numerous synthetic and natural polymers[4] to introduce thermo-responsiveness in cell adhesion materials[25]. These studies could lead to effective alternatives for tissue engineering materials.

Bovine serum albumin (BSA) is the most abundant animal protein available. Unlike collagen or fibronectin, native BSA does not have the β_1 integrin receptor (RGD sequence)[21]. Research of Kawamura et al.[22] showed that a cell adherent BSA based membrane could be created for some

non-adhesive cells. However, the function of this material was designed for cell anchoring and transferring, but not proliferation or differentiation of cells. To date, BSA has not been used as the scaffold material for tissue engineering *in vivo* or *in vitro*. Incorporating ECM simulating components into BSA could combine the merits of these components with affordable cost of the BSA based material.

In this study, BSA is grafted with a monosaccharide attached to PEG chains on specific sites to mimic glycoprotein and glycosaminoglycan in natural ECM, a model of artificial ECM that mimics the chemical components and structure of natural ECM. BSA was reduced to obtain a linear structure and crosslinked to form a mesh-like structure. Cell adhesion was tested on the BSA network and compared to the other scaffold materials. The result indicated that the material may possess advantageous properties over collagen, fibronectin or polypeptide based ones.

5. 2 EXPERIMENTAL SECTION

Materials:

Bovine serum albumin (BSA), collagen type I from bovine calf skin, tetramethylethylenediamine (TEMED), ethylenediaminetetraacetate (EDTA), and lactobionic acid (LA, 4-O-β-D-galactopyranosyl-D-gluconic acid) were obtained from Sigma-Aldrich (St. Louis, MO); polyethylene glycol diamine (PEGDA, molecular weight 200g/mol), dithioreitol (DTT), 1-ethyl-3-(3-dimethlyaminopropyl)carbodiimide (EDC) and gluconic acid (GA) were obtained from Alfa Aesar (Ward Hill, MA). Trypsin (1:250, tissue culture grade) and phosphate buffered saline (PBS) were purchased from Amresco (Solon, OH) and hydrogen chloride (HCl) was obtained from BDH (Poole, UK).

Synthesis:

The schematic of the BSA modification is shown in Figure 5.1. Briefly, 0.2 g (3 μmol) BSA was dissolved in 50 mL 0.05 M TEMED solution and reacted with 0.023 g (0.15 mmol) DTT for 12 h at room temperature[20,25]. Subsequently, 0.3 g (0.15 mmol) PEGDA was added, the pH of the solution adjusted to 4.5 with hydrochloride acid, and the reaction continued for another 12 h. Finally, 0.5 g sugar acid (SA, including GA or LA) and 0.05 g EDC were added and reacted for 24 h. The product was separated and purified multiple times by centrifugal filtration (MWCO 30 kDa) with DI water as the eluent.

Coating and lyophilization:

The coating solution consisted of 0.5 mL purified BSA-PEGDA-SAs aqueous solution (1%, 2% and 4% w/v, determined by UV-Vis) mixed with 4.5 mL DI water and dispersed onto 85 x 13 mm plastic petri dishes (VWR, non-treated polyethylene). Coating was achieved by removing solvent in a desiccator overnight at room temperature. EDC (0.05 mL, 1% (w/v)) in a methanol:water (9:1) solution was pipetted onto the coating and the samples were dried in a desiccator at room temperature.

For 3D topology, 0.5 mL purified BSA-PEGDA-SA aqueous solution (1%, 2% and 4% w/v, determined by UV-Vis) was added to each wells on a 24-well plate. Samples were prepared by adding EDC to each well in increasing amounts (10, 20, 50, 100, 200 and 500 mg, respectively). The plate was frozen overnight at -18 $^{\circ}$C and lyophilized under 5 mTorr vacuum for 24 h. The dried product was immersed in 0.01% (w/v) EDC solution (methanol:water 9:1, pH 4.5) for 24 h. EDC solution was carefully pipetted out and rinsed with solvent (methanol:water 9:1). The product was lyophilized using the previous conditions.

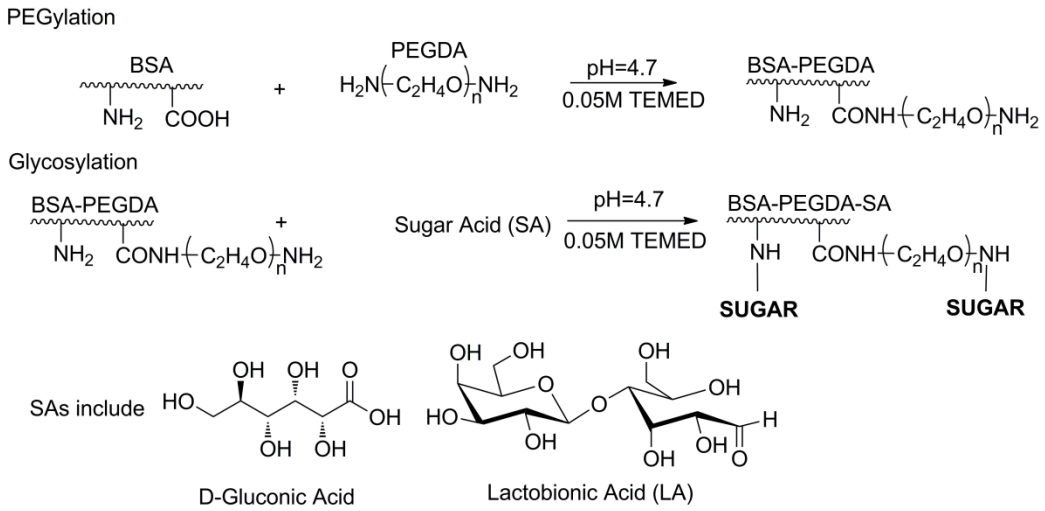

Figure 5.1. Synthesis of glycosylated PEGylated BSA (GA: Gluconic Acid, LA: Lactobionic Acid)

Characterization:

The samples were characterized by H^1-NMR spectroscopy using a Bruker 400MHz spectrometer. Samples were first dried in a desiccator under vacuum and dissolved in 0.5 mL D_2O solvent.

The molecular weights of modified BSA were measured by MALDI-TOF (Bruker Microflex LT MALDI-TOF mass spectrometer with the FlexControl software). The mass range was detected from 20-200 kDa with sinapic acid as the matrix.

UV-Vis spectroscopy was used (Thermo Scientific Genesys 6 spectrometer) to measure the concentration of the BSA moiety before the coating of the samples in quartz cuvettes with 10 mm path length. The absorption coefficient for modified BSA used 3443824 $M^{-1}cm^{-1}$ (280 nm).

The morphology of the coated samples was studied with a Carl Zeiss EVO 50 scanning electron microscope (SEM) at 20 kV scanning voltage. Gold coating was applied by a sputter coater prior to imaging.

Circular dichroism (CD) spectra were generated with a JASCO-810 spectropolarimeter (Jasco, Tokyo, Japan) within wavelength ranges from 180 to 300 nm. Quartz cuvettes with 2 mm path length were used and the average molecular weight of BSA residues used 114 g/mol. Samples were dissolved in 0.05 M phosphate buffer at pH 7.4 with 1 mg/mL protein. Protein moiety ellipticity was determined by equation (1)[24, 25]:

$$\theta = 114\theta_{\lambda}/10dc \quad (1)$$

Where θ_{λ} is the observed ellipticity, d is the light path and c the concentration.

Cell Culture:

NIH 3T3 cells (ATCC CRL-1658) were cultured in 4.5 g/L glucose Dulbecco's modified eagle medium (DMEM, Thermo Scientific) with 10% fetal bovine serum (FBS, Thermo Scientific), 1% Antibiotic-Antimycotic (10,000 units/mL of penicillin, 10,000 µg/mL of streptomycin, and 25 µg/mL of Fungizone, Gibco), in 100 x 20 mm cell culture petri dishes (Corning Costar, tissue cultured treated polystyrene (TPS)). Cells were incubated in 5% CO_2 at 37 $^{\circ}$C. Culture medium was changed every 72 h. Cells were detached with 1 mL trypsin-EDTA solution (0.25% trypsin, 0.02% EDTA) and the suspension was centrifuged at 1500 rpm for 5 min. Cells were diluted in 2 mL culture medium and counted using a hemocytometer.

Cell seeding and viability assay:

Harvested NIH 3T3 cells were seeded 5 X 10^3 cells per well onto a 24-well plate (Corning Costar) of coated BSA-PEGDA-GA/LA; uncoated and collagen coated; 6 wells per type. Then 0.5 mL BSA-PEGDA-GA/LA solution with 4 mg/mL concentration was coated onto each well and the samples dried under vacuum; 0.05 mL 1% (wt) EDC solution (methanol:water, 9:1) was added to the surface and rinse with methanol-water solution (9:1), then dried under vacuum. Collagen coated wells used 0.5 mL collagen (1 mg/mL 0.02 M acetic acid solution). For the 3D

structure, the preparation followed the same procedure as described above, except a 4% solution of BSA-PEGDA-SA containing 100 mg EDC was used. Plates were sterilized by long wavelengthUV light for 2 h prior to cell seeding.

The cells were incubated for 4, 10 and 20 days in the case of coated samples, and 1, 3, 7 days in case of samples with 3D structure. Cells were examined under optical and inverted phase microscopes; cells were fixed with 3% aqueous glutaraldehyde solution before imaging. Cells cultured on TPS were used as the control group. The viability of cells was examined by the MTT (3-(4,5-dimethylthiazol-2-yl)-2,5-diphenyltetrazolium bromide) assay (Biotium). Cells in each well were incubated with 0.05 mL MTT assay reagent with 0.5 mL full culture medium for 2 h. The culture medium was withdrawn and then 1.5 mL DMSO added. The resulting solution was transfer to the well in a 96-well plate and absorption examined by spectrophotometer at wavelengths of 570 and 630 nm (residual media absorption). The cell viability was determined by equation (2).

$$\text{Cell viability}=(OD_{570nm}(\text{Sample})-OD_{630nm}(\text{Sample}))/(OD_{570nm}(\text{control})-OD_{630nm}(\text{control})) \quad (2)$$

OD is the spectrophotometric reading of each well at the selected wavelength. The average values of six samples in each group were normalized and the significance level was determined by the student's T-test.

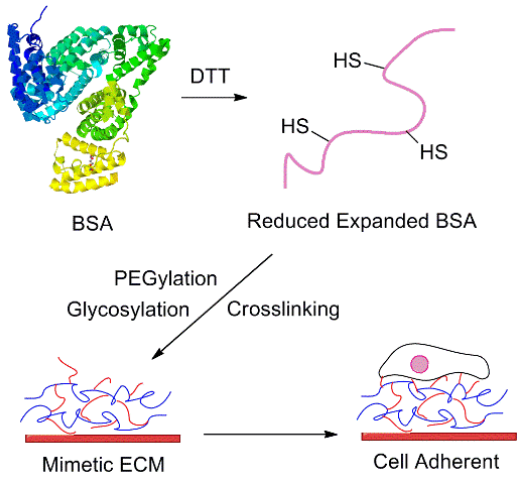

Figure 5.2. Schematic diagram of designing ECM mimicking glycosylated BSA

5.3 RESULT AND DISCUSSION

Synthesis

Figure 5.2 shows a schematic overview of the procedure to create BSA based ECM mimics. DTT reduced the disulfide bonds of BSA at alkaline pH. As a consequence of decreasing the pH, the globular structure of BSA began to unfold and transform into an extended form[25]. Grafting of the PEG chain occurred via the reaction of $–NH_2$ groups on PEGDA and acidic residual of the protein, creating a long hydrophilic chain that could mimic the glycosaminoglycan component in the glycoprotein receptors[20]. Finally, BSA molecules were intermolecularly crosslinked between -COOH and $–NH_2$ groups and a glycosylated BSA mesh structure was created, which mimics the molecular structure of natural ECM (Figure 5.2). It may have improved cell adhesion and growth by providing (1) a protein environment with both hydrophilic and hydrophobic domains; (2) a zwitterionic environment with both positive and negative ions for ionic interactions; and (3) polysaccharide-rich domain, often the composition of mammalian cell outer surface, to name a few.

The yield of BSA-PEGDA-GA was 67% (4% w/v solution, 3.5 mL); the yield of BSA-PEGDA-LA was 59% (4% w/v solution, 3.1mL). The BSA product was analyzed by Proton NMR spectroscopy (Figure 5.3). All the BSA-PEGDA-SAs showed characteristic peaks for both PEG and saccharide. In Figure 5.3a –OH groups of grafted saccharide acid shifted at δ 3.5-4.1 ppm for gluconic acid (GA) and δ 3.5-4.5 ppm for lactobionic acid (LA). The δ = 3.1-3.3 ppm peaks represent the ethoxyl groups and δ at 2.6-2.8 ppm the –NH groups bound to polyethylene glycol diamine. Shown in Figures 5.3b and 3c, by the 2D correlation spectra (COSY) method, the diagonal signals, indicating the bond formation between BSA-PEGDA and saccharide acid grafted via –NH groups of PEGDA. However, it is also possible that saccharide acid reacted to a lesser extent with other available $–NH_2$ groups in the BSA molecule since weak signals were detected off the diagonal regions.

The molecular weights of BSA-PEGDA-SAs were measured by MALDI-TOF. Compared to 66.5 kDa for BSA, the molecular weight of BSA-PEGDA-GA was at 78.4±0.5 kDa; for BSA-PEGDA-LA 78.1±0.4 kDa. Thus, the grafting ratio of the BSA-PEGDA to GA was approximately 1:30 and BSA-PEGDA to LA about 1:20. There was no indication of the presence of crosslinks or oligomers of BSA resulting from PEGylation and glycosylation reactions other than from the crosslinking by EDC.

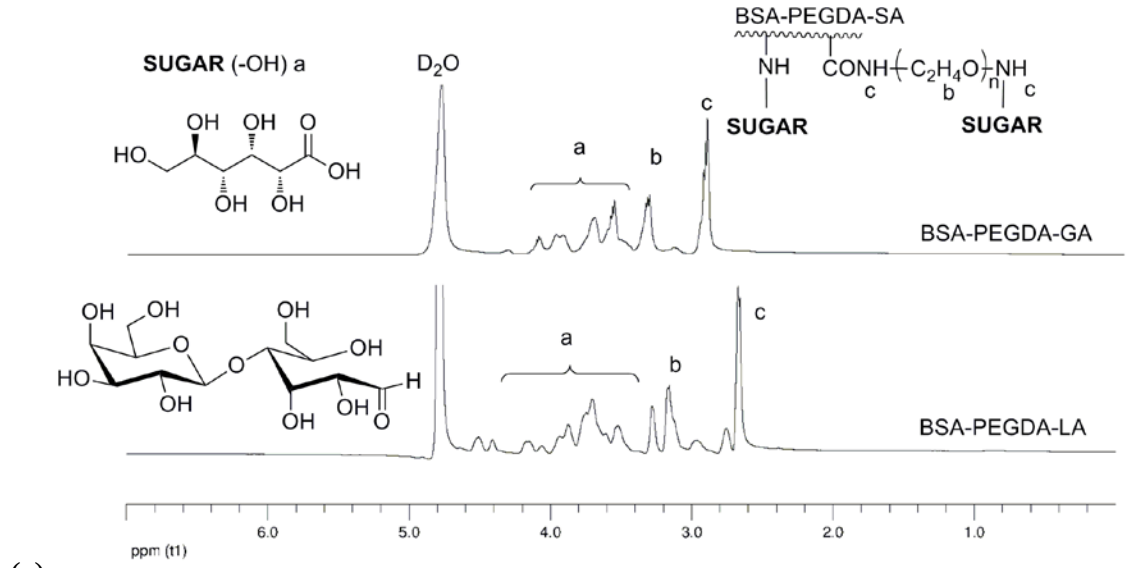

(a)

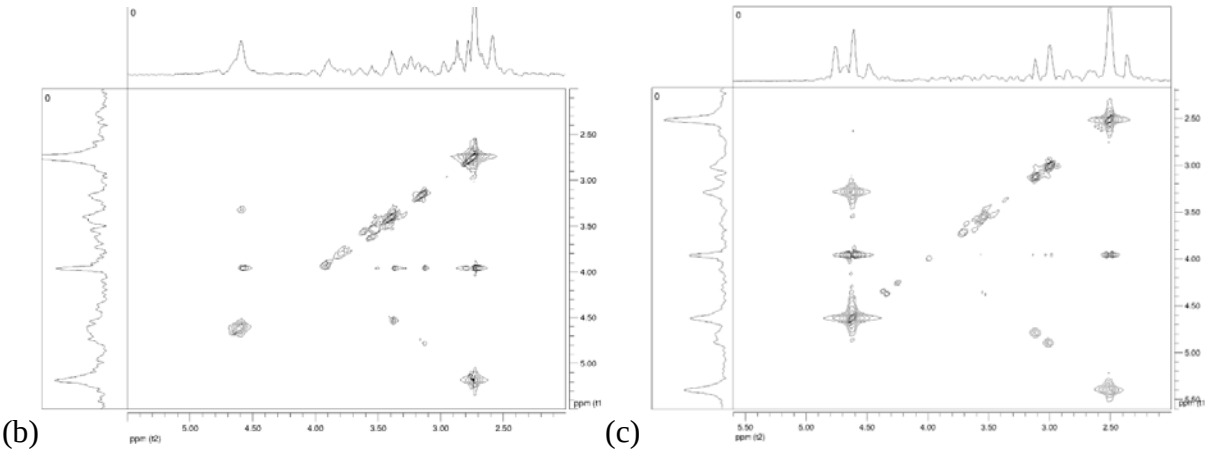

(b) (c)

Figure 5.3. (a) Proton NMR spectra of BSA-PEGDA-GA, BSA-PEGDA-GALA and BSA-PEGDA-LA (D_2O, 400MHz). 2D COSY Proton NMR spectra of (b) BSA-PEGDA-GA, (c) BSA-PEGDA-GALA and (d) BSA-PEGDA-LA (D_2O, 400MHz)

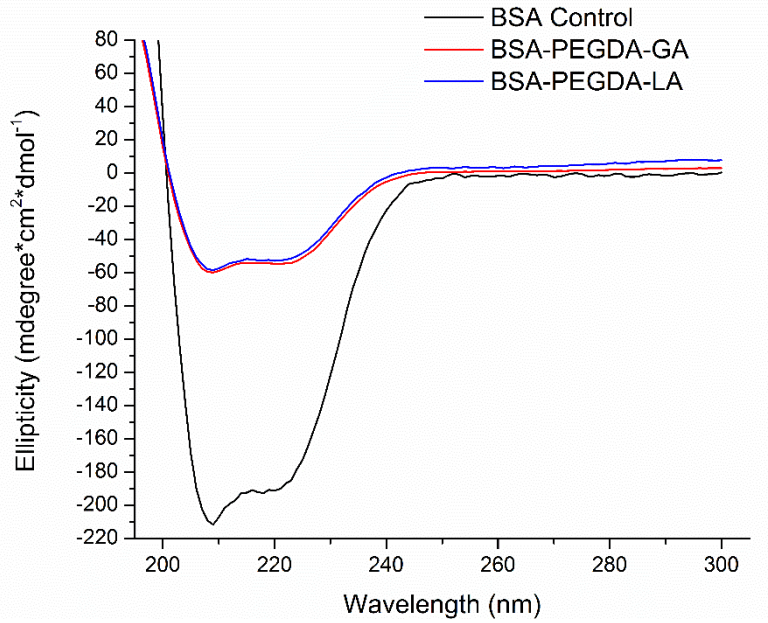

Figure 5.4. CD spectra of BSA-PEGDA-GA and BSA-PEGDA-LA in 0.05M pH=7.4 PBS

The CD spectra of BSA-PEGDA-SAs were compared with that of native BSA (Figure 5.4). A significant reduction in α-helix amount, about 2/3 compared to native BSA (absorption at 210 nm and 225 nm), clearly indicated that these molecules have unfolded under the reaction conditions (low pH) and provided an extended conformation.

Coating and aggregation

BSA-PEGDA-SAs samples were deposited onto polyethylene petri dishes and dehydrated under vacuum. Different morphologies were formed at different starting concentrations as shown in Figure 5.5a-c. At 1% (w/v), a dense structure of aligned fiber-like fragments was observed. It is possible that the aggregation at low concentration did not occur in a precise manner. When the concentration was increased to 2%, fine fibers were developed after dehydration[23]. Finally, with a concentration at/above 4%, a thin film appeared on the petri dish surface. It appears that a concentration of at least 4% is required to coat the area if a concise consistency of the coating is

desired. The cross-sections of the assembly revealed that the coating was less than 10 µm thick (Figure 5.5d).

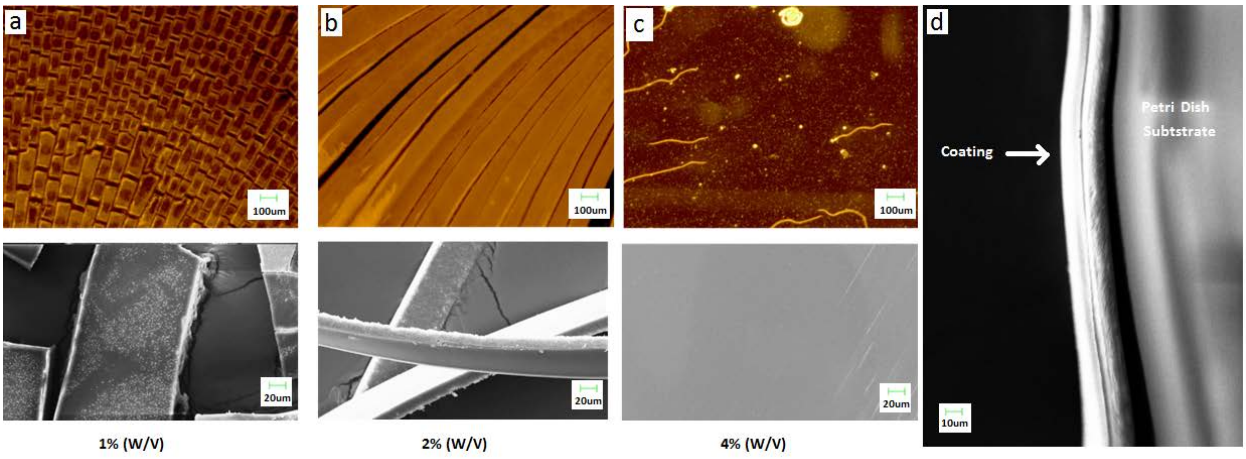

Figure 5.5. Topology of BSA coated with BSA-PEGDA-SA solution (a) 1% (b) 2% and (c) 4%; (d) SEM image of a cross section of BSA-PEGDA-SA coated on polyethylene surface

It has been found that the large surface area in 3D structure scaffolds allows for more effective accessibility to nutrients and other bioactive molecules [4,12]. This type of scaffold may also achieve superior performance with regard to cell proliferation. Under controlled vacuum, the 3D structures were created by removal of water via lyophilization. As illustrated in Figure 5.6, the concentration of BSA-PEGDA-SA was decisive for forming the porous skeleton. At concentrations of 1 and 2%, the structures collapsed after freeze-drying, indicating not enough molecules to sustain the structures with certain mechanical pressure. At 4% a sponge-like 3D structure could be supported. SEM images showed the pore sizes to range from 50-200 µm in diameter, which is about the size of 10 mammalian cells on average could survive comfortably.

This 3D scaffold may provide the surface area for cell adhesion and growth in depth, and simultaneously enable the exchange of nutrients and growth factors.

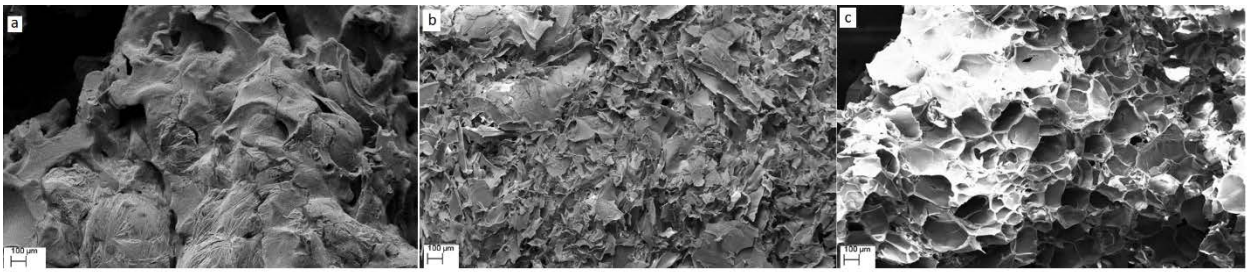

Figure 5.6. SEM images of the surface of 3D sponge-like structures from (a) 1%, (b) 2%, and (c) 4% BSA-PEGDA-SA; the dimension of the void space in (c) is 200 μm, the size of 10 mammalian cells

Cell culture assay

NIH 3T3 cells were seeded in a relatively low number, which allowed more time and space for the cells to migrate and proliferate. For the BSA-PEGDA-SA coating, cell confluence reached a relatively low level by day 4, 50-60% after 10 days, and a fully confluent after 20 days (Figure 5.7). It can be seen from Figures 5.7a-c cells seeded on BSA-PEGDA-SA samples have the cell morphology in a cluster pattern (a) and are on the way to confluent compared to the spindle shaped individual cells grown on collagen or TPS surface (Figures 5.7b and c). For the 3D scaffold structure, the cells can adhere to the surface or deep inside the pores which might provide the time-space cushion needed for cellular activities. This proves that BSA-PEGDA-SA coating is at least as good as that by collagen or TPS, but may be better with respect to cell proliferation. *In vitro*, BSA-PEGDA-SA is biocompatible on hydrophobic surfaces; *in vivo*, it is hypothesized to be compatible with tissue for having hydrophilic and/or hydrophobic surfaces.

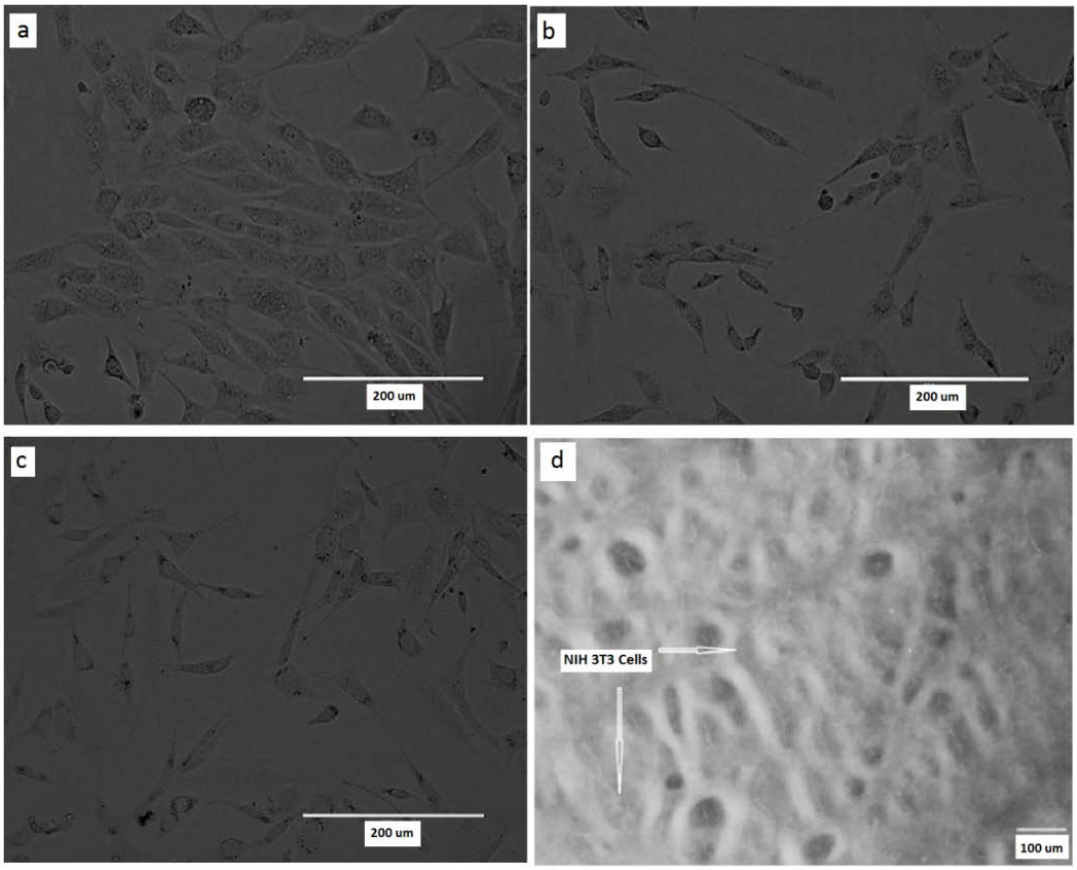

Figure 5.7. NIH 3T3 cell confluent on BSA-PEGDA-SA (a), collagen (b), TPS (c) surfaces (10 days), and on the surface of the 3D structure (d)

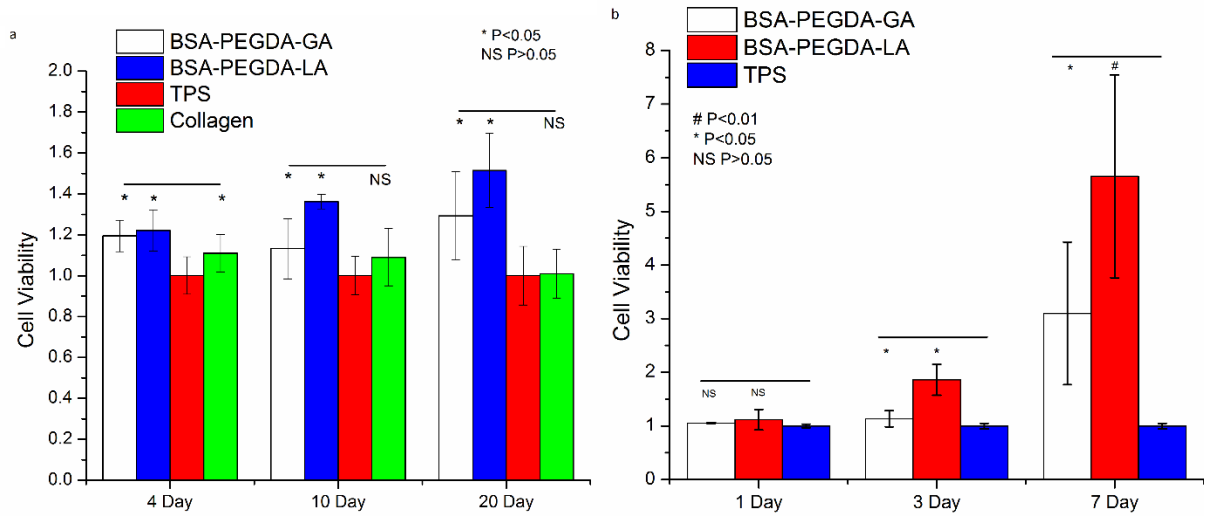

Figure 5.8. IH 3T3 cell viability from MTT assay on collagen, BSA-PEGDA-GA and BSA-PEGDA-LA coated with TPS control as (a) coating, and (b) on 3D structure

The viability of BSA-PEGDA-GA/LA grown cells was measured and compared with collagen and TPS controls. Pure collagen initially had 20% higher cell viability than TPS (Figure 5.8a); however, over time a downward trend was observed and after 20 days it was at the same level as TPS control. This may be due to the rapid degradation of pure collagen by cellular metabolic processes[4]. BSA-PEG-GA/LA, on the other hand, showed a consistent and significant increase in cell viability over time. BSA-PEG-LA was even more effective in facilitating cell proliferation than BSA-PEG-GA. Overall, both BSA based ECM enabled higher cell proliferation than controls. This result suggests strongly that they could be suitable for *in vitro* cell-based tissue culture.

Differences in cell viability from the 3D scaffold were more significant in the early phases of the test. There was no substantial difference after the first day of seeding, but after a few days the BSA-PEG-GA scaffold was 40% and the BSA-PEG-LA approximately 90% higher on average than the TPS control. After 7 days a significant difference between BSA-PEGDA-GA/LA and

control samples was observed, with BSA-PEG-LA by a factor of 2 higher than BSA-PEG-GA. These results suggest that the BSA-PEG-LA/GA 3D structures are indeed more effective in facilitating this particular cell growth. Introduced lactobionic acid (Galactose end groups) as glycoprotein receptor seemed to have improved the cell viability. Culturing of other cells, however, needs to be tested before a more general statement can be made.

5.4 CONCLUSION

PEGylation and glycosylation modified BSA has produced an organized polymer with controllable properties. The crosslinked product can mimic the mesh structure and components of those of natural ECM. Samples prepared in form of either a thin coating or a lyophilized 3D structure facilitated mammalian cell adhesion and proliferation. Compared to TPS matrix, this novel material were effective in improving cell growth and proliferation, and more durable than collagen coated matrix which has a very high degradation rate. BSA-PEG-LA as glycoprotein receptor showed a higher cell viability than GA in both thin film coating and 3D structure, and LA reached up to 5 times higher cell viability in the 3D structure than the TPS matrix. It will be interesting to create more sophisticated spatial structures by varying the reaction conditions and mixing with other materials/structures for eventual cell growth. This type of materials may serve as a cost effective alternative as a tissue culture adherent coating/scaffold with improved functionality to collagen or fibronectin based materials.

.

References

1. Patrick, C. W., Mikos, A. G., McIntire, L. V., editors. Frontiers in tissue engineering. Oxford: Pergamon; 1998

2. Daley, W. P., Peters, S. B., Larsen, M. Extracellular matrix dynamics in development and regenerative medicine. J. Cell. Sci. 2008;121: 255–264.

3. Kim, B. S., Park, I. K., Hoshiba, T., Jiang, H. L., Choi, Y. J., Akaike, T., & Cho, C. S. Design of artificial extracellular matrices for tissue engineering. Prog. Polym. Sci., 2011, 36(2), 238-268.

4. Badylak, S. F., Freytes, D. O., Gilbert, T. W. Extracellular matrix as a biological scaffold material: Structure and function. Acta Biomater 2009;5:1–13.

5. Rosso, F., Marino, G., Giordano, A., Barbarisi, M., Parmeggiani, D., Barbarisi, A. Smart materials as scaffolds for tissue engineering. J. Cell. Physiol. 2005;203:465–470.

6. Mano, J. F., Silva, G. A., Azevedo, H. S., Malafaya, P. B., Sousa, R. A., Silva, S. S., Boesel, L. F., Oliveira, J. M., Santos, T. C., Marques, A. P., Ves, N. M., Reis, R. L. Natural origin biodegradable systems in tissue engineering and regenerative medicine: present status and some moving trends. J. R. Soc. Interface 2007;4:999–1030.

7. Bhadriraju, K., Hansen, L. K. Hepatocyte adhesion, growth and differentiated function on RGD-containing proteins. Biomaterials 2000;21:267–272.

8. Fiegel, H. C., Havers, J., Kneser, U., Smith, M. K., Moeller, T., Kluth, D., Mooney, D. J., Rogiers, X., Kaufmann, P. M. Influence of flow conditions and matrix coatings on growth and differentiation of three-dimensionally cultured rat hepatocytes. Tissue Eng. 2004;10:165–174.

9. Zhao, Y., Xu, Y., Zhang, B., Wu, X., Xu, F., Liang, W., Du, X., Li, R. In vivo generation of thick, vascularized hepatic tissue from collagen hydrogel-based hepatic units. Tissue Eng. Part C Methods 2010;16:653–659.

10. Gruber, H. E., Hoelscher, G. L., Leslie, K., Ingram, J. A., Hanley, Jr E. N. Three dimensional culture of human disc cells within agarose or a collagen sponge: assessment of proteoglycan production. Biomaterials 2006;27:371–376.

11. Wu, C. H., Ko, C. S., Huang, J. W., Huang, H. J., Chu, I. M. Effects of exogenous glycosaminoglycans on human chondrocytes cultivated on type II collagen scaffolds. J Mater. Sci. Mater. Med. 2010;21:725–729

12. Nazarov, R., Jin, H. J., Kaplan, D. L. Porous 3-D scaffolds from regenerated silk fibroin. Biomacromolecules 2004;5:718–726.

13. Kim, J., Kim, I. S., Cho, T. H., Lee, K. B., Hwang, S. J., Tae, G., Noh, I., Lee, S. H., Park, Y., Sun, K. Bone regeneration using hyaluronic acid-based hydrogel with bone morphogenic protein-2 and human mesenchymal stem cells. Biomaterials 2007;28:1830–1837.

14. Bryant, S. J., Nicodemus, G. D., Villanueva, I.. Designing 3D photopolymer hydrogels to regulate biomechanical cues and tissue growth for cartilage tissue engineering. Pharm. Res. 2008;25:2379–2386.

15. Tan, H., Huang, D., Lao, L., Gao, C. RGD modified PLGA/gelatin microspheres as microcarriers for chondrocyte delivery. J Biomed. Mater. Res. B Appl. Biomater. 2009;91:228–238.

16. Hu, Y., Winn, S. R., Krajbich, I., Hollinger, J. O. Porous polymer scaffolds surface-modified with arginine-glycine-aspartic acid enhance bone cell attachment and differentiation in vitro. J Biomed. Mater. Res. A 2003;64:583–590.

17. Nuttelman, C. R., Tripodi, M. C., Anseth, K. S. Synthetic hydrogel niches that promote hMSC viability. Matrix Biol. 2005;24:208–218

18. Bogdanowich-Knipp, S. J., Chakrabarti, S., Williams, T. D., Dillman, R. K., Siahaan, T. J. Solution stability of linear vs. cyclic RGD peptides J. Pept. Res. 1999, 53(5):530-541.

19. Yang J, Goto M, Ise H, Cho CS, Akaike T. Galactosylated alginate as ascaffold for hepatocytes entrapment. Biomaterials 2002;23:471–479

20. Hong, S. R, Lee, Y. M., Akaike, T. Evaluation of a galactose-carrying gelatin sponge for hepatocytes culture and transplantation. J Biomed. Mater. Res. A 2003;67:733–741.

21. Seo, S. J., Choi, Y. J., Akaike, T., Higuchi, A., Cho, C. S. Alginate/galactosylated chitosan/heparin scaffold as a new synthetic extracellular matrix for hepatocytes. Tissue Eng. 2006;12:33–44.

22. Krieger, M., Scott, M. P., Matsudaira, P. T., Lodish, H. F., Darnell, J. E., Zipursky, L., Kaiser, C., Berk, A. (2004). Molecular cell biology (fifth ed.). New York: W.H. Freeman and CO. ISBN 0-7167-4366-3.

23. Kawamura, R., Mishima, M., Ryu, S., Arai, Y., Okose, M., Silberberg, Y. R. Nakamura, C. Controlled cell adhesion using a biocompatible anchor for membrane-conjugated bovine serum albumin/bovine serum albumin mixed layer. Langmuir, 2013 *29*(21), 6429-6433.

24. Wu, Y., Wang K., Buschle‐Diller G., Liles, M. R. Fiber formation by dehydration induced aggregation of albumin. J. Appl. Polym. Sci. 2013, 12(6): 3591-3600.

25. Wang, K., Buschle-Diller, G., Wu, Y. Thermoresponsive hydrogels from BSA esterified with low molecular weight PEG. J. Appl. Polym. Sci. (2014): DOI: 10.1002/APP.40946

CHARPTER 6 CONCLUSIONS

As a type of less developed renewable resources, BSA was investigated for materials in textile industry and biomedical applications. Directional dehydration converted the globular BSA protein to a beta-sheet core-shell structure with the formation of fibers, at isoelectric pH with Na_2SO_4. These fibers are long and smooth but show insufficient mechanical properties for most applications. Crosslinking by EDC significantly improved their mechanical properties. These fibers could be dyed and even twisted into yarns. It would be possible to scale up their production to industrial levels which could point to a future application as textile materials. Beyond the textile market, these fibers could also be developed into matrices for wound dressings that promote healing.

One-step PEGylation reaction introduced thermoresponsiveness into BSA to form hydrogels. By controlling the molecular weight of PEG, the Sol-Gel transition temperature could be controlled around the range of body temperature. This reaction kept the secondary and tertiary structure of BSA, and thus the product hydrogel still retained its capability to bind to hydrophobic drugs. This type of injectable biodegradable hydrogel may serve as vehicle for anti-tumor drugs right at the site of a tumor.

Mimicking of the natural ECM structure was conducted by using reduced BSA to be grafted with PEGDA and saccharide acid, and then crosslinked with EDC. The modified BSA could be assembled into a thin film and a 3D porous structure. It achieved improved cell viability in cell culture assay compared to collagen and tissue culture treated polystyrene. This type of material may be utilized as cost effective replacement of expensive collagen and fibronectin in tissue engineering.

In summary, applications of BSA were explored and could be expanded to the formation of fibers, injectable hydrogels and scaffold materials. In future research, a rapid response injectable hydrogel for drug delivery and tissue engineering may be developed.

VITA

Kai Wang, who is the son of Ziqiang Wang and Guanghui Cao, was born January 5, 1988 in Shandong Province, People's Republic of China. He entered Soochow University in 2006, and graduated with Bachelor of Engineering in Materials Engineering in July 2010. He entered the PhD program at the Department of Polymer and Fiber Engineering, Auburn University in August 2010. His current research area is protein based biomaterials from renewable resources.